

Seismic Stratigraphy and Sedimentary Dynamics of the Cenozoic Succession of the Offshore Indus Basin, Pakistan

Dissertation
with the aim of achieving a doctoral degree
at the Faculty of Mathematics, Informatics and Natural Sciences
Department of Earth Sciences
at Universität Hamburg

Submitted by

Khurram Shahzad

Pakistan

Hamburg 2019

Eidesstattliche Versicherung

Hiermit erkläre ich an Eides statt, dass ich die vorliegende Dissertationsschrift selbst verfasst und keine anderen als die angegebenen Quellen und Hilfsmittel benutzt habe.

I hereby declare that I have written this dissertation by my own and I have not used other than the acknowledged resources.

Hamburg, den 29.04.2019

Unterschrif

Accepted as Dissertation at the Department of Earth Sciences

Day of oral defense: 02.07.2019

Reviewers: Prof. Dr. Christian Betzler
Dr. Thomas Lüdmann

Chair of the Subject Doctoral Committee: Prof. Dr. Dirk Gajewski

Dean of Faculty of MIN: Prof. Dr. Heinrich Graener

Summary

The Offshore Indus Basin of Pakistan is a frontier geological province, located at the western continental margin of the Indian Plate. The basin preserves an exceptionally well-developed shallow marine carbonate record of the Paleocene-Eocene transition, which is buried under a thick succession of terrigenous sediments from the Indus Fan. However, the sedimentary dynamics of these carbonate platforms are poorly understood with respect to the Cenozoic stratigraphic evolution of the basin. Concerning the research gap, this thesis aims to reconstruct the Cenozoic depositional history of the Offshore Indus Basin, and to decipher the factors controlling the depositional architecture of the basin. The study involves extensive seismic sequence interpretation of a dense grid of high-resolution seismic data covering an area of 75000 km². Results are backed-up by lithological and biostratigraphic information from several industrial wells, towards establishing a chronostratigraphic framework and characterizing the post-rift depositional episodes of the western continental margin of India.

The interpretation of seismic profiles reveals the presence of nine complexes of isolated carbonate platforms that were established on the topographic highs inherited from the Deccan Volcanism. The subdivision of the carbonate succession into seven seismo-stratigraphic units constrains the stratigraphic evolution as phases of platform onset, of aggrading and backstepping margins, of platform top emersion, and drowning of the carbonate platforms. Fossil assemblages suggest that the development of the isolated carbonate platforms occurred during the early Paleogene greenhouse climate with a terminal drowning during the Early to Middle Eocene. The distinct shapes, sizes, and thicknesses of the carbonate platforms are the result of the antecedent topographic morphologies. Thermal subsidence primarily provided the accommodation for the accumulation of thick and wide carbonate succession. Decoding the internal reflection geometries and stratal patterns suggests strong imprints of the climate and sea level control upon the depositional architecture and platform-internal heterogeneity. The episodic syn-sedimentary reactivation of basement faults linked to the drifting and collision of the Indian Plate partially controlled the internal architecture and caused the backstepping of the carbonate margins. Further, the regional well correlation suggests that the isolated carbonate platforms are stratigraphically age-equivalent to the Laki-Ghazij lithostratigraphic unit of the coeval carbonate shelf.

Based on the planktonic foraminiferal assemblages, a depositional hiatus of around ~30 Ma is recorded at the top of the carbonate platforms, which encompasses a time period from the Early Eocene to Middle Miocene. However, the well to seismic correlation established the progradation of the Indus Fan sediments in the peripheries of the carbonate platforms during the Oligocene, which completely covered the platforms until the Middle Miocene.

Further, high-resolution seismic data allow distinguishing the internal geometries and the depositional elements of the canyon-channel system of the Indus Fan. The stratigraphic development of the Indus Fan is subdivided into an Oligocene to Miocene and a Plio-Pleistocene interval. The Oligocene to Early Miocene succession appears to be composed of small submarine channels with thin levees, alternating with repeated phases of mass transport

complex formation. In this study, the Middle Miocene times marks the development of the shelf prograding margins. The shelf margin is dissected by two sets of submarine canyons that developed during the Miocene and Plio-Pleistocene. The results show an increase in the size of channel-levee complexes during the Late Miocene until the Plio-Pleistocene. Furthermore, the results suggest that cyclic sea level fluctuations initiated the incision at the shelf margins with sediment by-passing to the deeper basin. This process ceased eventually coincident with a rising sea level halting fan development and establishing a system of shale-prone sediments.

In summary, this study aims at helping to understand the depositional responses regarding modern and ancient carbonate growth during warm climate conditions and proposes an extended approach towards investigating such carbonate platforms using seismic images. Further, the study concludes that the carbonate platform architecture was controlled mainly by the extrinsic factors of sea level changes and climate.

Zusammenfassung

Das der Küste von Pakistan vorgelagerte Indusbecken ist eine geologische Grenzprovinz, die sich am westlichen Kontinentalrand der Indischen Platte befindet. Das Becken weist ein außergewöhnlich gut entwickeltes Archiv flachmariner Karbonatgesteine des Übergangs vom Paläozän in das Eozän auf, welches von einer mächtigen Abfolge terrigener Sedimente des Indus-Fächers überlagert wird. Die Sedimentdynamik der dort vorkommenden Karbonatplattformen in Bezug auf die känozoische stratigraphische Entwicklung des Beckens ist jedoch wenig verstanden. Unter diesem Aspekt zielt diese These darauf ab, den Depositionsverlauf des Indusbeckens während des Känozoikums zu rekonstruieren und die Faktoren zu erfassen, die zur vorkommenden Architektur der Ablagerungen des Beckens geführt haben. Die Studie beinhaltet eine umfangreiche Sequenzinterpretation hochauflösender seismischer Daten welche eine Fläche von 75000 km² abdecken. Die Ergebnisse werden durch lithologische und biostratigraphische Informationen aus mehreren industriellen Bohrungen unterstützt, um einen chronostratigraphischen Rahmen zu erstellen und die Post-Rift-Ablagerungsepisoden des westlichen Kontinentalrandes von Indien zu charakterisieren.

Die Interpretation seismischer Profile zeigt das Vorhandensein von neun Komplexen isolierter Karbonatplattformen, die sich auf topographischen Höhen als Folge des Dekkan-Vulkanismus etablierten. Die Unterteilung der Karbonatabfolge in sieben seismostratigraphische Einheiten gliedert die stratigraphische Entwicklung in Phasen des Auftretens der Plattform, der Aggradation und des Zurückschreitens der Plattformränder, des Auftauchens der Plattformoberflächen und des Ertrinkens der Karbonatplattformen. Fossile Vergesellschaftungen deuten darauf hin, dass die Entwicklung der isolierten Karbonatplattformen während des frühen paläogenen Treibhausklimas stattfand, und durch die Überflutung der Plattformen während des frühen Eozäns beendet wurde. Die unterschiedlichen Formen, Ausbreitungen und Mächtigkeiten der Karbonatplattformen sind das Ergebnis vorangegangener topographischer Morphologien. Thermische Subsidenz bildete in erster Linie die Grundlage für die Akkumulation mächtiger und ausgebreiteter Karbonatfolgen. Die Interpretation der internen Reflexionsgeometrien und Schichtmuster deutet auf starke Auswirkungen der Klima- und Meeresspiegelveränderungen auf die Depositionsarchitektur und die plattforminterne Heterogenität hin. Die episodische synsedimentäre tektonische Reaktivierung von Störungen der topographischen Höhen, im Zusammenhang mit dem Abdriften und der Kollision der Indischen Platte, kontrollierte teilweise die interne Architektur und verursachte den Rückgang der Karbonatplattformränder. Darüber hinaus deutet die Korrelation der einzelnen Bohrungen darauf hin, dass die isolierten Karbonatplattformen stratigraphisch altersäquivalent zur lithostratigraphischen Einheit Laki-Ghazij, des gleichnamigen Karbonatschelfs sind.

Basierend auf planktischen Foraminiferen-Vergesellschaftungen wurde an der obersten Schichtgrenze der Karbonatplattformen zum terrigenen Material ein Hiatus von etwa ~30 Ma registriert. Diese Lücke umfasst einen Zeitraum vom frühen Eozän bis zum mittleren Miozän. Die Korrelation von seismischen und bohrlochgeophysikalischen Daten begründet die

Progradierung der Sedimente des Indus-Fächers in unmittelbarer Umgebung zu den Karbonatplattformen während des Oligozäns welche die Plattformen bis ins mittlere Miozän vollständig bedeckten.

Darüber hinaus ermöglichen hochauflösende seismische Daten die Unterscheidung der inneren Geometrien sowie der Depositionselemente des Canyon-Canal-Systems des Indus-Fächers. Die stratigraphische Entwicklung des Indus-Fächers gliedert sich in ein Oligozän - Miozän- und ein Plio - Pleistozän-Intervall. Die oligozäne bis miozäne Sukzession scheint aus kleinen Kanälen mit schmalen Levees zu bestehen, die sich mit wiederholten Phasen des zur Komplexbildung führenden Massentransports abwechseln. In dieser Studie markiert das mittlere Miozän die Entwicklung des progradierenden Schelfs. Der Schelfrand wird von zwei Sets submariner Canyonsysteme durchzogen, die sich im Miozän und Plio-Pleistozän entwickelten. Die Ergebnisse zeigen eine Vergrößerung der Channel-Levee Komplexe während des späten Miozäns bis zum Plio-Pleistozän. Darüber hinaus deuten die Ergebnisse darauf hin, dass zyklische Meeresspiegelschwankungen das Einschneiden an den Schelfrändern durch den Transport von Sedimenten in das tiefere Becken ausgelöst haben. Dieser Prozess endete schließlich mit einhergehendem Meeresspiegelanstieg, wodurch die Entwicklung des Fächers beendet wurde und sich ein System von fein-gradierten Tiefseesedimenten etablierte.

Zusammenfassend lässt sich sagen, dass diese Studie darauf abzielt, die Depositionsmechanismen bezüglich des rezenten und vorzeitlichen Karbonatwachstums unter warmen Klimabedingungen zu verstehen. Zusätzlich wird ein erweiterter Ansatz für die Untersuchung solcher Karbonatplattformen unter Verwendung seismischer Daten vorgeschlagen. Weiterhin wird in dieser Studie der Schluss gezogen, dass die Architektur der Karbonatplattform hauptsächlich durch die extrinsischen Faktoren von Meeresspiegeländerungen und Klima gesteuert wurde.

*This work is dedicated
to my father Muhammad Younas (Late)
and
to my mother Perveen Bano
for their endless love, support, encouragement and sacrifices.*

Acknowledgements

This Ph.D. thesis is a culmination of a life-long interest in geology and has turned into as much a labor of love as a scientific study. Therefore, I would like to thank numerous people who have helped me academically and socially through the course of my Ph.D. studies in Hamburg.

First and foremost, I would like to express my sincere gratitude to my advisors, as without their supervision and constant help the compilation of this dissertation was impossible. I am eternally grateful to my main advisor, Professor Dr. Christian Betzler, who accepted me as a Ph.D. student in his research group and provided me effective supervision, invaluable trust, time and overall guidance whenever it was needed throughout my Ph.D. His expertise, understanding, encouragement and affirmative advice have helped me to grow as a researcher. I would like to thank my second advisor Dr. Thomas Lüdman for his continuous support and insightful advisory on my dissertation work. I am very grateful to Dr. Sebastian Lindhorst for his valuable suggestions and administrative support during the period of my Ph.D. studies. Especially, I am indebted and thankful to Dr. Nadeem Ahmed for sharing his knowledge about the regional geology of Pakistan and introducing me to the fascinated world of marine geology. Words of gratitude are also for Dr. Anwar Qadir from the University of Haripur, Farrukh Qayyum from Saudi Aramco KSA, Humaad Ghani from the University of Potsdam, Germany for their friendly discussions on my scientific results and helping me in finding ways to tackle scientific challenges during my Ph.D. research. I am especially thankful to Prof. Dr. Gerhard Schmiedl from the Institute of Geology, and Prof. Dr. Silvia Spezzaferri from the University of Fribourg for their kind help in looking into the fossils and dating the rocks.

The colleagues at the Institute of Geology meant like a family to me, they have contributed vastly to my memorable stay in Hamburg and has been a source of continuous motivation and learning. I would like to thank Juliane Ludwig, Huaqing Bai and Jesus Reolid and, especially, Marco Wunsch for amazing discussions on carbonate geology and other aspects. I would like to also thank Dr. Annemarie Gerhard for her help during my early days in Hamburg and doing paperwork during my Ph.D. I would also like to thank Dirk Eggers in providing logistic support during my Ph.D. studies. I also thank Muhammad Zafar and Faisal Iqbal for providing me access to the core-repository and thin section preparation in Hydrocarbon Development Institute of Pakistan.

I am grateful to all the funding sources that helped me to complete my doctoral dissertation. Mainly, I acknowledge the University of Hamburg for providing me funding for my Ph.D. that made my stay in Hamburg comfortable. Further, I am also thankful to my supervisor again for providing me funding for attending international conferences that benefited my research in millions of ways. Acknowledgements are also given to the German Research Foundation (DFG) for providing me financial support during my stay in Germany.

I thank my Pakistani friends, Muhammad Abid, Sohail Aftab, and Malik Abdullah among other friends for their continuous support during the period of stay and study in Hamburg. At

the best of all, I thank Muhammad Zeeshan Saeed for his company and for regular fights that helped me a lot in releasing my work stress. Altogether, I have been luckily surrounded by such a delightful group of people who helped and inspired me throughout my Ph.D. tenure.

Special thanks go to my family. Words cannot express how grateful I am to my mother for her unconditional love, support, affection and constant prayers at home. I am eternally grateful to my sisters for their love and unconditional support. I also express my sincere gratitude to my brothers Muhammad Ilyas, Muhammad Ayaz and Muhammad Mudassar for their support and sympathy during all these years with various difficulties involved in producing a thesis.

List of Publications

1. **Shahzad, K., Betzler, C., Qayyum, F.** (2019) Controls on the Paleogene carbonate growth under greenhouse climate conditions (Offshore Indus Basin). *Marine and Petroleum Geology*, 101, 519-539.
2. **Shahzad, K., Betzler, C., Ahmed, N., Qayyum, F., Spezzaferri, S., Qadir, A.** (2018) Growth and demise of a Paleogene isolated carbonate platform of the Offshore Indus Basin, Pakistan: Effects of regional and local controlling factors. *International Journal of Earth sciences*, 107, 481-502.

Contents

Summary	i
Zusammenfassung	iii
Acknowledgement	vi
List of Publications	viii
Chapter I: Introduction	1
1.1 Research rationale	1
1.2 Research aim and objectives	3
1.3 Study area: Offshore Indus Basin.....	3
1.4 Material and methods	4
1.4.1 Seismic data	4
1.4.2 Well data	6
1.4.3 Biostratigraphy and age control	6
1.5 Thesis outlines.....	6
Chapter II: Tectonic and stratigraphic framework of the Offshore Indus Basin	8
2.1 Regional settings	8
2.2 Basin development	8
2.3 Cenozoic stratigraphy.....	10
2.3.1 The Indus Fan	10
2.4 Paleogeography of the Indian Ocean	13
Chapter III: Growth and demise of a Paleogene isolated carbonate platform of the Offshore Indus Basin, Pakistan: Effects of regional and local controlling factors	14
3.1 Outline of the chapter	14
3.2 Geological background	14
3.3 Data and methods	15
3.4 Results and interpretation.....	16
3.4.1 Seismic facies.....	16
3.4.2 Seismic stratigraphy.....	19
3.4.2.1 Deccan volcanics	19
3.4.2.2 Seismic unit S1	19
3.4.2.3 Seismic unit S2	21
3.4.2.4 Seismic unit S3	22
3.4.2.5 Seismic unit S4	23
3.4.2.6 Seismic unit S5	24
3.4.2.7 Seismic unit S6	26
3.4.2.8 Seismic unit S7	26
3.5 Calibration with biostratigraphy.....	26
3.6 Discussion	28
3.6.1 Paleocology and biostratigraphy	28
3.6.2 Platform evolution	30
3.6.2.1 Platform initiation stage (S1-S2)	30
3.6.2.2 Aggrading and escarpment stage (S3-S6)	31
3.6.2.3 Late stage buildup and final drowning stage (S7)	32

3.6.3	Factors controlling the carbonate platform growth and architecture.....	32
3.6.3.1	Subsidence and sea level changes	32
3.6.3.2	Climate and paleoceanography.....	34
3.6.4	Partial drowning mechanism of the carbonate platform.....	35
Chapter IV: Controls on the Paleogene carbonate platform growth under greenhouse climate conditions (Offshore Indus Basin)		37
4.1	Outline of the chapter	37
4.2	Regional settings	38
4.3	Data and methods	39
4.3.1	Well to seismic tie and stratigraphic correlation.....	39
4.4	Results	43
4.4.1	Seismic facies analysis.....	43
4.4.2	Seismic morphology and distribution of isolated carbonate platforms	43
4.4.3	Seismic stratigraphy of the isolated carbonate platforms	47
4.4.3.1	Top Basement (Cretaceous-Paleogene).....	47
4.4.3.2	Seismic unit S1 (Middle to Late Paleocene)	47
4.4.3.3	Seismic unit S2 and S3 (Late Paleocene)	49
4.4.3.4	Seismic unit S4 (Late Paleocene to Early Eocene).....	50
4.4.3.5	Seismic unit S5 (Early Eocene)	51
4.4.3.6	Seismic units S6 and S7 (Early to Middle Eocene).....	51
4.4.4	Seismic interpretation and paleogeography	53
4.4.4.1	Carbonate platform evolution.....	53
4.4.4.2	Carbonate platform margin development	54
4.4.5	Structural trends	55
4.4.6	Subsidence and accommodation	57
4.5	Discussion	59
4.5.1	Controls on carbonate platform evolution	59
4.5.1.1	Volcanic ridges as antecedent topography	59
4.5.1.2	Platform geometries: sea level vs climate	59
4.5.1.3	Tectonic influence and platform backstepping.....	61
4.5.2	Comparison with the Indian Ocean carbonate platform	62
Chapter V: Seismic architecture and stratigraphy of the Indus Fan		63
5.1	Outline of the chapter	63
5.2	Regional settings	63
5.2.1	Geological settings.....	63
5.2.2	Fan morphology	64
5.3	Data and methods	65
5.3.1	Seismic and well data.....	65
5.3.2	Methodology	65
5.3.3	Terminology.....	68
5.4	Results and discussion.....	69
5.4.1	Architectural elements of the Indus Delta and Fan system.....	69
5.4.1.1	Shelf Edge Delta.....	71
5.4.1.2	Submarine canyons and gullies	71

5.4.1.3	Submarine channel fills	71
5.4.1.4	Inner levee and intra-channel terraces	71
5.4.1.5	Outer levee/overbanking.....	71
5.4.1.6	Sediment waves	72
5.4.1.7	Mass transport complexes	72
5.4.1.8	Hemipelagic deposits.....	73
5.4.1.9	Unconfined lobes and sheet deposits.....	73
5.4.2	Seismic stratigraphy	73
5.4.2.1	Cretaceous-Paleogene boundary and prefan stratigraphy	73
5.4.2.2	Oligocene to Miocene.....	77
5.4.2.3	Pliocene – Pleistocene	80
5.4.2.4	Holocene Hemipelagic drapes	81
5.4.3	Sedimentary dynamics and growth of Plio-Pleistocene CLCs	81
5.4.3.1	Stage 1: Channel incision	81
5.4.3.2	Stage 2: Channel fills and levee deposition.....	83
5.4.3.3	Stage 2a: Channel migration and channel bifurcation.....	83
5.4.3.4	Stage 3: Passive channel filling and channel abandonment	85
5.5	Controlling factors of the Indus Fan sedimentation	85
Chapter VI: Conclusions and synthesis		88
References		91

Chapter I

Introduction

1.1 Research rationale

Passive continental margins are important repositories of depositional archives that contain significant information about tectonic-climate interactions. Advances in the seismic stratigraphy have largely evoked great interest in unraveling these stratigraphic records of passive continental margins (Mitchum et al., 1977; Posamentier et al., 1988). Interpreting these depositional archives provide essential information about paleo-terrestrial and marine climate (Zachos et al., 2001), paleo-sea level changes (Haq et al., 1987; Miller et al., 1987, 2005), rate of erosion and sediment influx from hinterlands (Clift et al., 2008, 2014), and ocean circulations (Rebesco et al., 2014).

According to the principles of sequence stratigraphy, the development of stratigraphic sequences depends on the climate and sea level changes (Mitchum et al., 1977; Posamentier et al., 1988; Schlager, 2005; Catuneanu, 2006). Climate primarily controls the type and supply of sediments, together with tectonics and eustasy that determine the accumulation and accommodation of the sediments. The interplay between these mechanisms controls the formation of the distinctive depositional geometries. Through the study of sedimentary archives, it is established that the Earth's Cenozoic climate history has experienced fundamental long-term climatic changes (Zachos et al., 2001). Following the mass extinction at the Cretaceous–Paleogene boundary, the Paleogene is characterized as a period of greenhouse climate that culminated with the inception of the Neogene icehouse world. The triggering mechanisms for this temperature increase was linked to a substantial rise in the atmospheric carbon dioxide (CO₂) level (Pearson and Palmer, 2000; Zachos, 2003). Consequently, these environmental conditions affected the ecosystem of marine and terrestrial biota and resulted in a major extinction event of deep-sea benthic foraminifera with a reported Tethyan-wide reduction of coral reef species (Scheibner et al., 2005). These long term hyperthermia ended in the Late Cenozoic with the development of Antarctic Ice sheets (Zachos et al., 2001). Further studies suggest that higher chemical erosion rates of the Himalayan region and Tibetan plateau repose a drawdown of atmospheric CO₂ and global cooling (Raymo and Ruddiman, 1992).

Located on the western continental margin of India (Fig. 1.1), the Offshore Indus Basin is one of the largest sedimentary basins of the world that comprise a well-developed but unexplored Cenozoic stratigraphic succession. As an Indian marginal basin, the Offshore Indus Basin has experienced significant climatic changes in the Paleogene period during its multiphase rifting, drifting and ongoing collision of the Indian-Eurasian Plates (Chatterjee et al., 2013). The stratigraphy of the basin includes up to 10 km of Cenozoic sediments that can be primarily subcategorized into Paleocene-Eocene tropical carbonate platforms and Oligocene to recent submarine fan and turbidite systems.

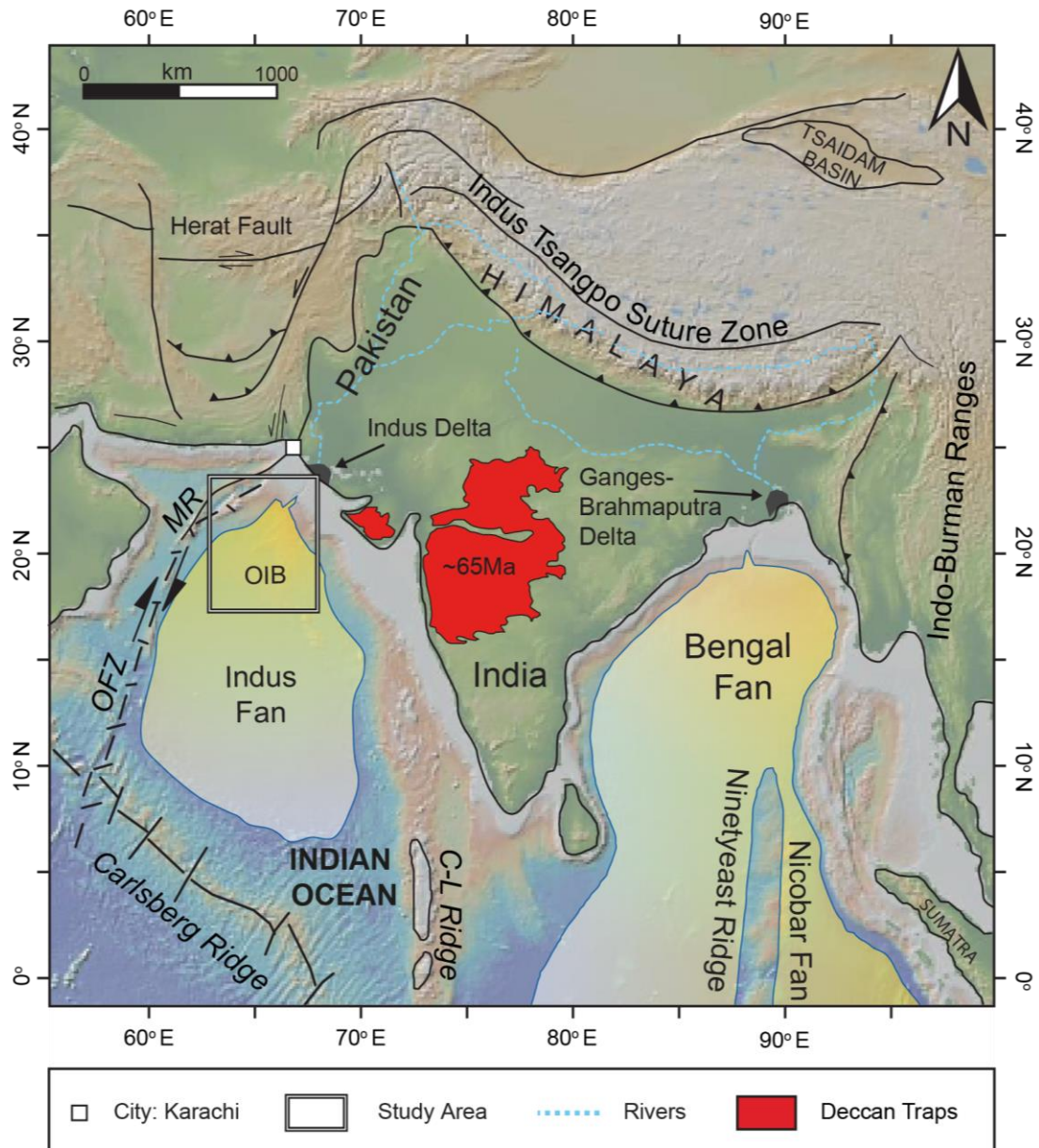


Figure 1.1: Geographical position of the Offshore Indus Basin. Bathymetry after Ryan et al. (2009). C-L: Chagos-Laccadive Ridge, MR: Murray Ridge, OFZ: Owen Fracture Zone

The Offshore Indus Basin has been the focus of numerous scientific investigations to understand its complex stratigraphic history (Clift et al., 2001; Daley and Alam, 2002; Gaedicke et al., 2002b; Carmichael et al., 2009; Corfield et al., 2010; Calvès et al., 2011). These studies primarily focus on the Indus Fan sedimentation and constrain the tectonic-erosional history of the Himalayan Orogeny, which explain the regional climatic events of the Neogene period such as development and strengthening of the South Asian Monsoon, and a drastic decrease in CO₂ and global cooling (Clift et al., 2001; Gaedicke et al., 2002a). In contrast, the Paleogene stratigraphic record developed during the drifting phase of the Indian margin has received much less attention and has remained a significant gap in attempting to reconstruct the stratigraphic history of the basin. Thus, the lack of attention has severe consequences for an improved understanding of the regional climate evolution and in describing the correct sediment depositional history of the Indus Fan. Further, the study of the

tropical succession of the shallow water carbonate platform developed during the climatic perturbation of the Paleogene period can provide clues about the drastic impact of the climate on the paleogeography of the Indian Plate. This will not only increase our understanding of the evolution of the basin but also the least understood carbonate factory of the Cenozoic time. As a result of scarce examples of such carbonate system, the study of the Offshore Indus carbonate platforms become significantly valuable. These carbonate platforms are buried under a thick succession of terrigenous sediments of the Indus Fan derived from the Indian-Eurasian continent collision. As a consequence of Indian-Eurasian Collision, the effect of orogeny and active sediment supply modified the depositional architecture of the Offshore Indus Basin. Sea level fluctuations and thermal subsidence created accommodation for extensive sedimentation but hindered the reactivation of the carbonate factories.

Therefore, the primary target of the study is to establish a comprehensive stratigraphic framework of the Cenozoic succession and investigate the evolution of the Indus Offshore Basin by integrating commercially acquired seismic data with the well information. Improved understanding of the depositional processes is also vital for the successful delineation of natural resources that received considerable attention by the hydrocarbon exploration industry in recent years.

1.2 Research aim and objectives

The objective of this study is to answer the questions: i) *what types of stratigraphic and sedimentation processes occurred in the Offshore Indus Basin during the Cenozoic time, and ii) what are the intrinsic and extrinsic controlling factors?*

The following work package allows to achieve this objective:

- Revision of the established stratigraphic framework for the Cenozoic succession of the Offshore Indus Basin Pakistan based on newly available seismic data.
- Bio-and lithostratigraphic correlation of the Paleogene and the Neogene succession of the Offshore Indus Basin to the onshore through industrial wells.
- Characterization of the seismic architecture and depositional geometries of Paleogene and Neogene successions and establishment of a sequence stratigraphic framework for the shallow water carbonate sequences, and Indus Fan deposits, respectively.
- Analysis of the regional and global mechanisms controlling the development of the Cenozoic sedimentary systems, and to determine the relationship between the development of carbonate platform and submarine fan deposits to the sea level change and tectonic dynamics of the Northern Indian Ocean.

1.3 Study area: Offshore Indus Basin

The study area is located ca. 300 km southeast of the city of Karachi at the proximal setting of the Indus Fan in the Northern Indian Ocean (Fig. 1.1). The study area covers the continental shelf to deep-water settings of the western continental margin of the Indian Plate, with water depth ranging between 100 to 3500 m (Fig. 1.2). The geology of study area and regional settings have been discussed in detail in section 2.1 of chapter II.

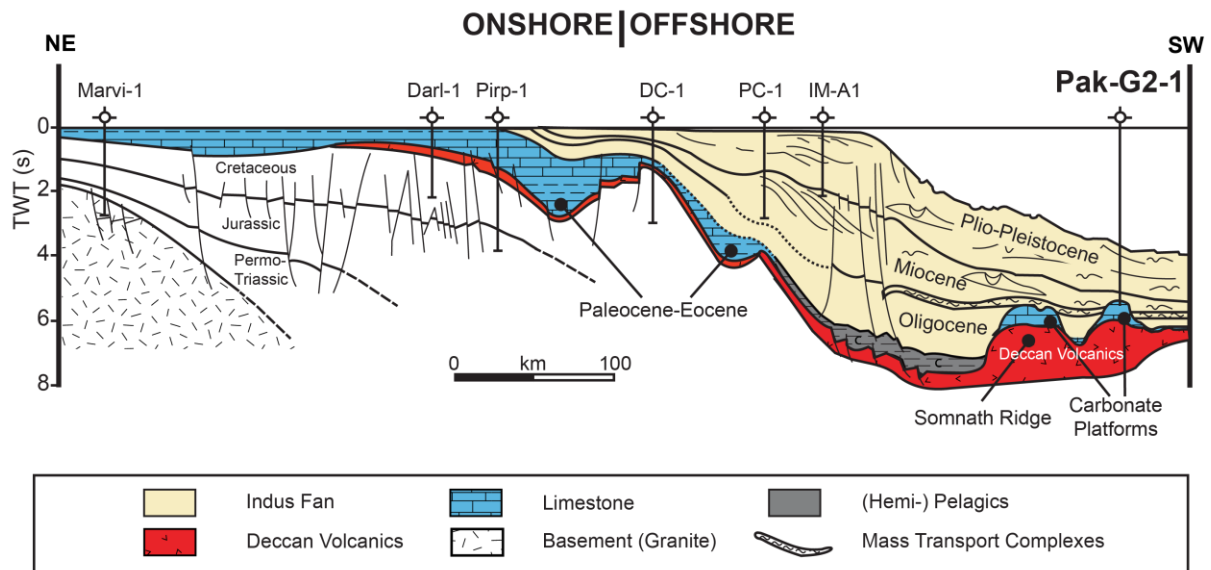


Figure 1.2: Regional cross-section of the Offshore Indus Basin and adjacent onshore basin, modified after Carmichael et al. (2009). DC-1: Daboo Creek-1, PC-1: PakCan-1, IM-A1: Indus Marine A1

1.4 Material and methods

In the Offshore Indus Basin, research and hydrocarbon exploration activities during the last 50 years has compiled an enormous amount of seismic and well data. This study integrates a variety of datasets acquired for the commercial and academic purposes including 2D seismic data and well data from commercial boreholes and public domain bathymetry datasets (Fig. 1.3).

1.4.1 Seismic data

The seismic survey, named TEPP2000, was acquired by Total Exploration and Production, Pakistan in 2002. This seismic survey covers a region from the continental shelf edge to the deep-water basin covering the continental slope, and the Upper Indus Fan, and provides a baseline for the seismic interpretation (Fig. 1.3). The acquisition was carried out with the following parameters: a 3410 cubic inches air gun array placed 6 m below the sea surface, 37.5 m shot-point interval, a 6000 m long streamer with 480 channels and a group interval of 12.5 m. With a grid interval of 5 X 5 km, the record length reached 10s two-way time (TWT), with a sampling interval of 2 ms and a fold of 160. Standard industrial processing produced seismic data with the deconvolved, zero-phased, time migrated seismic display using Society of Exploration Geophysicists (SEG) reverse polarity (Brown, 2004). The quality of the seismic imaging is good with a vertical seismic resolution of ~25m, estimated from a dominant frequency of 45 Hz. However, the seismic imaging is compromised in the proximity of the volcanic basement and structural highs. The data set is the property of Government of Pakistan, and is obtained on request and special permission by C. Betzler to use in the research and publish the outcome of the results to make them accessible to the scientific community. Another seismic survey acquired in 1997 was also procured from the Bundesanstalt für Geowissenschaften und Rohstoffe (BGR) for the seismic interpretation of peripheries of the study area.

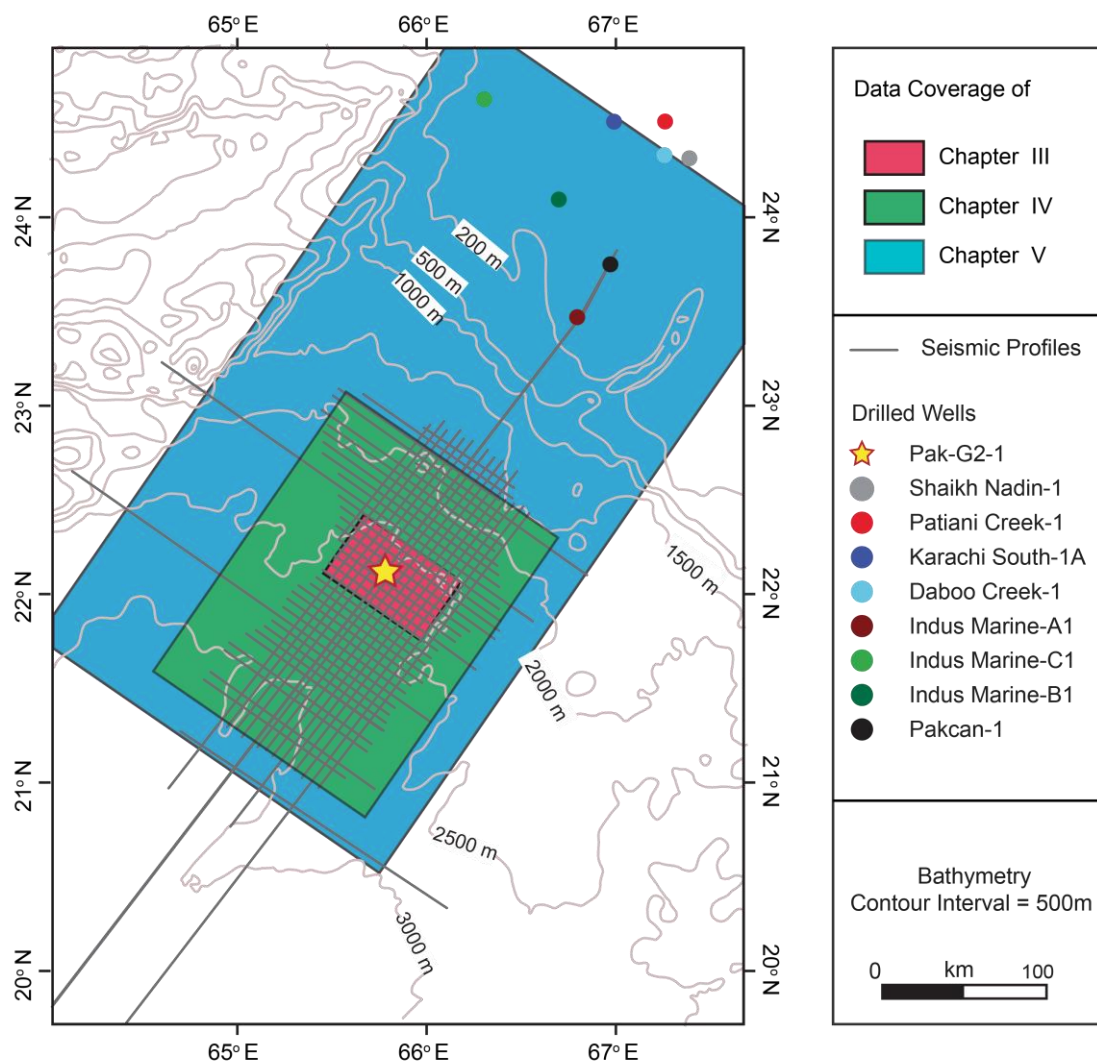


Figure 1.3: Basemap showing the location of the seismic survey and wells used in this study. Wells drilled in the study area are shown with the solid colored dots.

The post-stack time-migrated seismic sections and well data were introduced in the Petrel (Schlumberger) software suit for stratigraphic and structural interpretation. The stratigraphy from the exploration wells located on the present-day continental shelf was extrapolated to the seismic dataset. This provided a chronostratigraphic framework for the carbonate and the younger sedimentary succession. For the deep-water settings of the Offshore Indus Basin, the stratigraphic model developed by Carmichael et al. (2009) was adopted along with the available information of well Pak-G2-1. The seafloor surface was mapped on the seismic grid and was converted to the bathymetry by using the standard water velocity of 1500 m/s. This bathymetric surface was then incorporated with the satellite bathymetric data from Smith and Sandwell (1997). The mapped seafloor was then utilized to identify the various morphologic features present in the Northern Indian Ocean. The excellent resolution and depth of penetration of these datasets allow detailed observation of internal geometry over a large area of the Offshore Indus Basin. Based on these observations, the depositional history of the region has been investigated.

1.4.2 Well data

In addition to seismic data, digital log motifs from the 11 industrial wells were used for the stratigraphic correlation and calibration of the seismic data. The well-to-seismic correlation was achieved by the use of Vertical Seismic Profile (VSP) and check-shot data. The well data consists of a standard wireline log suit comprising gamma ray (GR), sonic (DT), density, and neutron porosity logs.

1.4.3 Biostratigraphy and age control

For the age control of the Cenozoic succession, microfacies and micropaleontology analysis was performed on the well cuttings of the industrial wells. Samples were taken on variable intervals coinciding the seismic stratigraphic surfaces established through the seismic stratal patterns. The identification of the type of fossil assemblages helps us to reconstruct the prevailing environmental conditions as well as sea level changes through time. Samples were taken from the carbonate succession bearing well-preserved larger benthic foraminifera. Larger benthic foraminifera are adapted to specific light conditions, depth, and trophic regimes, as well as to a well-defined temperature range. This approach helped us mark the transition from the deep to the shallow marine environment. The planktonic foraminifera biostratigraphy of the overlying pelagic deposits helped us to identify and date the post drowning deep marine succession. For the biozonation of larger benthic foraminifera bearing Paleocene-Eocene carbonate succession, we followed the biostratigraphic scheme of Serra et al. (1985).

1.5 Thesis outlines

This dissertation is comprised of six chapters including this introductory chapter (Chapter I). The regional geological setting of the Offshore Indus Basin is described in Chapter II. Chapter III investigates the architectural evolution and drowning history of one of the Paleogene carbonate platforms of the Offshore Indus Basin, Pakistan through a comprehensive analysis of regional 2D seismic profiles and well data. In the light of seismic stratigraphic concepts and facies analysis, this chapter focuses on internal reflection geometry to trace the development phases and assess the intrinsic and extrinsic factors that governed the carbonate growth and demise. Furthermore, the chapter documents the biotic assemblages and constrains the ages of the major evolutionary stages of platform growth and final drowning based on the biostratigraphic analysis of well cuttings from the exploration wells. This chapter is based on the findings of the peer-reviewed article entitled “Growth and demise of a Paleogene isolated carbonate platform of the Offshore Indus Basin, Pakistan: effects of regional and local controlling factors” published in the *International Journal of Earth Sciences* (for details, please refer to Shahzad et al., 2018).

Chapter IV of the dissertation further extends the results driven from chapter III for the regional interpretation and correlation. In this chapter, we present the stratigraphic evolution, the morphological features, and the distributions of the nine composites of the Paleocene-Eocene carbonate platforms, covering an area of almost 9000 km². The isolated carbonate platforms are developed on the NE-SW oriented volcanic basement highs and volcanic ridges

Chapter I

of the Réunion Hotspot trace. Further, using the seismic stratigraphic principles, this chapter emphasizes the depositional geometries and decipher mechanisms controlling the stratigraphic architecture of the carbonate platforms developed under the greenhouse climatic conditions. Findings of this study will directly or indirectly enhance our understanding of greenhouse carbonate platforms that can be applied to similar deposits elsewhere. The work presented in this chapter has also been published in the *Journal of Marine and Petroleum Geology* (Shahzad et al., 2019) and titled “Controls on the Paleogene carbonate platform growth under greenhouse climate conditions (Offshore Indus Basin).”

Chapter V presents the seismic interpretation of the multichannel seismic profiles across the Indus Fan region and establishes the stratigraphic subdivision of the Indus Fan and associated deposits. This study distinguishes the mega-stratigraphic units and establishes a correlation between deep-water setting and coeval deposits of the continental shelf. The results suggest time-stratigraphic bounded relations of the erosional and depositional elements of the Indus Delta and Fan system. Further, this chapter describes the changes in depositional history through Cenozoic and explains the different depositional elements in the stratigraphy.

Finally, Chapter VI summarizes the main findings and synthesis of the work presented in the thesis.

All the chapters were written by Khurram Shahzad, and are based on the seismic data analysis, and digital well logs and biostratigraphic analysis of well cuttings samples, granted to Mr. Khurram Shahzad on special request of Prof. Dr. Christian Betzler by the Directorate General of Petroleum Concessions (Ministry of Petroleum Pakistan), LMKR and Hydrocarbon Development Institute of Pakistan. Another data set was granted to the Institute of Geology, the University of Hamburg by Bundesanstalt für Geowissenschaften und Rohstoffe (BGR) on an agreement between BGR representatives and Prof. Dr. Christian Betzler (University of Hamburg).

Chapter II

Tectonic and stratigraphic framework of the Offshore Indus Basin

2.1 Regional settings

The Offshore Indus Basin is bounded by the Murray Ridge - Owen Fracture Zone in the west-northwest (Fig. 2.1), which is a major plate boundary between the Indian and Arabian Plate (Edwards et al., 2000). To the north, it is facing the continental shelf that is incised by the Indus Canyon. The Laxmi Ridge is located in the southeast of the basin, which is a subsurface buried structure and assumed to be a continental product of the early stages of the Indian Plate's drift (Fig. 2.1; Naini and Talwani, 1982; Talwani and Reif, 1998). The crustal thickness in the region varies between 9 km and 12 km (Calvès et al., 2008). The tectonic history suggests a thermal subsidence phase coeval with the cooling of the Pakistan volcanic margin followed by the induced flexuring responsible for the development of basin in the Cenozoic (Mohan, 1985; Agrawal and Rogers, 1992; Whiting et al., 1994).

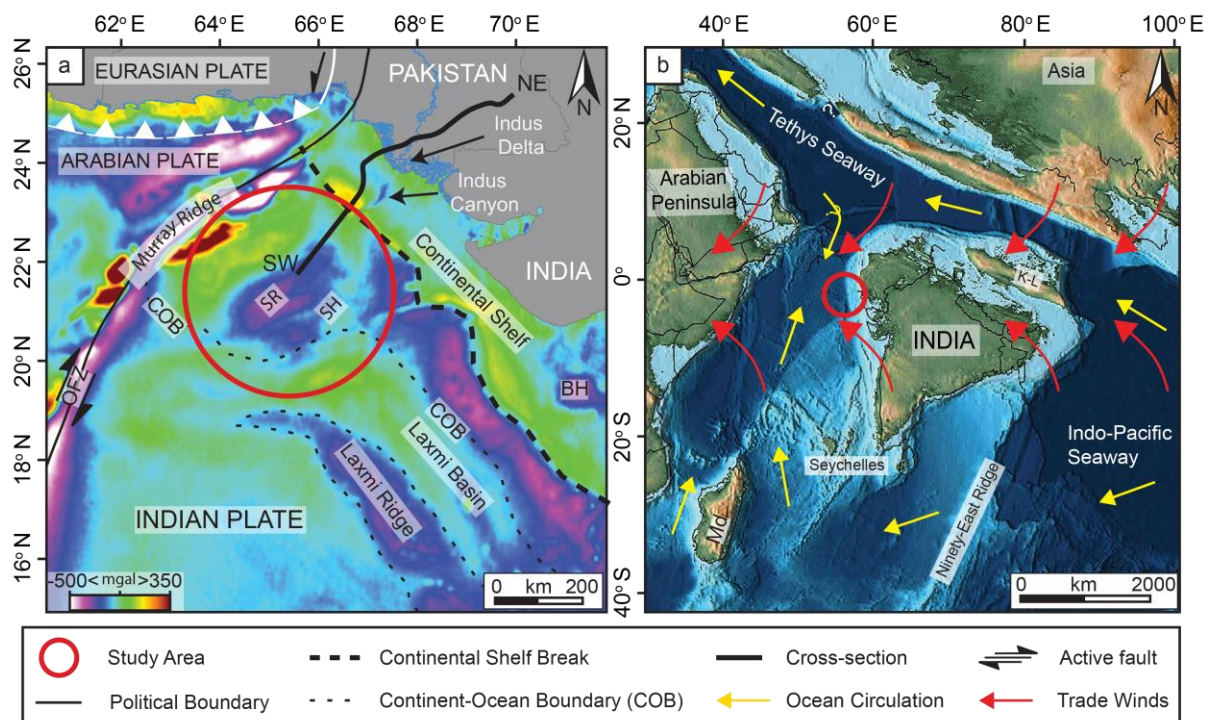


Figure 2.1: (a) Map of tectonic and structural elements of the northwestern margin of the Indian Plate and surroundings with the free air gravity (Sandwell et al., 2014). NE-SW: cross section shown in figure 1.2. The dotted line labeled with “COB” marks the continent-ocean boundary after Carmichael et al. (2009). OFZ: Owen-Fracture Zone, SR: Somnath Ridge, SH: Saurashtra High, BH: Bombay High (b) Late Paleocene reconstruction (~56 Ma) and paleogeography of Indian Plate to show the tropical environment with ocean circulation and prevailing wind direction (Haq, 1981; Aubert and Droxler, 1996; Scotese, 2001). Md: Madagascar.

2.2 Basin development

The tectonic evolution of the basin encompasses over 200 million years of geological history (Fig. 2.2). The development of the western continental margin of India started with the

breakup of the East Gondwanaland in the Cretaceous (Chatterjee et al., 2013). During the Early Cretaceous, the Indian Plate started to detach from the Antarctic and the Australian Plates and drifted northward (Chatterjee et al., 2013). At this time, the conjoined India-Madagascar-Seychelles was moving south with respect to Africa. This movement ceased around ~100 Ma (Edwards et al., 2000) and turned into two successive phases of rifting. The first phase of rifting took place with the separation of India-Seychelles from Madagascar during the Late Cretaceous leading to the formation of a spreading ridge in the Mascarene Basin (Edwards et al., 2000). This rifting event was followed by the second phase of rifting, separating Seychelles from the Indian Plate during the Late Cretaceous and Early Paleocene times (Corfield et al., 2010). The separation is contemporaneous with the voluminous extrusive volcanism of Deccan volcanic episode while India and Seychelles passed over the Réunion hotspot. As a result, a chain of volcanic ridges was formed. The separation of Seychelles from the Indian Plate was also accompanied by the formation of a new sea-floor spreading center (Carlsberg Ridge) in the Indian Ocean (White and McKenzie, 1989; Todal and Edholm, 1998; Whiting et al., 1994). Passive margin developed during the post-volcanic event that would become the modern-day continental shelf.

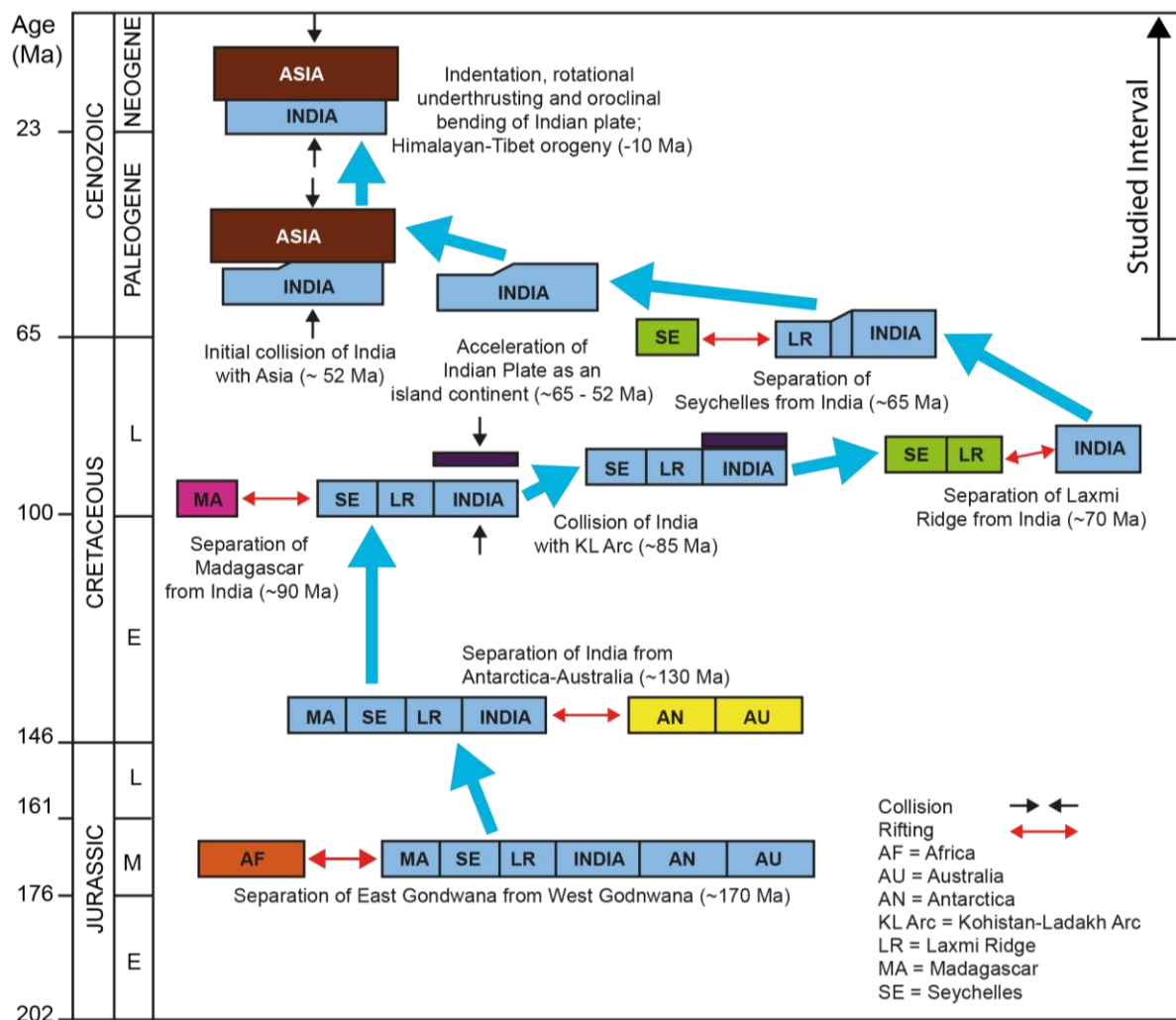


Figure 2.2: Tectonic history of the Indian Plate over the 200 million years of its geological history (Chatterjee et al., 2013).

Following the event of Deccan volcanism and seafloor spreading, the Indian Plate started moving northward rapidly towards the Eurasian Plate. This northward voyage of the Indian Plate was slowed by the oblique collision with the Eurasian Plate and docking with the Kohistan-Ladakh Island Arc in the Late Paleocene to Middle Eocene time. Subsequently, the Tethyan Seaway located in the northwest closed during the Late Eocene to Oligocene. This event was followed by the orogeny and a massive influx of terrigenous sediments in the adjacent seas and nearby foredeep which developed the world's second largest submarine fan system in the Indian Ocean, the Indus Fan (Clift et al., 2001; Wandrey et al., 2004).

2.3 Cenozoic stratigraphy

The offshore region of Pakistan is still considered as a frontier basin and no formal lithostratigraphic scheme has yet been established. However, based on the regional seismic surveys and well data, numerous authors have documented first order stratigraphic outlines of the Offshore Indus basin (Fig. 2.3; Clift et al., 2001; Gaedicke et al., 2002a; Carmichael et al., 2009; Khan et al., 2016; Shahzad et al., 2018, 2019). The stratigraphy of the area of interest is subdivided into four main stratigraphic units (Figs. 2.3 and 2.4): (1) a Late Cretaceous to Early Paleocene igneous basement, equivalent to the Deccan Volcanics, (2) Paleocene–Eocene shallow marine carbonate platforms, nested on the volcanic highs, surrounded by (3) the Paleocene–Oligocene hemipelagic deep marine deposits (discussed in chapter III and IV), (4) the Oligocene to Recent siliciclastic succession of the Indus Fan with distinctly large-scale Plio-Pleistocene channel-levee systems (discussed in chapter V).

The Cenozoic sedimentary section of the offshore basin overlies the Deccan Volcanics (Figs. 2.3 and 2.4; Carmichael et al., 2009). However, the oldest sedimentary succession reported in the exploration wells of the adjacent onshore region is the Late Cretaceous in age and comprises of deltaic sandstones alternating with basalts (Daley and Alam, 2002). The overlying Paleogene succession is dominated by a series of tropical attached and detached, shallow marine carbonate platforms that developed on the continental shelf and the pre-existing paleo-highs, respectively, during the equatorial and subequatorial position of the basin (Shahzad et al., 2018, 2019). The intervening topographic lows and basin floors are covered by pelagic to hemipelagic sediments intercalated with siliciclastics (Rodriguez et al., 2014). Onshore the Paleogene comprises the Paleocene-Rankiot Group, the Early Eocene Laki-Ghazij Formation, the Middle to Late Eocene Kirthar Formation and the Oligocene Nari Formation (Fig. 2.3; Carmichael et al., 2009; Daley and Alam, 2002). Biostratigraphically, the detached carbonate platforms in the Offshore Indus Basin are time-equivalent to the Laki member of the Ghazij Group, comprising nummulitid and assilinitid bearing, low-energy carbonate banks with interbedded transgressive shales in the lower part.

2.3.1 The Indus Fan

In the Offshore Indus Basin, the Middle Eocene time marked the onset of the Indus Fan deposition (Clift et al., 2002). Further, an increase of the sediment supply to the Indus Fan is known since the Late Oligocene. Increased sedimentation rates between the Early and Middle Miocene (~16-11 Ma) may reflect the prominent uplift of the Himalaya (Clift et al., 2002).

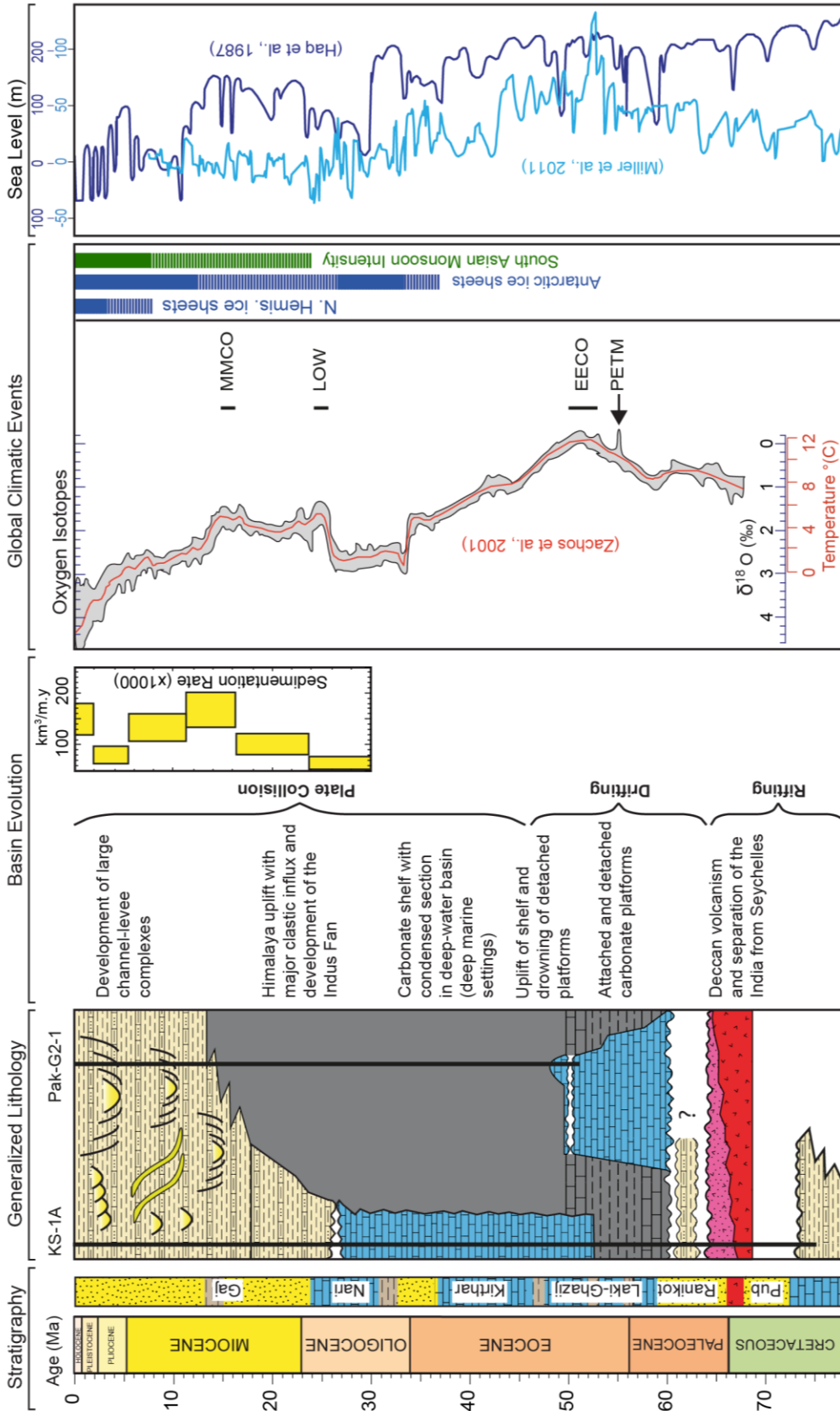


Figure 2.3: Regional stratigraphic column and basin evolution of the Offshore Indus margin and reported sediment thickness of the Indus Fan (after Clift et al., 2002) with global climatic events are illustrated, modified after Zachos et al. (2001), and compared with the global sea level curves (Haq et al., 1987; Miller et al., 2011). MMCO: Middle Miocene Climatic Optimum, LOW: Late Oligocene Warming, EEEO: Early Eocene Climatic Optimum, PETM: Paleocene-Eocene Thermal Maximum.

Furthermore, Clift et al. (2001) speculated that the exhumation of the Indus drainage basin was later followed by a decrease in sediment influx in the Late Miocene. Fan deposits rapidly leveled the relief between the basement structural highs (Clift et al., 2001; Gaedicke et al., 2002a; Clift and Gaedicke, 2002). Today, the offshore region is one of the major deltaic basins and is characterized by large scale channel-levee systems. The Indus Fan is also the world's second-largest submarine fan system with a volume of $5.0 \times 10^6 \text{ km}^3$. It is up to 960 km wide and stretches around 1500 km in front of the Indus Delta into the Indian Ocean (Clift et al., 2001; Gaedicke et al., 2002). At the proximal setting, the basin currently contains a 9 km thick succession of the fan deposits (Gaedicke et al., 2002c; Carmichael et al., 2009).

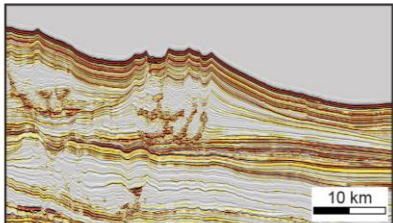
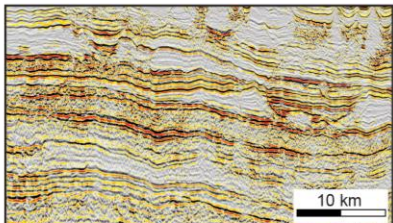
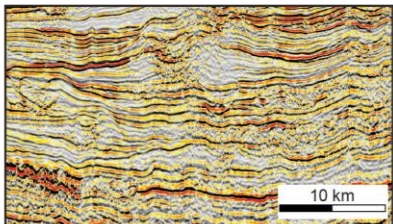
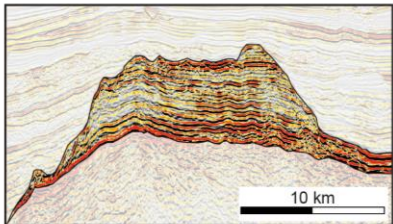
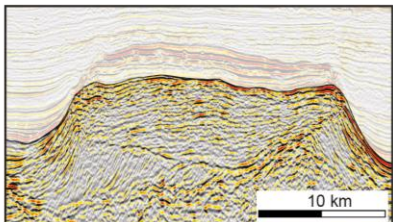
Stratigraphic Framework	Seismic Expression	Depositional (Seismic) Characteristics
Plio-Pleistocene Channel-Levee Complexes with Hemipelagics succession on top.		Below the seafloor, a thick succession of hemi-pelagics deposits on the top of turbidites are the most recent sediments. Plio-Pleistocene deposits are characterized by the very large scale channel flanked by the gull-winged shaped levees. Channels are separated by the (hemi-) pelagics condensed sections.
Oligocene-Miocene Megasequences of the Indus Fan		Oligocene and Miocene composed of the small scaled leveed channels and repeated phase of the mass transport complexes.
Paleocene-Eocene Hemipelagic Deposits with overlying Oligocene Fan deposits		The lower Paleogene succession is predominantly rich in the (hemi-) pelagics. The upper unit consist of small channels and mass flows in the form of mass transport complexes.
Paleocene-Eocene Carbonate Platforms		The stratigraphic unit of Paleocene-Eocene consist of isolated carbonate platforms, sitting on the top of the Early Paleocene volcanic mounds. Carbonate platforms are rich in larger benthic foraminifera encasing the shallow benthic zones SBZ-5 to 10 of Serra-Kiel et al. (1998).
Late Cretaceous to Early Paleocene Basalts		Volcanic mounds developed during the volcanism event of Reunion hotspot, equivalent to the Deccan Traps in age. Dominantly consist of hyaloclastite mounds and lava flows, emplaced during the separation of India-Seychelles.

Figure 2.4: Seismic expressions of the stratigraphic intervals studied in this research project and their corresponding depositional interpretation.

2.4 Paleogeography of the Indian Ocean

Paleo-oceanographic studies indicate that the changing positions of continents, archipelagos, and island arcs of the geologic past also changed coeval wind and ocean circulation patterns (Parrish, 1987). Today, the geomorphology of India deflects the northern subtropical gyre, and the monsoonal circulation disturbs the trade-wind system. In the past, the oceanographic setting of the region was quite different. The Cretaceous oceans were characterized by warm and high sea levels. Cooling initiated with the beginning of the Cenozoic and eventually culminated with the Neogene glacial climate (Zachos et al., 2001). During the Paleogene period, the Tethys currents, which dominated the tropical circulations, were actively flowing westward through the Tethys Seaway and the Panama Straits to form a Circum-Tethyan global tropical current contributing to the widespread dispersal of marine biota from the eastern to the western of the Tethys Sea (Fig. 2.1b). The Indian landmass arrived at the subduction zone on the north between the Latest Paleocene to and the Eocene. The northern Tethys seaways began to restrict, until the end of the Eocene, which is evident by the presence of extensive neritic and marginal marine deposits of the Middle to Late Eocene in an age in Pakistan (Haq, 1981). Furthermore, in Oligocene, this flow sharply reduced and finally closed in the Miocene.

Chapter III

Growth and demise of a Paleogene isolated carbonate platform of the Offshore Indus Basin, Pakistan: Effects of regional and local controlling factors

3.1 Outline of the chapter

In the early Paleogene, the Offshore Indus Basin was a part of the eastern Tethys and an equatorial province that characterized by widespread attached and isolated carbonate platforms. However, concerning the regional stratigraphic settings, the sedimentary dynamics of Paleogene carbonate platforms of the Offshore Indus Basin (Pakistan) were unknown. Under the premise, this chapter documents the age of the carbonate successions and investigates the architectural evolution and drowning history of one of the carbonate platforms. The subsurface geometries of the isolated carbonate platform are well imaged on the seismic data, further offering the opportunity to catalogue their seismic facies and depositional changes. In the light of seismic stratigraphic concepts and facies analysis, the study emphasizes the internal reflection geometries to trace the development phases. Biostratigraphic analysis of the larger benthic foraminifera and planktonic foraminifera assemblages permit constraining the ages of the main evolutionary steps including onset, episode of emersion and drowning of the carbonate platform, and assist in distinguishing the different depositional environments. Further, the results describe the growth history of the Paleocene-Eocene carbonate platform in the context of regional tectonics, sea level, and climate changes.

3.2 Geological background

The south-southwest trending basin developed as a result of repeated phases of rifting in Cretaceous. During the Paleogene Period, the Indian Plate drifted from the southern hemisphere to the northern hemisphere and collided with the Eurasian Plate (Chatterjee et al., 2013). Today, the northwestern margin (Pakistan & India) of the Indian Ocean contains several tropical carbonate platforms of the Paleocene and Eocene epochs (Carmichael et al., 2009; Clift et al., 2008). The sedimentary package overlies the Late Cretaceous to Early Paleocene igneous complexes of the Deccan volcanics and has a conformable contact with the overlying thin sequence of deep marine shales. In deep-water, the time equivalent succession appears as a condensed section and may be composed of pelagic deposits. These carbonate successions recorded diverse changes of the paleo-oceanographic setting of the Paleo-Tethys Ocean under conditions of a changing position and anticlockwise movement of the Indian Plate (Copley et al., 2010) as well as changes in climate and sea level. The seismic data from this area provides a unique opportunity to unravel the Paleogene depositional record and the growth history of the carbonate platform through an integrated approach linking core, seismic and well log data.

3.3 Data and methods

This study is based on the analysis of industrial 2D seismic data that was acquired and processed in 2002 for hydrocarbon exploration. The 160-fold seismic survey was recorded with SEG reverse polarity, where the increase in acoustic impedance is reflected as negative amplitude. Standard processing yielded data length ranges between 8 to 10 s with a 4 ms sampling interval. With a grid interval of approximately 5 km in each direction, the regional dataset covers an area between the continental shelf and the deep basin. Most of the seismic lines concentrated over the buried isolated carbonate platform of the Paleocene to Eocene succession (Fig. 3.1).

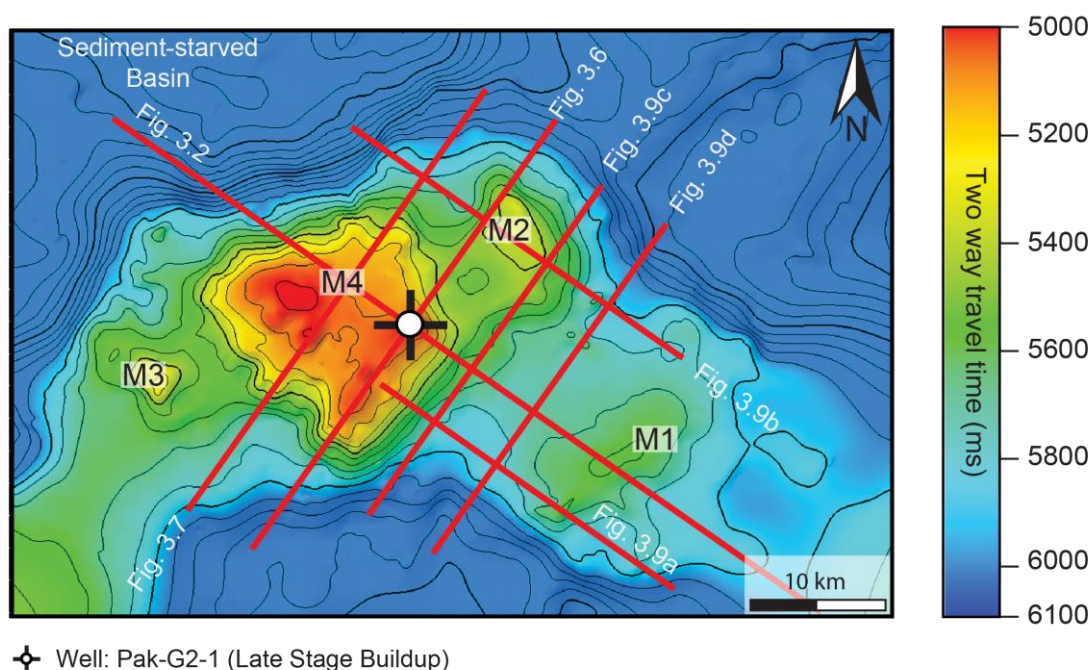


Figure 3.1: Time structure map (two way travel time) of the top surface of the carbonate platform with the position of seismic transects presented in this study. M1, M2, M3, and M4 are four carbonate buildups identified. Contour line interval is 100 ms.

The seismic interpretation was conducted using Petrel software. Key reflections were identified and mapped on seismic data based on reflections discontinuity criteria. Further, data from three exploration wells (Pakcan-1, Indus Marine-A1, and Pak-G2-1) were incorporated to support the seismic interpretation. The time-depth relationship was established using VSP and check shot dataset. The well Pak-G2-1 was drilled in 2004 to test the hydrocarbon potential of the Paleocene-Eocene carbonate succession. It penetrated approximately 2050 m thick Early Eocene to Pleistocene sedimentary sequence (Fig. 3.2). The stratigraphy from the Well Pak-G2-1 was extrapolated to the seismic dataset that provided a chronostratigraphic framework for the carbonate and the younger sedimentary succession (Fig. 3.2). The well data consists of a standard wireline log suite comprising gamma ray (GR), sonic (DT), density, and neutron porosity. Furthermore, the biostratigraphic analysis of the drill cuttings brought additional dating constraints and depositional environment interpretation of the carbonate sequence.

The seismic stratigraphic framework was established using standard seismic stratigraphic interpretation techniques (Mitchum et al., 1977; Fontaine et al., 1987; Embry, 1993). Depositional sequences in carbonate buildups are defined by unconformities and their correlative conformities as sequence boundaries. These sequence boundaries are based on reflection terminations (onlap, downlap, and truncation), erosional surfaces, truncations, and downlap events (Mitchum et al., 1977). The detailed mapping for the understanding of stratigraphic succession was achieved using advanced seismic interpretation techniques such as Horizon cube method by dGB OpendTect software (de Groot et al., 2010; Qayyum et al., 2012). This approach is used to produce densely mapped seismic sections and allow defining the HorizonCube density attribute, which helps to determine the intervals of reflection convergence (dense) and divergence (less dense). The convergence areas are mostly related to unconformities, condensed sections, reef tops, and flooding surfaces.

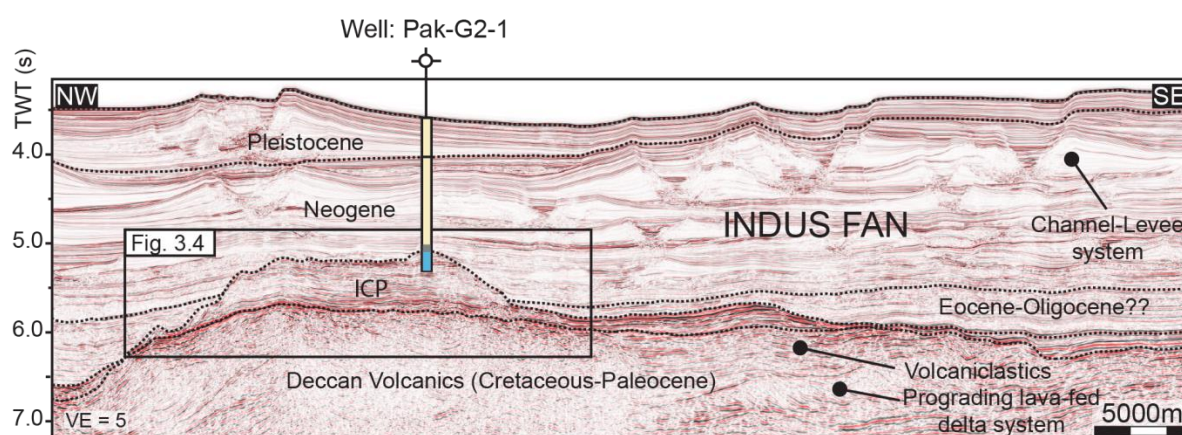


Figure 3.2: Interpreted NW-SE oriented regional seismic profile showing the stratigraphic framework of the Paleocene-Eocene isolated carbonate platform (ICP = Paleocene-Eocene isolated carbonate platform). (For location, see map in Fig. 3.1).

3.4 Results and interpretation

3.4.1 Seismic facies

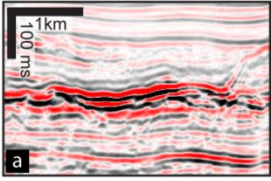
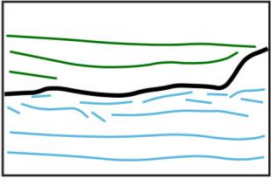
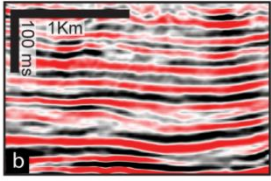
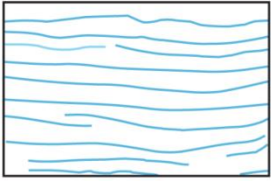
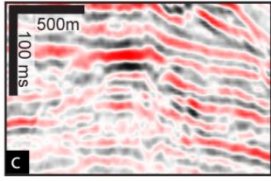
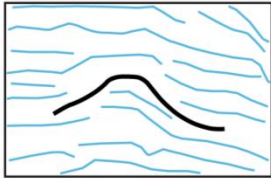
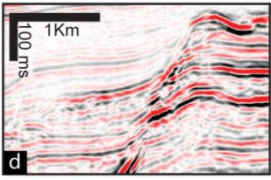
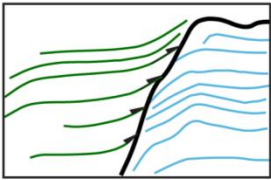
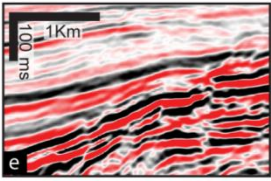
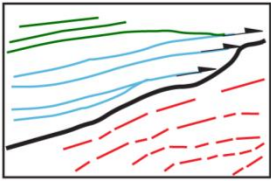
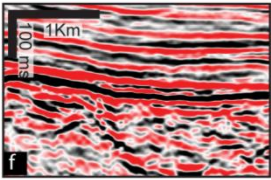
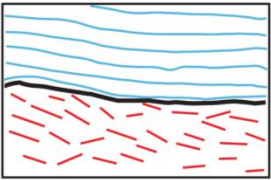
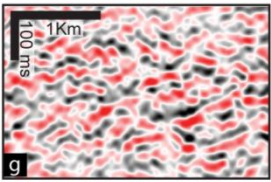
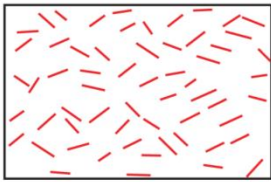
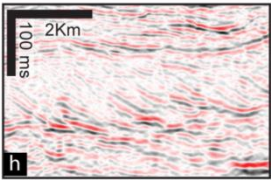
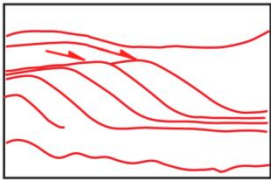
Eight types of seismic facies are described from seismic profiles, differentiated by their internal reflection configuration and external geometry (Fig. 3.3). The isolated carbonate platform is seismically characterized by medium- to high-amplitude reflections as compared to the younger siliciclastic deposits of the Indus Fan. The irregular top surface of the platform appears as a high-amplitude reflection, covering irregular and semi-continuous reflections with several parabolic shapes (Fig. 3.3a). This pattern is most likely produced by intensive karstification, possibly with formation of caves at the platform top before its final demise. Some patch reefs that in the data are imaged as pinnacle shaped bodies (Fig. 3.3a) may overlie this irregular surface. The inner platform facies are characterized by medium- to high-amplitude reflections with strong continuity and parallel relationship (Fig. 3.3b). This variance in reflection amplitude is interpreted as the alternating succession of a lagoonal to the shallow marine environment. Reflections of these facies often have low-angle dips thus forming localized packages with internal shingling. Often inner platform facies are laterally interrupted by the convex-upward or bidirectional mound facies, having a high impedance

contrast at the top (Fig. 3.3c), which is interpreted as an indication of the possible presence of reefs and mounds. The juxtaposition of the inner platform facies with the mound facies is proposed to represent the contact of inner platform deposits with reef and reef debris.

The slopes of the carbonate platform appear as sharp boundaries with the surrounding strata arranged in an onlap configuration (Fig. 3.3d). High- to medium-amplitude basinal and hemiplegics seismic facies are present basin-ward of the carbonate platform slopes and the toe of the slopes (Fig. 3.3e). The boundary between the carbonate and volcanic basement is sharp because of high acoustic impedance contrast between carbonate and volcanic rocks (Fig. 3.3f). The volcanic basement contains reflection-free seismic facies and chaotic reflections with low amplitude (Fig. 3.3g). At places, sigmoidal shaped reflections with high acoustic impedance contrast are imaged on the seismic data, which represent lava-fed delta systems comparable to those described by Jerram et al. (2009) in Faroe-Shetland Basin (Fig. 3.3h).

Table 3.1: Description of the seismic units.

Seismic units	Top surface	Identification Criteria	Maximum thickness (TWT) Amplitude	Intraplatform facies
S7	DU	Seismic; Drill cutting and log character	T= 80 ms Medium amplitude, continuous reflections	Aggrading late-stage buildup
S6	SB6	Seismic and log character, and drill cuttings	T= 60 ms Medium to high amplitude Discontinuous to chaotic	Chaotic and discontinuous reflections
S5	SB5	Seismic and log character drill cuttings	T=120 ms Medium amplitude Continuous to semi-continuous	Progradation, thickness decreases towards the northwest.
S4	SB4	Seismic character	T=100 ms Low amplitude and semi-continuous	Mostly progradation and onlapping on the base surface
S3b	SB3	Seismic character	T=100 ms High amplitude, parallel to sub-parallel and continuous	Aggrading facies minor progradation towards the north-northwest
S3a	SB3a (?)	Seismic character	T=100 ms High amplitude, parallel to sub-parallel and continuous	Aggrading and progradational facies south to southeast
S2	SB2	Seismic character	T= 200 ms High to low amplitude, continuous to discontinuous	Aggrading basal part with localized progradation towards the south to southeast
S1	SB1	Seismic character, interval velocity	T=220 ms High amplitude discontinuous reflections	Aggrading, backstepping, and progradation
Deccan Volcanic	Top volcanics	Seismic character, Interval velocity	Seismic dipping reflection (Inner and outer SDRs)	Reflection-free, sometime with prograding and high amplitude facies

	Seismic Expression	Seismic Reflection Geometries	Depositional Environment
Carbonate Facies			Karst facies with high amplitude, broken reflections topped by a drowning surface. Carbonates are overlain by siliciclastics.
			Inner platform facies with high amplitude reflections. Often these reflections are inclined with a dip of less than 1°.
			Mound facies which appears as isolated bodies within the platform and/or at the platform margins.
			Platform margin facies with onlapping basinal siliciclastics.
			Hemipelagic and pelagics off-platform deposits onlapping the volcanic basement.
			Inner platform facies with high amplitude reflections overlying a strong reflection making the top of the volcanic basement.
Volcanic Facies			Basalt facies with chaotic and attenuated reflections.
			Lava delta facies with prograding clinoforms.

Legend:

— Basalts — Carbonates — Siliciclastics

Figure 3.3: Catalogue of seismic facies recognized in the high-resolution seismic dataset.

3.4.2 Seismic stratigraphy

Detailed analysis of seismic reflection configuration identified seven seismic stratigraphic units within the studied isolated carbonate platform based on stratal terminations, seismic reflection geometries, and stratal stacking patterns, bounded by key sequence stratigraphic surfaces (Figs. 3.4-3.7; Tab. 3.1). The seismic survey is time migrated, and depth control is inadequate. Thus, the vertical scale and time structure maps are in two-way travel time or TWT (Fig. 3.8). The stratigraphic framework is summarized in Table 3.1, with each unit described below. The location of the seismic lines used for the stratigraphic subdivision is displayed in Fig. 3.1 in a time structure map.

3.4.2.1 Deccan volcanics

The Deccan volcanics form a chain of seamounts and guyots, dominated by basaltic flows with interlayered sedimentary packages (Carmichael et al., 2009). A strong seismic peak with positive amplitude, which marks a pronounced regional sub-aerial unconformity at the Cretaceous-Paleogene boundary (K-Pg), defines the top of the volcanics. Often the unit contains sigmoidal reflection bundles of the prograding lava basalt (Figs. 3.2 and 3.3h). Apart from these features, this unit mostly includes the basalt facies with chaotic and attenuated reflections (Figs. 3.2 and 3.3g). The thickness and nature of the volcanic unit are highly variable. Laterally, age equivalent rocks attributed to the Khadro Formation of the Ranikot Group were encountered in wells in the onshore areas of the Greater Indus Basin (Ahmad and Ahmad, 2005). This unit has not been drilled until today in the studied area. However, its tentative age assignment is as old as Late Cretaceous to Early Paleocene (Calvès et al., 2008; Torsvik et al., 2013).

3.4.2.2 Seismic unit S1

Seismic unit S1 is the oldest sequence developed above Deccan volcanics with an onlapping reflection pattern and early transgressive mounds. Internally, high amplitudes and sub-continuous reflections, with frequent mound facies in the basal part (Figs. 3.4 and 3.6), dominate this unit. Toward the southeast, the seismic frequency decreases in areas where the confined package consists of mixed chaotic reflections (Fig. 3.5a). This configuration indicates a complex assemblage of lithofacies that may range from volcanoclastic to shallow marine carbonates. Following the early transgressive event, a local prograding complex is observed, reflecting a normal regression (Figs. 3.4 and 3.5a). From the top, this unit is bounded by sequence boundary SB1.

In the map view, four distinct buildup areas are identified as M1, M2, M3, and M4 (Figs. 3.1 and 3.8a). On the isochron map, the thickest interval is located in the eastern part of the volcanic ridge at the M1 buildup, which is considerably deeper and is the oldest succession of the carbonate platform (Fig. 3.8: S1). Thinning and onlapping of the unit toward the west suggest that the regions of M2, M3, and M4 were topographically higher during the deposition of the seismic unit S1. The maximum thickness represented by this unit is about 220 ms (TWT) on isochron map with an aerial extension of approximately 1700 km².

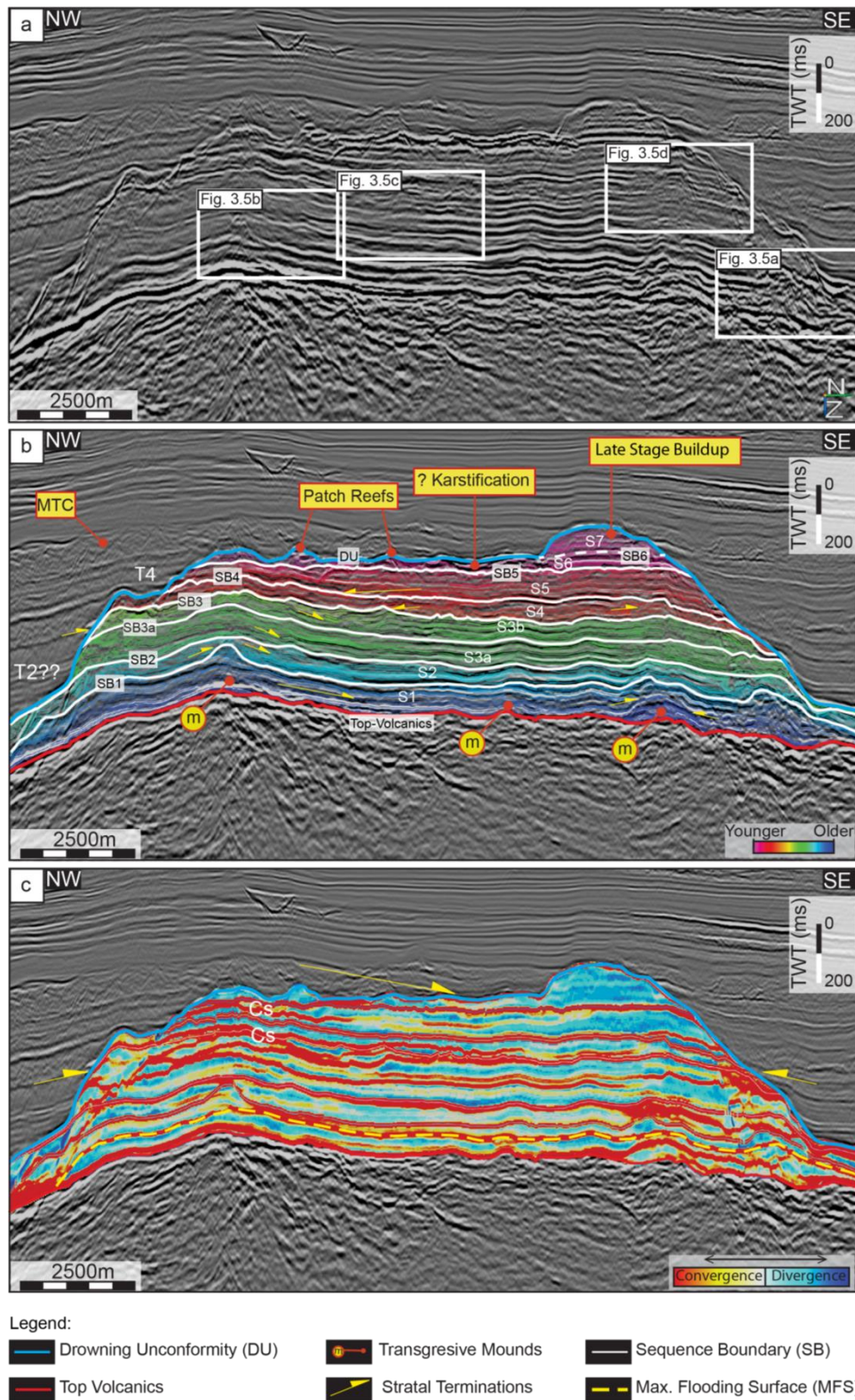


Figure 3.4: Seismic profile crossing the carbonate platform in an NW-SE direction. (a) Uninterpreted view. (b) Interpreted section of the M4 carbonate buildup with all seismic characteristics and seismic reflection configurations. MTC – Mass transport complex; m: mound facies; SB: sequence boundary. (c) Interpreted section of M4 carbonate buildup with horizon cube attribute and showing the region of convergence and divergence seismic of reflections patterns; Cs: condensed section.

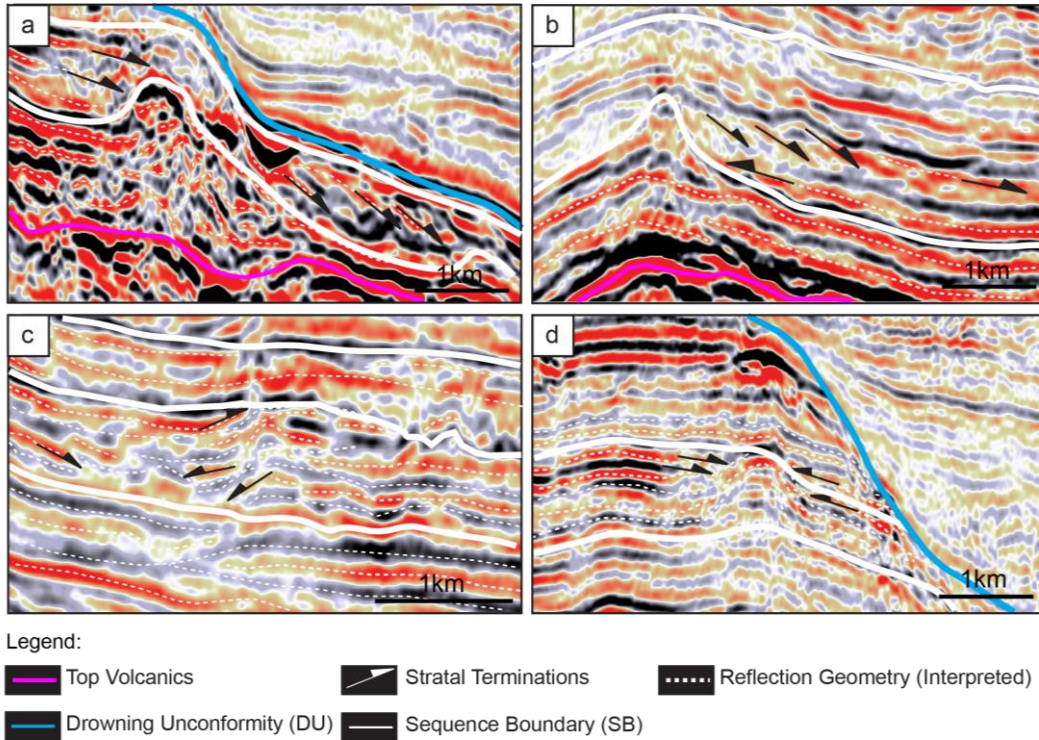


Figure 3.5: Seismic characteristics of the M4 buildup: (a) a confined chaotic reflection pattern, (b) shingling reflections against the basal transgressive system, (c) development of mound and shift in the depositional unit, (d) mound facies in the margin.

3.4.2.3 Seismic unit S2

Seismic unit S2 is characterized by a distinct reduction of the platform surface area and retreated margins (T1; Figs. 3.6 and 3.7). It is a relatively thin unit with mostly medium- to low-amplitude reflections. In the lower part of the S2, some high amplitude, and continuous seismic reflections are observed (Fig. 3.4). These reflections sometimes onlap the top surface of S1 (SB1), forming a thinly defined basal transgressive package. The overall growth of this unit shows an aggrading stacking pattern. Often, subtle localized clinofolds are observed dipping towards the southeast and downlap onto the basal transgressive unit (Fig. 3.5b). Numerous small mounds and pinnacles are observed within this unit (Figs. 3.9). The top of this unit is identified by a high-amplitude surface with an irregular relief, defined as horizon SB2 (Figs. 3.4, 3.6 and 3.7).

Overall, this unit is thin in the middle part of the carbonate platform, across the buildup M4. It is thicker along the northeastern and southwestern margins of the platform, identified as buildups M2 and M3, respectively (Fig. 3.8). During the formation of this unit, M1 build-up area is consistently the thinnest, with small patches and mound facies. The total surface area covered by this unit is ultimately limited to about 1315 km², with a maximum thickness of less than 200 ms.

3.4.2.4 Seismic unit S3

Seismic unit S3 conformably overlies the unit S2. The facies in the lower part are analogous to the seismic unit S2, whereas the upper part shows high amplitude, sub-parallel, continuous seismic reflection patterns with subtle clinofolds toward the central platform, forming a condensed section to the west (Figs. 3.4c and 3.5c). Often, some onlaps and in-fills are partially truncated at the top of this unit (Fig. 3.5c). Several mound facies with chaotic reflection and terminations are observed (Fig. 3.6b). The platform margin facing the open ocean retreated and developed a terrace that was around 850 m in width (T2), whereas the eastward margin exhibits a continuous aggrading stacking pattern (Figs. 3.6 and 3.7). The top of this unit is delimited by SB3, which is imaged as a high amplitude continuous surface.

An isochron map of this unit reveals a remarkable upward growth with a maximum relief of around 200 ms (TWT) and steepening of the platform margins by more than 15°. The thickest interval lies in the center of the platform, at the location of buildup M4 (Fig. 3.8b: S3). A distinct succession characterized by strong reflections with hummocky to chaotic pattern piles up as off-platform deposits between these buildups.

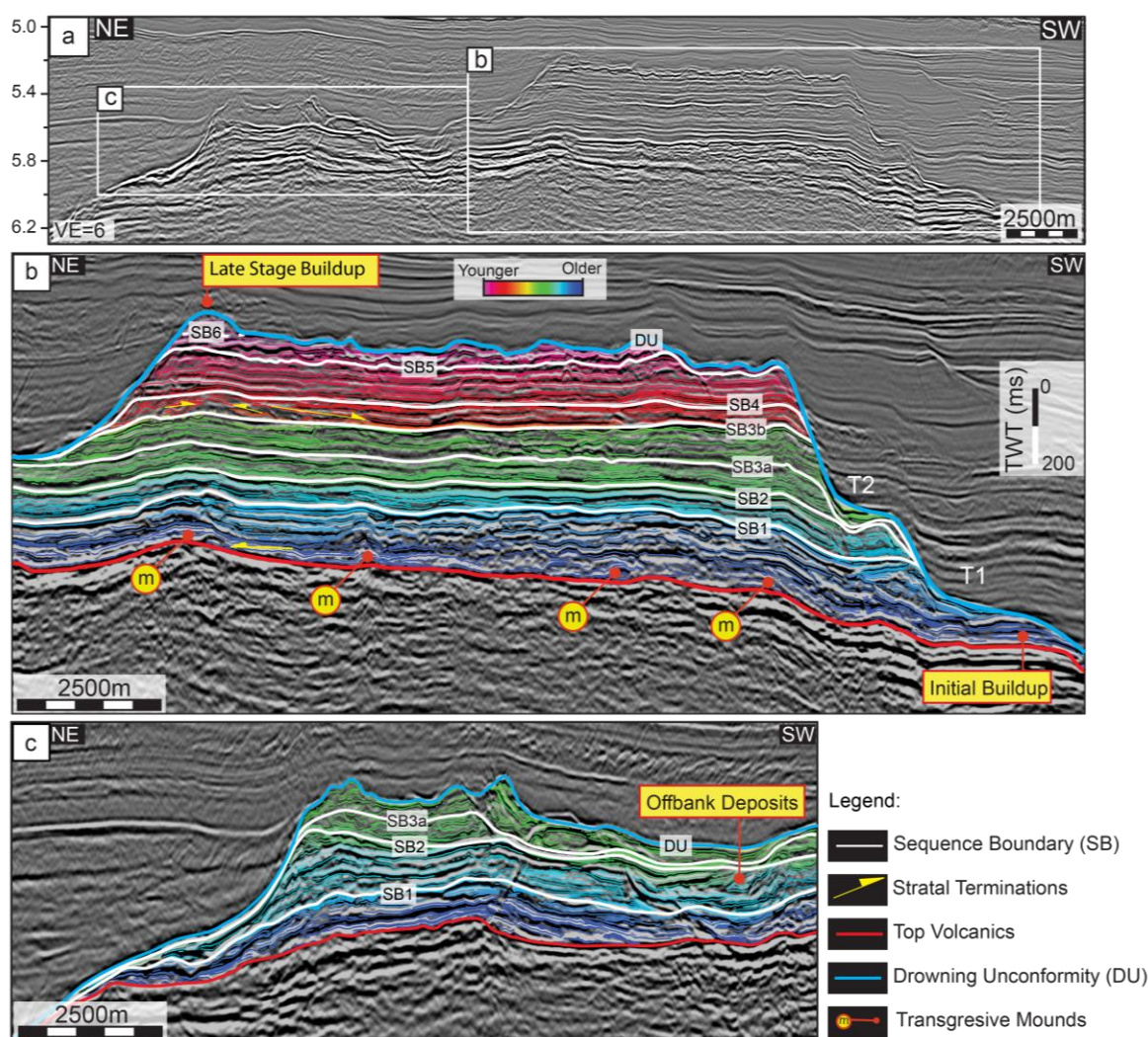


Figure 3.6: (a) NE-SW trending seismic profile across the carbonate platform (b) and (c) are interpreted seismic sections of the M4 and M2 buildups respectively. (See map in Fig. 3.1 for location).

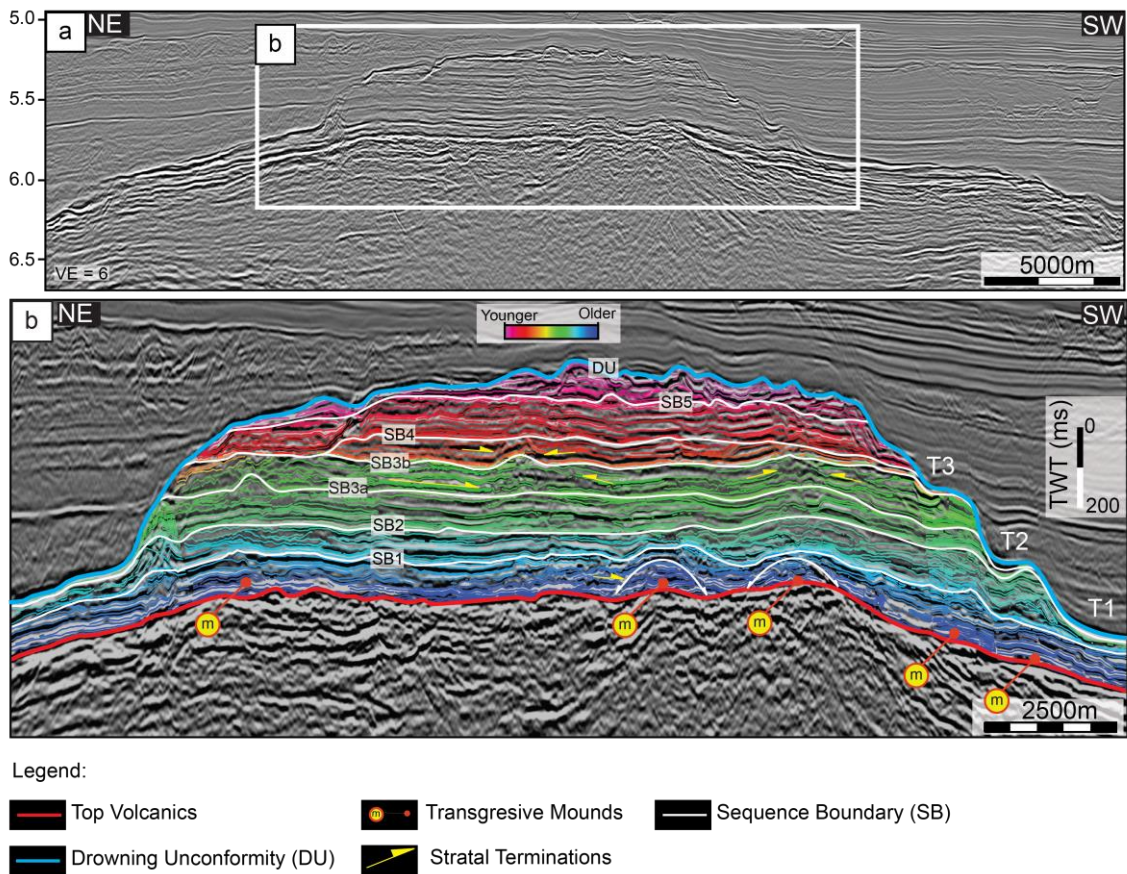


Figure 3.7: (a) NE-SW trending seismic profile across the central part of the platform. (b) Interpreted section of M4 buildup. (See map in Fig. 3.1 for location).

3.4.2.5 Seismic unit S4

S4 is mainly characterized by medium amplitude, wavy, and semi-continuous seismic reflections with minor lateral facies changes. The lower part of the unit onlaps onto SB3, forming a wedge-to-sheet-like body which thins out toward the northwest (Figs. 3.4b and 3.4c). Within this unit, two bodies with convex upward reflections and bidirectional downlaps are interpreted as the mound seismic facies, which are separated from each other by the inner platform facies (Figs. 3.5d, 3.6 and 3.7). These mounds measure around 70 ms (TWT) in height and 550–650 m in width (Figs. 3.5d, 3.6 and 3.7). Unit S4 is bounded at the top by the sequence boundary SB4.

In contrast to the seismic unit S3, this unit marks a significant change in a deposition. In this unit, the main thickness lies at the south-eastern margin of the buildup M4. The unit thins toward the northwest with mound facies on the top. The average thickness of this unit is less than 100 ms (TWT) with a maximum surface area of about 350 km² (Fig. 3.8b: S4).

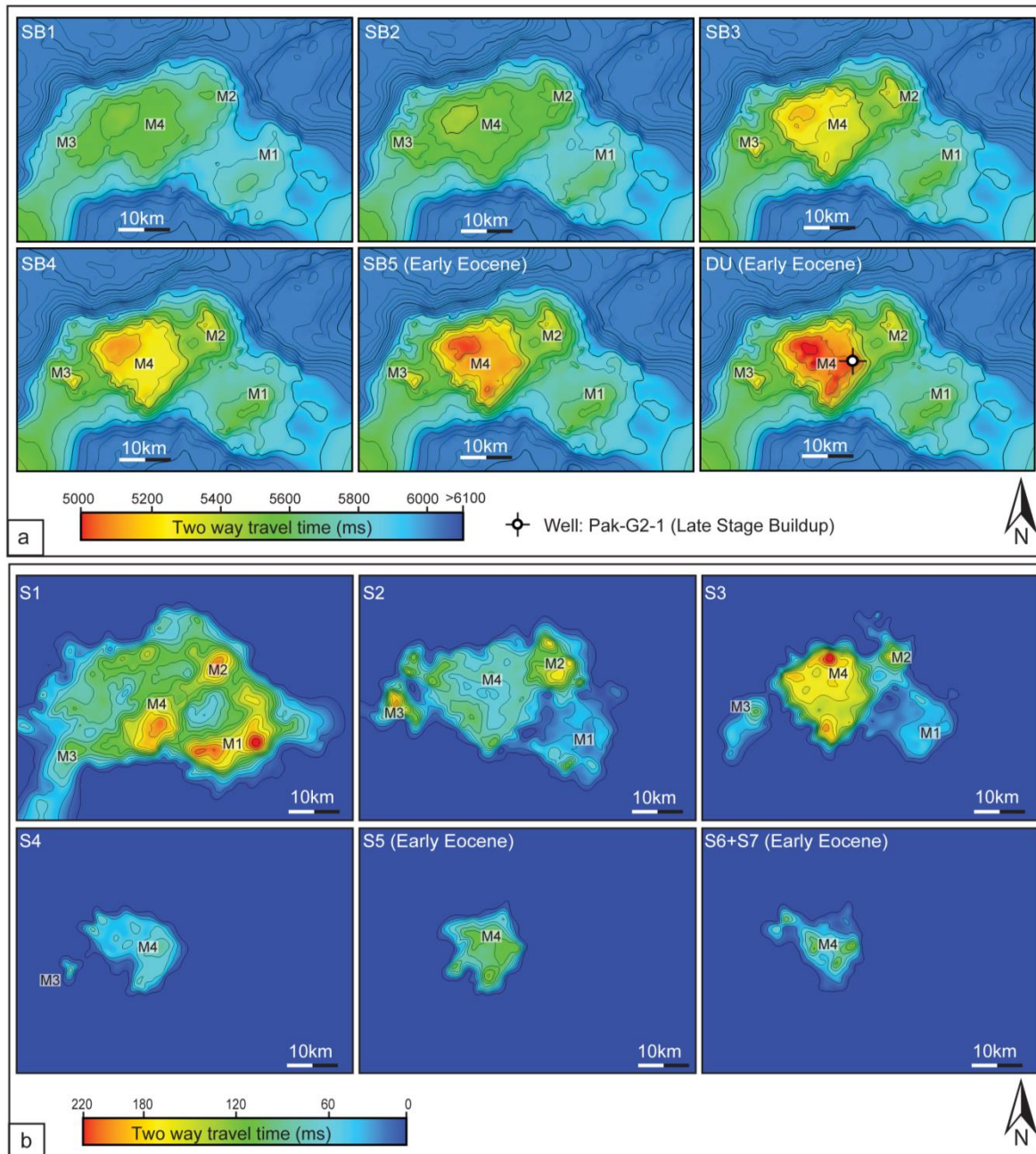


Figure 3.8: (a) Time structure maps of the interpreted stratigraphic surface (SB1-DU) described in the chapter. M1, M2, M3, and M4 are four carbonate buildups identified in the isolated carbonate platform. The well Pak-G2-1 is located on the late stage buildup. Contour lines are every 100 ms (thin black lines) and 500 ms (thick black lines). (b) Isochron maps which represent the two way travel time thickness maps calculated by the thickness difference between the top and the bottom bounding surface of each seismic stratigraphic unit. The area with zero thickness is depicted as a blue color.

3.4.2.6 Seismic unit S5

With seismic characteristics similar to those of S4, seismic unit S5 is a wedge-shaped unit becoming thinner toward the north-western margin of the platform, passing from about 120 ms to about 40 ms (TWT) (Figs. 3.4, and 3.8b). Its basal part onlaps over the inclined surface of SB4 since the unit is thinner toward the northwest margin. In contrast, this unit shows an average thickness of approximately 120 ms on the seismic profiles-oriented northeast to

southwest (Figs. 3.6b and 3.7b). Reflection amplitude is moderate, and reflection continuity is low to high, with decreasing frequency toward the northwestern margin. At the eastern margin, the internal reflections are conformably overlying SB4. Internally, this unit displays mostly sigmoidal clinoforms prograding to the west. At the western margin, there is a terrace of around 1000 m in width (T4: Fig. 3.4b). The top surface of unit S5, identified as SB5, is a relatively flat surface.

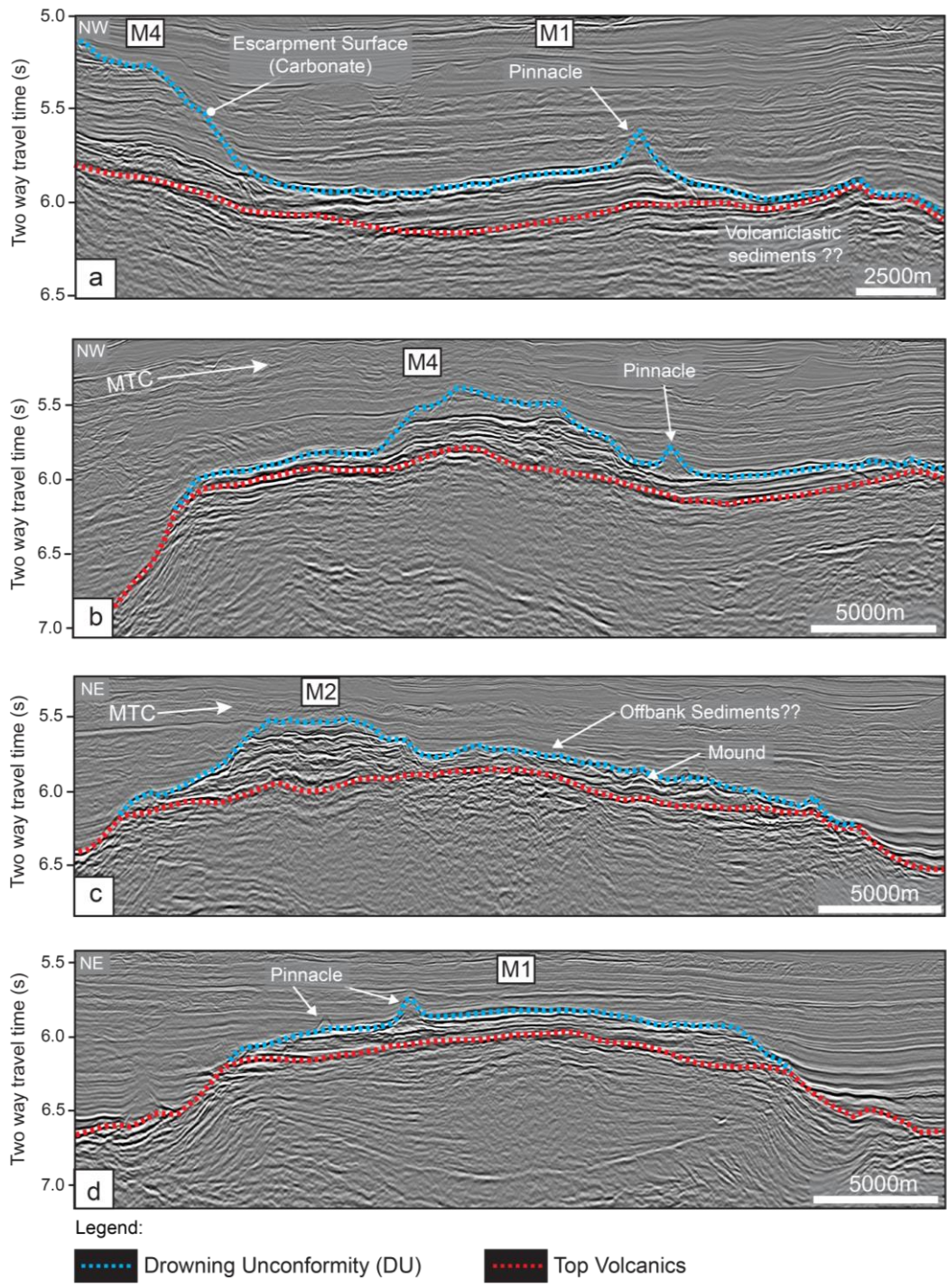


Figure 3.9: Seismic characteristics of the isolated carbonate platform. MTC: Mass transport complex (See figure 3.1 for seismic line positions).

3.4.2.7 Seismic unit S6

Seismic unit S6 is mainly characterized by medium- to high-amplitude and discontinuous seismic reflections. High-amplitude continuous and parallel seismic facies are confined to the east margin of the carbonate buildup (Figs. 3.4 and 3.6). This unit is bounded on the top by a high-amplitude uneven surface, picked as a regional unconformity across the platform with mounds and troughs (Fig. 3.4b). However, this surface becomes continuous and smooth toward the eastern margin of the buildup, where it marks the onset of the late stage buildup as seismic unit S7.

On isochron maps, seismic unit S6 is restricted to a surface area of approximately 260 km². The maximum thickness is about 60 ms on average, which separated the buildup M4, from the late stage buildup.

3.4.2.8 Seismic unit S7

Seismic unit S7 is the youngest unit of the carbonate platform and consists of a convex upward late stage buildup (Figs. 3.4 and 3.6). This unit is located and restricted to the southeastern side of the underlying M4 buildup and consists mostly of medium- to low-amplitude with semi-continuous to parallel seismic reflections. The internal geometries of the late-stage buildup, with a mostly aggrading growth pattern, are coupled with retrograde margins (Fig. 3.4). At the top, this unit is bounded by a strong-peak surface, interpreted as drowning unconformity, which marks the cessation of carbonate platform growth in the analyzed dataset. This unit covers an area of less than 8 km², the maximum thickness of which is approximately 80 ms as mapped on the seismic profile (Fig. 3.4).

3.5 Calibration with biostratigraphy

Cutting samples from the well Pak-G2-1 were investigated for the facies and the microfaunas of the carbonate platform (Fig. 3.10). The well penetrated ± 320 m of shallow water carbonates, encompassing seismostratigraphic units S5, S6, and S7 (Fig. 3.11). Larger benthic and small benthic foraminifera, planktonic foraminifera, gastropods, and brachiopods with some siliciclastic rock fragments dominate biogenic components. Further detailed investigation of the samples coupled with well logs and seismic interpretation leads to the following results.

Samples from 4750 m to 4630 mMD (meters—measuring depths) depth correspond to the upper part of the seismic unit S5 that predominantly consists of creamy-white fossiliferous limestone with abundant benthic foraminifera and some other bioclasts. The abundance of larger benthic foraminifera, which are represented by *Lokhartia* (Figs. 3.10a and 3.10b), *Alveolina* (Figs. 3.10c and 3.10d), *Nummulites* (Figs. 3.10e, 3.10f and 3.10k), *Operculina*, and *Orbitolites* in absence of planktonic specimens is taken as an indication of shallow, open marine to inner neritic environment. In conjunction with the cuttings samples, the wireline log characters show a rather clean carbonate succession. The GR-log display low amplitude response of less than 45 API (Fig. 3.11), indicating a lack of any argillaceous materials with minor heterogeneity (Lucia, 2007). The estimated average porosity ranges between 20% and

30%, with a bulk density of about 2.3 g/cm³. The upper bounding surface ‘SB5’ coincides with relatively high GR-log values (greater than 50 API). However, there is a slight mismatch between the wireline log and seismic data, attributed to the poor depth control (± 5 m).

On the depth scale, seismic unit ‘S6’ ranges between 4630 and 4530 m. It is mainly composed of wackestone to packstone and is rich in benthic foraminifera such as *Nummulites* (Figs. 3.10e and 3.10f) (*N. atacicus*, *N. globulus*) *Alveolina* sp. (Figs. 3.10h), *Assilina* sp., and miliolids (Fig. 3.10i). In the well log suite, the GR facies shows serrated low- to medium-amplitude values of around 45 API to 39 API in the basal part of the unit. Uphole, the log shows an increase in the values to up to 65 API, and then a decrease again to 51 API at the SB6. The DT and density logs also show similar features, varying between 60 and 100 μ s/ft. and 2.0 to 2.3 g/cm³ respectively. Similarly, the average porosity is 20–25%, but values vary highly between 10% and 30% (Fig. 3.11). The variations observed in the log suite correlate to the high amplitude reflection and chaotic seismic facies. These features are interpreted to represent a secondary porosity developed due to the dissolution and leaching of the formation during subaerial exposure and karstification (Fig. 3.11). Therefore, it is proposed that the top surface of the unit is a subaerial unconformity.

Seismic unit S7 corresponds to the late stage buildup, which was penetrated between 4530 m and 4433 mMD. Below 4505 mMD, this unit is dominated by bioclastic packstone to grainstone. The succession contains fragments of litho- and bioclasts with the large benthic foraminifera *Glomalveolina lepidula*, *Alveolina* sp., *Orbitolites* sp., and *Nummulites* sp. together with some small miliolids. Overall, in this unit, fossil shells are often recrystallized, and therefore, the preservation of fossils is poorer as compared to the older units. This deterioration in preservation points towards post-depositional fluid migration and dissolution. Planktonic foraminifera replaces this assemblage in the upper part of this unit. At a depth of 4450 mMD, a mixture of deep marine sediments with shallow marine carbonate is noticed. The ratio of gray shale to carbonate sediments increases toward the top of the platform implying a deepening of the environment. This is confirmed by a fining upward sequence in the GR log (Fig. 3.11). The average density of the formation is about 2.3 g/cm³. Just 2 meter below the top of the drowning unconformity—at a depth of 4335 mMD—the collected samples are rich in planktonic foraminifera and benthic species are entirely absent. The age diagnostic planktonic species identified are *Catapsydrax* sp. and *Globigerinatheka* sp. (Berggren, 2005; Wade et al., 2011). On the GR and DT, a gradual increase in the basal part of the unit is noticed (Fig. 3.11). This pattern is followed by the serrated values, which again decrease toward the interpreted drowning unconformity (DU), recognized at 4433 mMD (Fig. 3.11) on the digital well logs motifs. In the GR and DT logs, a sudden low- to the high-amplitude pattern is observed along the shale/carbonate boundary. The GR log jumped from 50 API below to around 130 API above. The same trend appears in DT and density logs, which seem to have increasing values. At 4320 mMD depth (at 13 m above the DU), the assemblage is rich in age-diagnostic planktonic fossils with predominantly pelagic mudstone or marine shales. Some lithoclasts are also present in this unit.

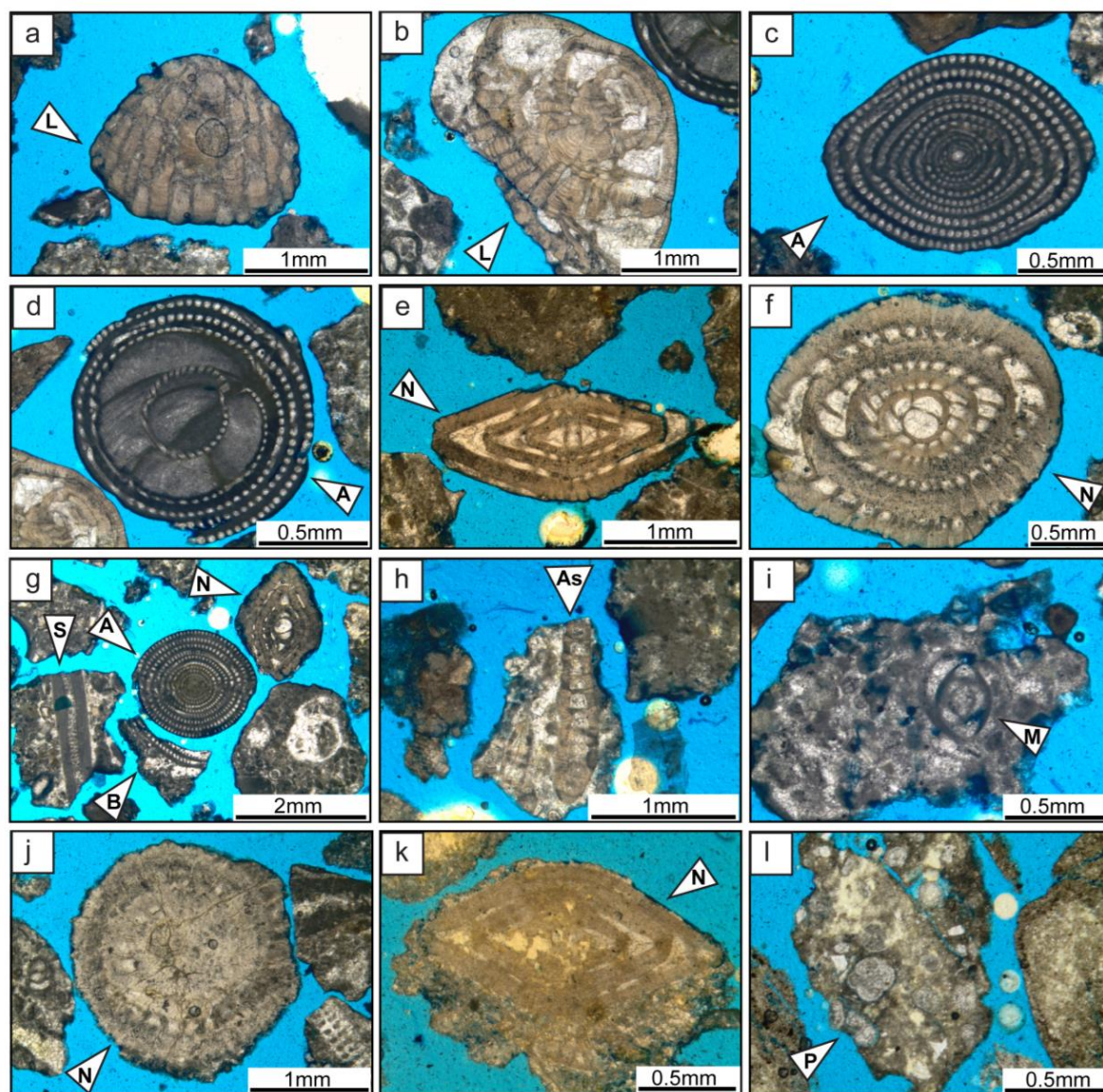


Figure 3.10: Biostratigraphically significant larger benthic foraminifera from Late Paleocene to Early Eocene. a & b. *Lokhartia* sp., (L) c. *Alveolina* sp., (A) (axial section), d. *Alveolina* sp., (A), (equatorial section) e. *Nummulites* sp., (N) (axial section) f. *Nummulites* sp., (N) (equatorial section). g. Bioclasts (B) and some other Eocene larger benthic foraminifera (*Somalina* sp., S) h. a broken piece of *Assilina* sp., (As), i. Milliolid foraminifera, (M), in lithoclast j & k. *Nummulites* sp., with poor preservation. l. A lithoclast with abundant planktonic foraminifera (P).

3.6 Discussion

3.6.1 Paleocology and biostratigraphy

The large benthic foraminiferal assemblages indicate that the carbonate succession accumulated in a tropical environmental setting under oligotrophic conditions (Hallock and Glenn, 1986; Jorry et al., 2006). The large benthic foraminifera together with the planktonic foraminifera allow an age assignment of the carbonate platform. For the age model, the work of (Serra-Kiel et al., 1998) on larger benthic foraminifera biozones was applied together with the documented stratigraphic distribution of these fossils in the Greater Indus Basin by Afzal et al. (2009, 2011).

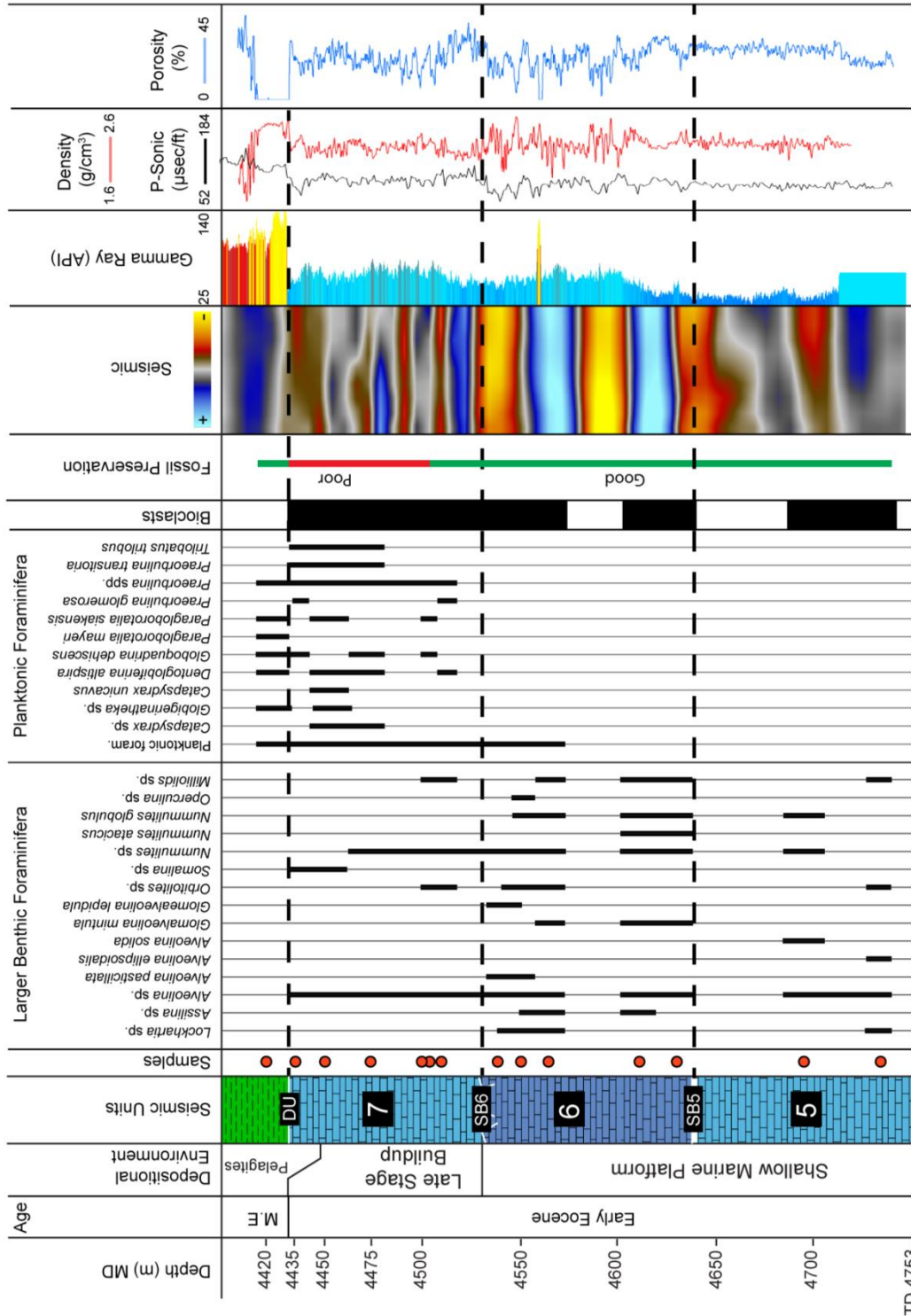


Figure 3.11: Stratigraphic ranges of some important foraminiferal species in the studied section of well Pak-G2-1 and their corresponding seismostratigraphic units on depth converted seismic. The gamma ray curve increasing from left to right. The black and red well curves are compressional sonic and density logs respectively.

The earliest appearance of *Lokhartia* sp. is documented as SBZ3 (Serra-Kiel et al., 1998) which extends into the Early Eocene age in the region of the eastern Tethys (Akhter and Butt, 1999; Afzal et al., 2009, 2011). The first appearance of *Alveolina* sp. marks the biozone SBZ5/6 at the base of the Eocene (Hottinger, 1971; Serra-Kiel et al., 1998). However, the analyzed samples were void of common large benthic foraminifera of SBZ3 and SBZ4 Zones in the Greater Indus Basin (Afzal et al., 2011), such as *Ranikothalia* and *Miscellanea*. Therefore, the presence of *Lokhartia* sp. and *Alveolina* sp. together suggests an earliest

Eocene age for the shallow marine carbonate platform (Fig. 3.11), equivalent to Zone SBZ5/6 by Serra-Kiel et al. (1998). Later, the first appearance of *Nummulites atacicus* and *Nummulites globulus* is attributed to the Zone SBZ8. These results are consistent with the biostratigraphic assemblage of other Tethyan carbonate platforms (Afzal et al., 2011). This foraminiferal assemblage indicates that this carbonate unit dates to an Early Eocene age.

The final drowning event of the carbonate platform is placed in the interval encompassing the Early Eocene to earliest-Middle Eocene (~49 to ~45 Ma) by considering the appearance of the age-diagnostic planktonic foraminifera *Catapsydrax* sp. and *Globigerinatheka* sp. as evidence (Berggren, 2005; Wade et al., 2011). Hence, the stratigraphic data of Calves et al. (2008) proposing the platform drowning age as 37 Ma, are evidently challenged.

3.6.2 Platform evolution

Regional seismic interpretation and the biostratigraphy indicate that the carbonate platform has evolved during the Paleocene to Early Eocene times. Seismic stacking patterns, platform architecture, and depositional facies allow the identification of three-platform evolution stages—platform initiation stage, development of aggrading and escarpment stage, and late stage buildup and drowning stage.

3.6.2.1 Platform initiation stage (S1-S2)

Investigation of seismic profiles and isochron maps depict an atoll-shaped flat-topped volcanic complex. The evidence of subaerial exposure of this volcanic complex is a debatable subject. Subsequent localized growth of carbonates on the volcanic complex is evident in the data presented herein. These carbonates formed small mounds and patches which are interpreted as the first recognizable flooding event of the volcanic complex (Fig. 3.12A). This initial stage of carbonate development is interpreted as a start-up to catch-up phase, which mostly forms the lower part of the seismic unit S1. This phase, with a backstepping of the mounds, seems to match with the global Early to Middle Paleocene sea level rise (Miller et al., 2011). During the further growth of this unit, carbonate production expanded and localized patches and mounds coalesced thus forming a low relief flat-topped platform with small mounds and four distinct buildups areas M1, M2, M3, and M4.

Following the seismic unit S1, the carbonate factory kept up with significant local growth. This episode is marked by the presence of subtle clinofolds away from the mound observed in the seismic unit S1 (Fig. 3.4b) and interpreted as a localized lowstand on the carbonate platform which was later overlapped by a transgressive event of the seismic unit S2. This growth phase culminated with the drowning of the M1 buildup, which restricted the growth of neritic carbonates to the western margin of the volcanic ridge (Fig. 3.8b: S1). Several small mounds and pinnacles are present in the central and peripheral areas above the sequence boundary SB1. At the end of this stage, the carbonate platform developed a low relief with an estimated height of almost approximately 450 m (velocity 4500 m/s) and slope angles of less than 10°.

3.6.2.2 Aggrading and escarpment stage (S3-S6)

With a subsequent relative sea level rise, the carbonate platform significantly aggraded until the mid of the seismic unit 3 (SB3a). During this time, the platform margin retreated inwards, which is taken as an indication of insufficient carbonate production to fill up the available accommodation space, giving way to a ‘give-up’ sequence. With the onset of the seismic unit 3b, a significant shift in the depositional trend is observed. The trend marks a subtle intraplatform prograding complex towards the NW and may, in fact, be the downlapping on the underlying aggradational geometries. Considering the seismic resolution as a limitation, interpreting this as an abrupt change in depositional trend could be misleading. However, the downlapping patterns mark another event, genetically different from the underlying carbonate factory. A few possible explanations for this shift may be:

- (1) A lag time and re-establishment of the carbonate factory may have occurred between the sub-units S3a and S3b. If this was the case, the underlying keep-up cycle must have terminated for a particular period before a new factory was established at another location. There is no clear seismic evidence of exposure between the sub-units S3a and S3b, but such a feature may lie below seismic resolution.
- (2) The development of local mounds was due to a significant increase in the carbonate growth potential under decreasing accommodation (see Fig. 3.5c). This would imply that the underlying keep-up cycle continues until the end of the seismic unit S3.
- (3) A transgressive event may have temporarily shut down the carbonate factory, due to a significant rise in sea level, but could not develop a seismic scale reflection. In this case, a drop in sea level at a later point of time re-established the carbonate factory, which was prograding toward the north and northwest.

In summary, the entire stage is characterized by large-scale aggrading margins until the end of seismic unit 3 (SB3b). Further, this unit is overlapped by a thin transgressive event of the seismic unit S4 overlain by normal regressive events of the seismic unit 5. This entire stage is interpreted as a localized keep-up cycle, with the subsequent drowning of buildups M2 and M3 (Fig. 3.12C). The margins of buildup M4 became starved and accumulated vertically to form an escarpment surface with a relief of approximately 1100 m (velocity 4500m/s), with progressively steepening slopes reaching angles between 15° and 20°. The buildup M4 growth continued until the next fall in sea level (SB6), which apparently marks a depositional hiatus and subaerial exposure on a seismic scale as high amplitude (Figs. 3.11 and 3.12D). This observation matches with more erratic log values and infers a possible karst development. However, the impact of this exposure is not observed in the limited record provided by the well cuttings. An alternative interpretation for the discontinuous and mounded facies could also infer the presence of patch reefs in the shallow lagoon, enclosed by reef rims similar to examples provided by numerous ancient and modern carbonate buildups. The topographic lows between these buildups received some of the platform-derived sediments characterized by strong amplitudes with hummocky reflections (Figs. 3.6 and 3.12).

3.6.2.3 Late stage buildup and final drowning stage (S7)

Following the exposure event which interrupted the formation of S6, the platform was inundated again by a rise in relative sea level thus re-establishing a neritic carbonate production. During this time, the increase in accommodation space restricted the carbonate factory to the eastern margin of the M4 buildup. In this scenario, the carbonate factory did not have an opportunity to re-occupy the full platform. It rather formed a distinctive mound, approximately 120 m thick and covering a surface of 8 km². This growth episode is herein referred to as late-stage buildup (Fig. 3.12E). Hemipelagics and pelagics covered the surrounding platform area at this time. The gradual change from shallow marine benthic foraminifera to deep marine planktonic species is recorded, which is indicative of the deepening paleoenvironment. From the biostratigraphic data, it appears that the shallow water carbonate factory completely drowned during the Early Eocene followed by the pelagic deposition, which persisted, from the Middle Eocene to the Middle Miocene (see Fig. 3.11). This hemipelagic to pelagic episode terminated with the advance of the southward prograding Miocene Indus Fan. The platform was therefore buried under a thick pile of Neogene to Recent siliciclastics turbidites and marine shales.

3.6.3 Factors controlling the carbonate platform growth and architecture

The Indus Basin is a classical area for the development of models for the facies, the stratigraphy and the paleoenvironmental evolution of Paleogene neritic carbonates (Akhter and Butt, 1999; Afzal et al., 2011). In this study, for the first time, an overview of the geometrical and sequence stratigraphic evolution of these depositional systems is introduced, along with an insight into global and regional factors controlling the buildups growth in the region.

3.6.3.1 Subsidence and sea level changes

In the line of previous studies (Agrawal and Rogers, 1992; Calvès et al., 2008; Mohan, 1985), the subsidence history of western Indian margin can be separated into a main thermal subsidence phase, linked with the Early Paleocene volcanism and coeval development of the passive margin, and a secondary phase of the flexuring induced subsidence by the loading of excessive Indus Fan sediments and accompanied by the Indian Plate reorganization (Mohan, 1985; Agrawal and Rogers, 1992; Whiting et al., 1994). The first phase of thermal subsidence further consists of slow subsidence during the Late Paleocene to Early Eocene and a rapid subsidence event occurred thereafter. The stratigraphic development of the carbonate platform in the Offshore Indus Basin was controlled by thermal subsidence. This continuous subsidence was responsible for creating the accommodation space for the growth of an approximately 1400 m thick shallow marine carbonate succession.

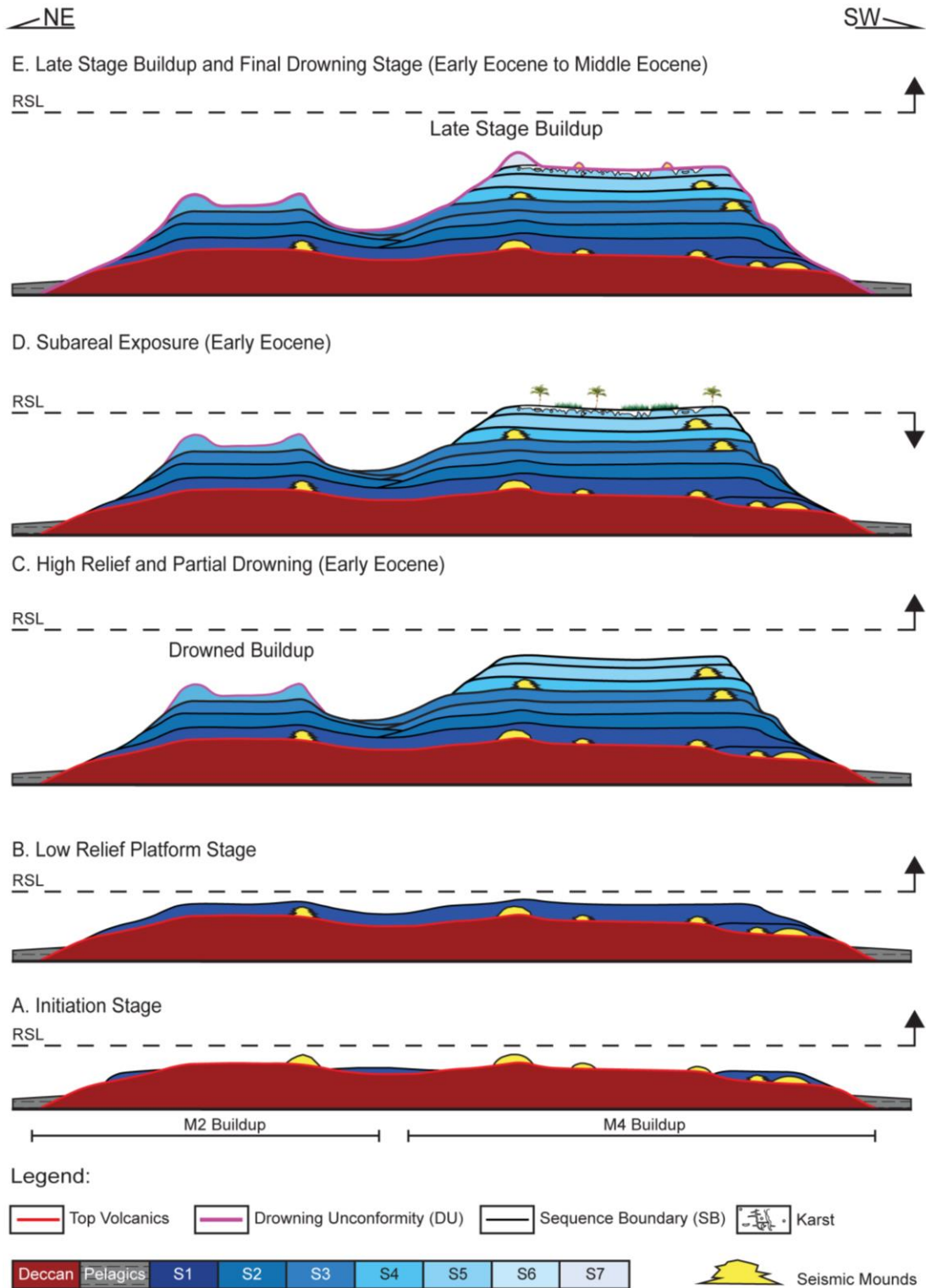


Figure 3.12: Schematic model of the studied isolated carbonate platform. (A) Initial establishment and start-up phase. Carbonate platform deposition first began as mounds and patches at the top of the submerged volcanic high with early transgression. (B) The development of low relief platform with low angle flat-top surface. (C) Carbonate platform retreated from the margins and catch-up with the relative sea level rise. M4 buildup accumulated vertically and M2 buildup subsequently drowned. (D) A fall in relative sea level was recorded, and erosional features were formed. (E) The quick rise in sea level caused the terminal drowning of carbonate platform with subsequent formation of late-stage buildup in Early Eocene. The deep-water settings prevailed and pelagic continuous to develop till the Middle Miocene when carbonate platform was covered by the terrigenous succession of the Indus Fan. RSL: Relative Sea Level

During this time, the carbonate platform continuously reduced its surface area between the seismic units S1 to S7, from 1650 to 260 km², without any interruption by a margin progradational phase. However, the contemporaneous intra-platform progradation and the subaerial exposure of the platform suggest that the main global eustatic changes can still be recognized as a secondary overprint despite the strong control on deposition by subsidence. Further, a gradual change in the carbonate facies, from shallow marine limestone to the deep marine pelagic is indicative of a rapid change in accommodation space where the carbonate platform could not keep pace with the relative sea level rise and drowned. Calves et al. (2008) connected this demise of the platform with the rapid subsidence by thinning and cooling of the lithosphere. It was further speculated that the Indian margin shows significant slow thermal subsidence until Middle Eocene (~37Ma) which was followed by an episode of a rapid subsidence.

The present study, on a contradictory note, presents a different age of the platform drowning. Results derived from the biostratigraphic data propose an age bracket of ~ 49 to 45 Mas for the onset of the drowning of the carbonate platform. This infers that the rapid subsidence started prior to this time, where initial slow subsidence is recorded within the time span of 16–20 Ma. This resulted in the deposition of thick limestone units. These results validate the drowning age suggested by Carmichael et al. (2009). However, the exposure surface preceding the development of the late stage buildup is suspicious. We propose that a high-amplitude eustatic sea level lowering occurred in the corresponding time interval that may be responsible for the platform emersion. Although the herein presented biostratigraphic data are inadequate to document the precise age and interval of the emersion, the best correlation of the emersion preceding the late stage buildup seems to match with a eustatic fall of more than 100 m around ca. 49 and 51 Ma (Haq et al., 1987; Miller et al., 2011).

3.6.3.2 Climate and paleoceanography

The type of carbonate producers and rate of deposition are known to be strongly influenced by climate (Jones and Desrochers, 1992; Schlager, 2005). The carbonate succession of the Greater Indus Basin was dominated by larger benthic foraminifera during the Paleogene period. This period witnessed long-term climatic changes that led to the transition from global greenhouse conditions to icehouse conditions (Zachos et al., 2001). Scheibner and Speijer (2008a) suggested that Paleogene global warming events caused a Tethyan-wide massive decline in coral reefs and a coeval shift of carbonate platforms with large benthic foraminifera.

(Scheibner and Speijer, 2008b) subdivided the evolution of Paleogene Tethyan carbonate platforms into three stages linked to climate perturbations. Platform Stage I (~58.9 to 56.2 Ma; SBZ 1–3) is represented by the dominance of corallgal assemblages throughout the Tethys. Platform Stage 2 (~56.2 to ~55.5 Ma; SBZ 4–5) is linked with a noticeable reduction of coral taxa and a proliferation of larger foraminifera communities such as ranikothalids and micellanids in lower latitudes (0–20°) with a global rise in sea surface temperature, and Platform Stage III (~55.5 to 40.4; SBZ 5/6–16) with a massive transient temperature peak causing a Tethyan-wide scarcity of coral communities. At the same time, Paleocene

ranikothalids and miscellanids were substituted by nummulitids and alveolinids at the Paleocene - Eocene limit. This evolutionary trend is known as the Larger Foraminifera Turnover (LFT) and is directly coupled to the Carbon Isotope Excursion of the Paleocene-Eocene Thermal Maximum (Scheibner et al., 2005). The drilled section of carbonate platform sequences S5 to S7 shows a high abundance of *Nummulites* and *Alveolina* species. This may assist in treating this part of carbonate succession to Platform Stage III of the Tethyan carbonate platforms. Undoubtedly, the lower platform part, which is more than 1000 m thick, records the LFT but this needs further drilling for confirmation. Correspondingly, the seismic units overlying SB3 show a decrease in relative thickness with the absence of any seismic mound facies. This is taken as an indication that a turnover of the type of carbonate factory occurred after this time and the lowest carbonate production rates due to the lack of a mound-building capacity can be expected.

The Early Paleogene climate perturbation climaxed with the Early Eocene Climatic Optimum responding to a decline in the global temperatures. The global cooling event was accompanied by the demise of many symbiont-bearing larger benthic foraminifers species and a recovery of coral taxa in the southern Tethys (Hallock et al., 1991; Höntzsch et al., 2013). This persistent cooling trend eventually led to a glacial climate condition near the Eocene-Oligocene boundary (Kent and Muttoni, 2008). The Early Eocene Climatic Optimum is apparently not a signature in the platform, but its possible effects cannot be neglected in the final demise of the carbonate platform.

(Hallock, 1987) presumed that the Paleogene evolutionary events of large benthic and planktonic foraminifera were linked to the effects of varying trophic resources in the oceans, resulting in eutrophic conditions on the continental shelves. Further, (Speijer and Wagner, 2002) outlined the intensification of deeper water upwelling on the continental shelf bordering the Tethyan Ocean. Considering these scenarios, the orientation of the Indian margin during the Late Paleocene was almost -32° clockwise from the present-day position (Copley et al., 2010). The Indo-pacific seaways were not closed yet and acted as a passage for ocean currents to the western Tethys (Scotese, 2001). Perhaps these conditions developed a local geostrophic flow along the western margins of the Indian Plate, which enhanced the seasonal upwelling and productivity in the surface water with a possible additional influence of trade winds. Scotese and Summerhayes, (1986) predicted the presence of upwelling phenomena during the Early Eocene, which might be a source of the seasonally induced nutrient influx in the Offshore Indus Basin. As a consequence, the deposition of organic-rich shale occurred along the coast of the western Indian margin during the Late Paleocene to Early Eocene, which is taken as evidence of an increase in productivity (Ahmad and Ahmad, 2005). Such enhanced eutrophic conditions on the continental shelves may have been a factor for controlling the proliferation of the large benthic foraminifera.

3.6.4 Partial drowning mechanism of the carbonate platform

Tropical shallow water carbonate factories drown if the rate of increase of accommodation exceeds the carbonate growth and accumulation rate (Schlager, 1981; Kim et al., 2012) and growth and accumulation rates are reduced through ecological disturbance and the platform

submerged beneath the photic zone (Schlager, 1981; Hallock and Schlager, 1986).

Our results suggest that the flanks of the carbonate platform show asymmetric growth. The eastern margin shows continuous aggrading margins whereas the western margins stepped back episodically during its growth to form three successive terraces. These types of terraces are also identified within the other modern and ancient carbonate systems. The reason of such terrace-formation is attributed to the differential tectonics, changes in climate and biota, and environmental conditions (Betzler et al., 2009; Courgeon et al., 2016; Fürstenau et al., 2010; Ward, 1999). The origin of this asymmetrical appearance of the platform margins, on the studied platform, is not entirely clear because of the data restraints. By comparison with the other platforms in the region, several hypotheses can be formulated to explain the external architecture of the platform history.

1. The western margin of the platform could be a response of differential subsidence subjected to the Cenozoic reorganization of the Indian Plate with respect to the Arabian-African Plate. However, this hypothesis cannot be fully tested on this platform as the seismic data resolution also abruptly decreases beneath the carbonate platform due to the sub-basalt-imaging problem. Therefore, resolving the basement faults which could reflect such a process is not possible on 2D seismic.
2. Courgeon et al. (2016) also reported successive terrace formation in an Early Paleogene carbonate bank in the Mozambique Channel seamounts. This example was proposed to be associated with the major long term climatic warming of the Paleocene-Eocene transition during which much Tethyan coral reef system declined.
3. The backstepping could also be the response of environmentally triggered eutrophic regimes in the western Indian Ocean as seen in the archipelago of the Maldives (Betzler et al., 2016, 2009), the South China Sea (Zampetti et al., 2004). It is suggested that the deterioration of the environmental conditions are linked with the trade-wind driven upwelling as discussed earlier. Eventually, this nutrient injection threatened the carbonate factory and the platform could not keep-up with the relative sea level rise in the aforementioned scenarios.

Nevertheless, future drilling, high-resolution geochemical, and microfacies analysis of the western margin of the platform may help to test the validity of these hypotheses.

Chapter IV

Controls on the Paleogene carbonate platform growth under greenhouse climate conditions (Offshore Indus Basin)

4.1 Outline of the chapter

The evolution of tropical carbonate platforms is dictated by the interplay between multiple controlling factors including antecedent topography, type of carbonate factory, eustasy, tectonics, and climatic and environmental conditions (Fournier et al., 2005; Betzler et al., 2013; Paumard et al., 2017). Paleocene-Eocene carbonate factories differ drastically in terms of carbonate producer from other Cenozoic carbonate factories, and in general seem to be characterized by a Tethyan-wide decline of coral species and abundance in larger benthic foraminifera at the Paleocene-Eocene transition (Scheibner and Speijer, 2008b). The Paleocene and Eocene epochs were characterized by a warm and ice-free climate with pronounced hyperthermals with 5-8° C higher sea surface temperatures than today (Zachos et al., 2001). Such environmental conditions affected marine and terrestrial biota and resulted in a major extinction event that terminated many deep-sea benthic foraminifera and produced a turnover in shallow benthic foraminiferal associated concomitant with a Tethyan wide reduction of coral reef species. In the past, several studies have evaluated the carbonate platforms for their biotic assemblages and facies distribution with regard to climatic and ecological signals affecting the neritic carbonate factories (Scheibner and Speijer, 2008b). In contrast, little attention has been devoted to the observation of the architectural and geometrical response of Paleocene-Eocene carbonate platforms to the paleoecological conditions of the greenhouse climatic state.

During the Paleocene-Eocene, carbonate deposition took place around shallow-water equatorial basins of the Tethyan realm extending further north and south of the 30° latitude which today is the general limit of coral reef growth (Schlager, 2005; Kiessling and Flügel, 2002). Stratigraphic and architectural models of carbonate platforms from these ages were derived mainly from the outcrop in the Pyrenees (Spain) and Galala (Egypt) (Baceta et al., 2005; Eichenseer and Luterbacher, 1992; Höntzsch et al., 2011). However, modern analogs of such carbonate factory do not exist today, leaving some gaps in our understanding of the dynamics of these carbonate depositional systems. To address this research gap, this chapter establishes the regional stratigraphic framework of the Paleogene carbonate platform using seismic data supported with lithological and biostratigraphical data gathered from several exploration wells to analyze the Offshore Indus Basin carbonate platforms (Fig. 4.1). The data characterize the depositional geometries and to decipher mechanisms controlling the stratigraphic architecture of one of the best-quoted example of the Paleocene-Eocene carbonate platforms developed under greenhouse climate conditions. Findings of this study will directly or indirectly enhance our understanding of greenhouse carbonate platforms that can be applied to similar deposits elsewhere.

4.2 Regional settings

Located on the western continental margin of India, the Offshore Indus Basin of Pakistan in the subsurface preserves a spectacular record of isolated Paleocene and Eocene carbonate platforms and contemporaneous shelf-attached platforms (Fig. 4.1; Carmichael et al., 2009; Shahzad et al., 2018). The carbonate platforms developed on the northeast-southwest trending isolated Saurashtra Volcanic Platform (SVP) are separated from the Eocene continental shelf by a deep-water trough (Fig. 4.2; Corfield et al., 2010; Chatterjee et al., 2013). Located in the southeast of the Murray Ridge, the volcanic platform represents the fundament of the isolated carbonate platforms (Fig. 4.3). SVP encompasses two volcanic highs (Somnath Ridge and Saurashtra High), and consists of extrusive basalts covering an area of 42,500 km² within the limit of the Pakistan Exclusive Economic Zone (Calvès et al., 2011) and is more than 15 km thick. An additional 300 km² extend into the Indian national territory. In the southeast, the SVP is bounded by the Laxmi Basin/Gop Rift and Laxmi Ridge (Bhattacharya et al., 1994). The structural evolution of the SVP is poorly understood and has been linked to the strike-slip strain accommodation during the separation of the Indian Plate from Madagascar (Calvès et al., 2011; Chatterjee et al., 2013). The crust beneath the SVP is interpreted either as a stretched continental crust or as an oceanic crust older than 64 Ma (An 28) (Malod et al., 1997) (Fig. 4.2).

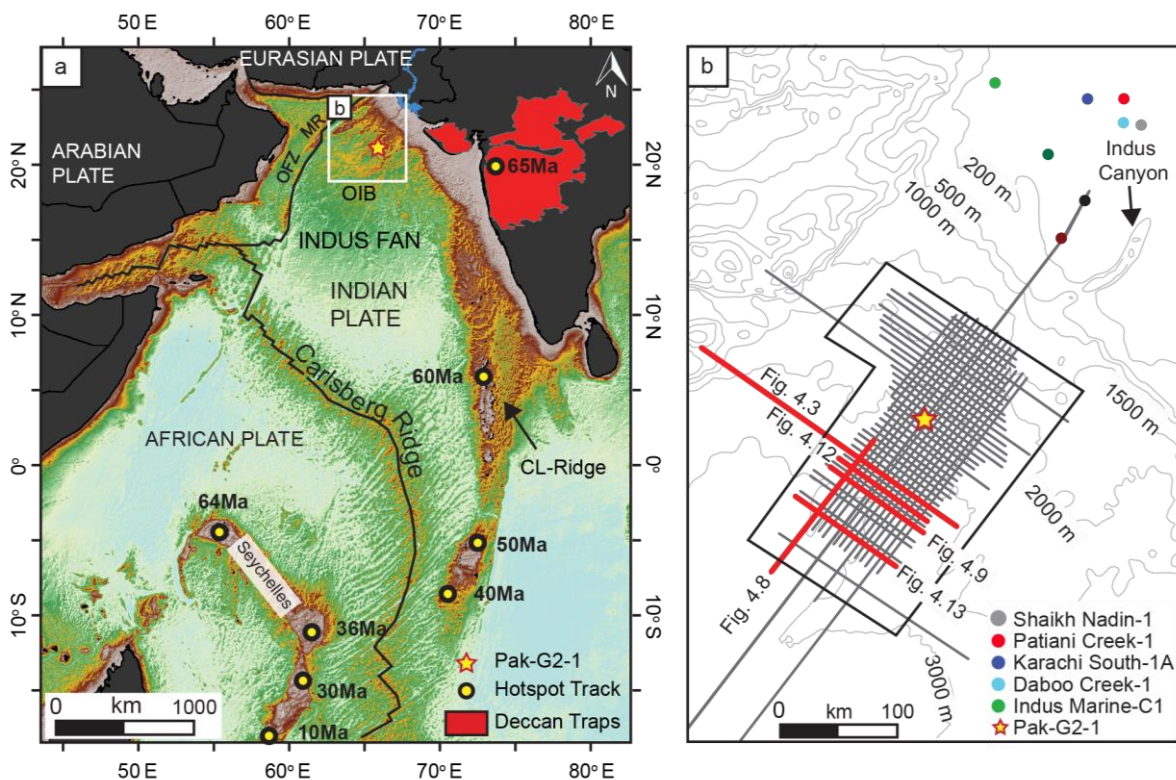


Figure 4.1: (a) Regional index map of the Indian Ocean, annotated with major tectonic and structural elements (Smith and Sandwell, 1997). The yellow points represent the approximate path and age of the deposits of the Deccan/Reunion Plume (Corfield et al., 2010). OFZ: Owen Fracture Zone; MR: Murray Ridge; OIB: Offshore Indus Basin CL-Ridge: Chagos-Laccadive Ridge. The small white rectangle shows the seismic and well data coverage enlarged in part b. (b) Seismic and well coverage with present day bathymetry. The highlighted seismic lines are shown in the corresponding figures.

Detached and at a distance of 150 km from the present-day shelf-margin, the carbonate succession developed during the northward drift of the Indian Plate following its separation from Seychelles and the oceanic spreading at the Carlsberg Ridge. These carbonates recorded diverse changes of the tectonics, paleoceanographic and atmospheric conditions of the Paleo-Tethys Ocean. Thus, the region can be considered as a natural laboratory for the investigation of growth patterns and depositional architectures of greenhouse carbonate platforms.

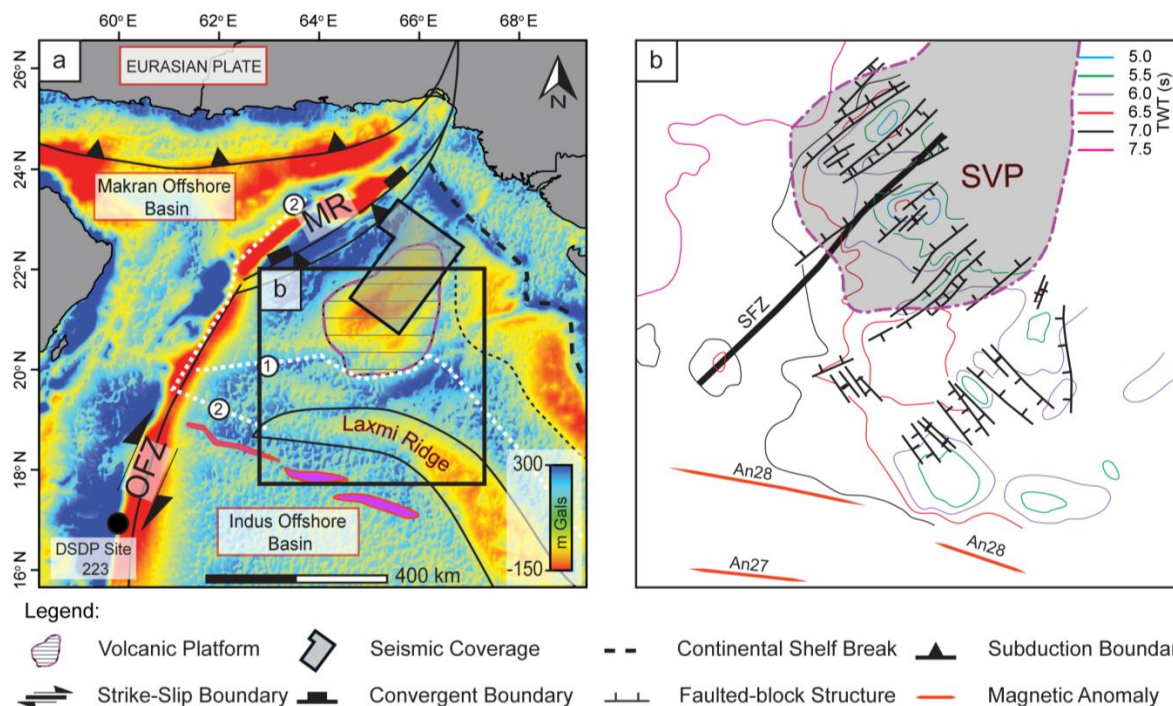


Figure 4.2: (a) Tectonic elements of the Offshore Indus Basin, Pakistan with an overlay of free-air gravity map (Corfield et al., 2010; Minshull et al., 2015). Primary study area is the Saurashtra Volcanic Platform (SVP). Key to symbols: The thick stipple black line denotes the present-day shelf-break, white dotted line is the ocean-continent boundary (1. after Corfield et al., 2010; 2. after Minshull et al., 2015). MR: Murray Ridge, OFZ: Owen Fracture Zone. A zoomed map of the structural characteristics of the basin (after Malod et al., 1997). (b) The zoomed area shows the structural framework of the area of interest. SFZ: Somnath Fracture Zone.

4.3 Data and methods

Data from 2002 vintages are time-migrated 2D seismic reflections data and comprise line lengths of approx. 9000 km covering an area of 75000 km² in the proximity of the Indus Fan (Fig. 4.1b). The data are zero-phase processed and displayed with the negative (SEG) polarity whereby an increase in acoustic impedance is recorded negative in numbers or trough. The quality of the seismic imaging is good with the vertical seismic resolution of ~25 m, estimated from a central frequency of 45 Hz and velocity of 4500 m/s in the carbonates.

4.3.1 Well to seismic tie and stratigraphic correlation

The workflow started with the establishment of a regional stratigraphic correlation between the isolated carbonate platforms and the continental shelf margin stratigraphy based on the identification of time-significant key surfaces in seismic profiles. Nature and ages of the surfaces were constrained using well data from nine exploratory wells (Fig. 4.1). Out of the nine wells, eight are located on the continental shelf in less than 150 m water depth, and only

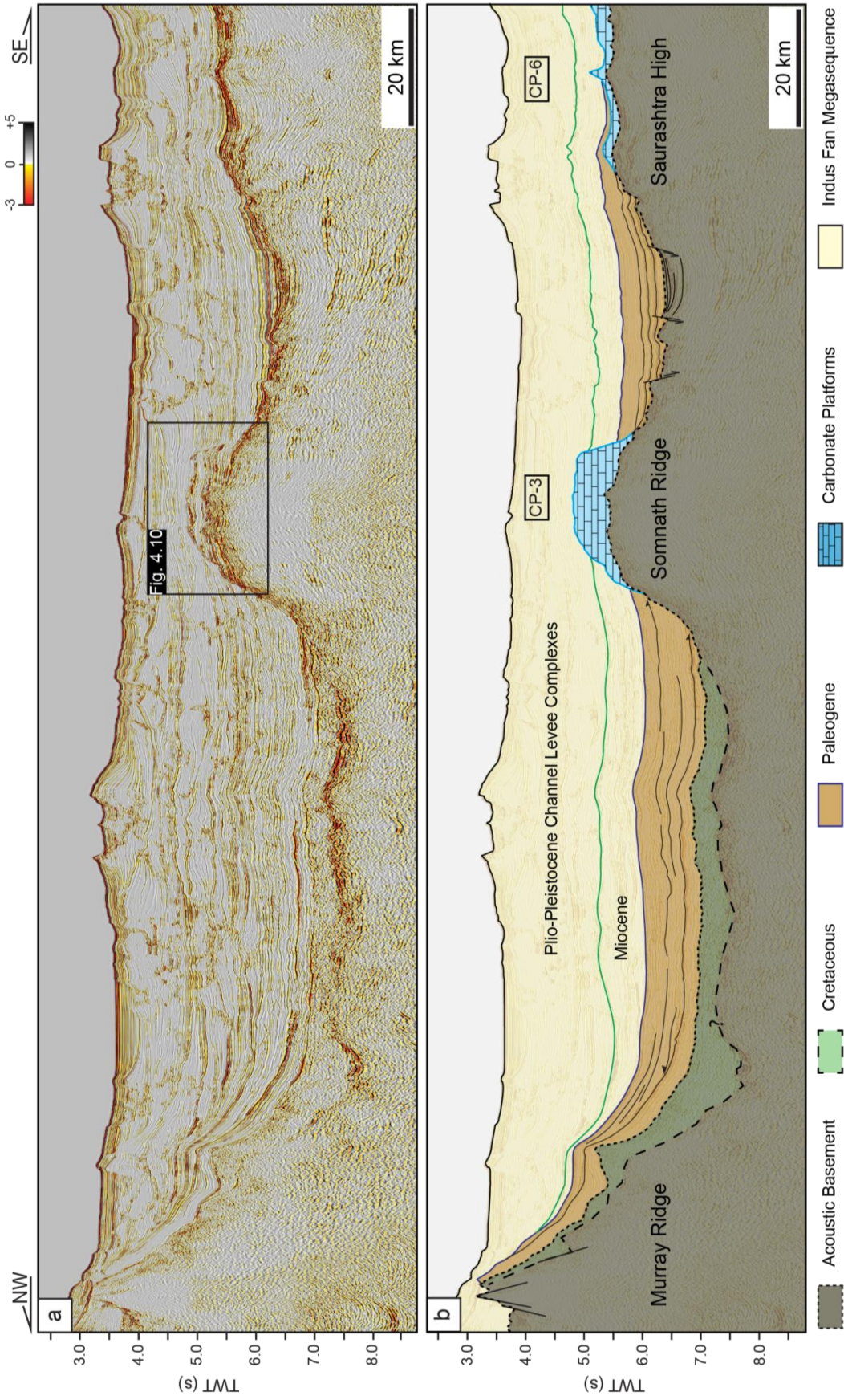


Figure 4.3: (a) Regional northwest-southeast oriented seismic profile. (b) Interpretation illustrating the stratigraphic framework of the carbonate platforms with the indicated regional structural features. Location of profile is marked in Fig. 4.1b. (Vertical Exaggeration=10)

the well Pak-G2-1 is located on the continental rise at water depth more than 2700 m (Figs. 4.1 and 4.4). Wireline log data were calibrated with lithological and biostratigraphic data obtained from cuttings. VSP and check-shot data were utilized to calibrate the wells with 2-D seismic lines. The carbonate lithofacies, the paleobathymetric evaluation, and the biostratigraphic age determination of the isolated carbonate platforms were provided by correlation of seismic data to the wells Pak-G2-1 and Karachi South-1A.

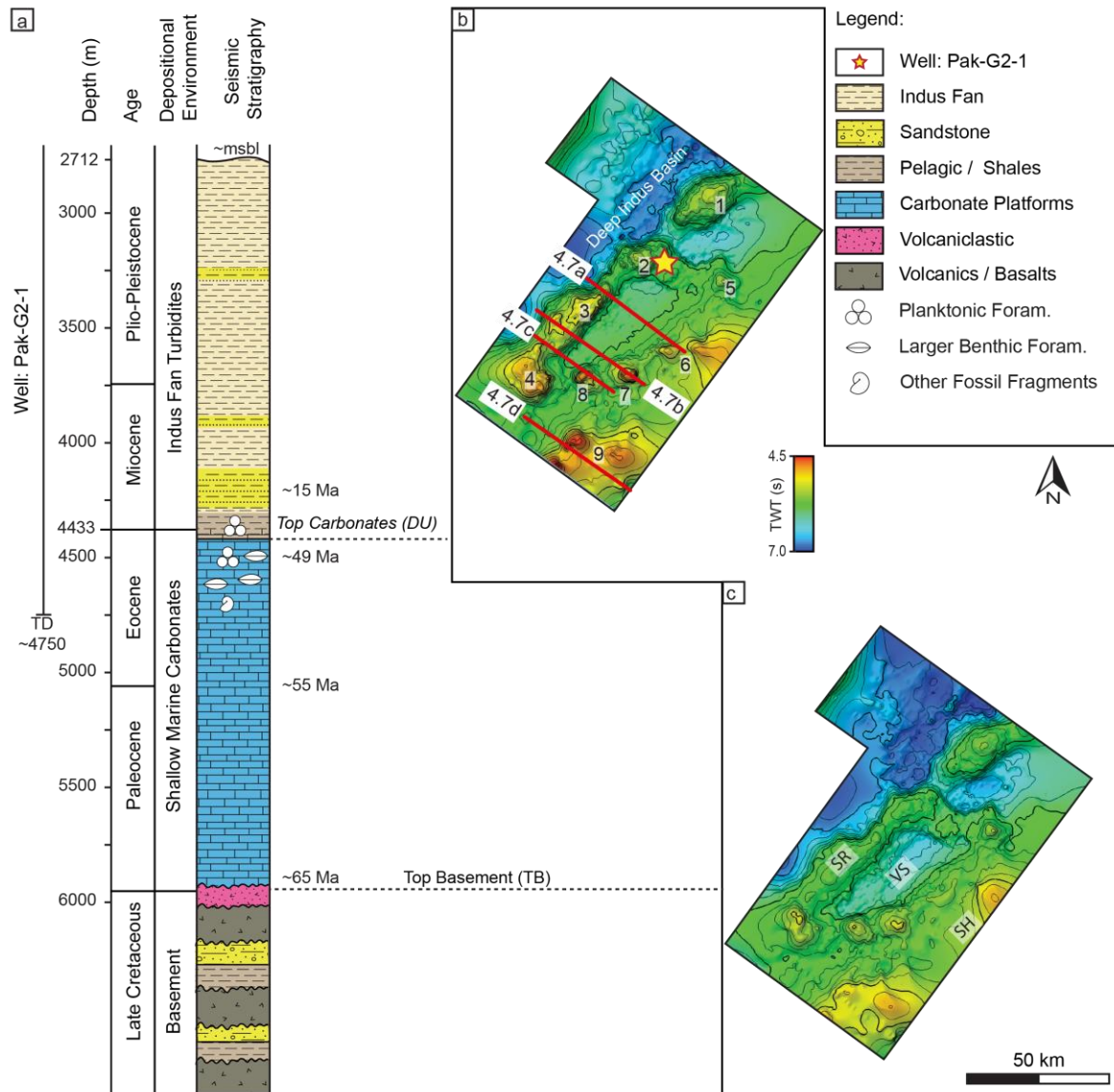


Figure 4.4: (a) A simplified lithological column of industrial well Pak-G2-1 with the possible extension to the interpreted acoustic basement (Shahzad et al., 2018). (b) and (c) are mapped surfaces Top carbonate and Top basement, respectively in the time domain. Numbers in b refer to the carbonate platforms (CP) whereas the red lines indicate the position of seismic lines shown in figure 4.7. SR: Somnath Ridge, SH: Saurashtra and VS: Volcanic sub basin.

The exploration well Pak-G2-1 was drilled in the apex of a drowned, isolated carbonate platform. The well penetrated three major stratigraphic units (Fig. 4.4a), which are from bottom to top: Late Paleocene-Early Eocene shallow-water carbonates, Middle Eocene to Middle Miocene deep marine pelagics, and megasequences of Indus Fan deposits comprising Miocene and Pliocene-Pleistocene channel-levee systems. The microfauna in the carbonates is characterized by *Nummulites sp.*, *Alveolina sp.*, and *Lokhartia sp.*, which corresponds to the SBZ4/5 to SBZ8-10 zones, of Late Paleocene to Early Eocene age (Serra-Kiel et al., 1998; Shahzad et al., 2018). The top of the shallow-marine carbonate succession is at a depth of 4433 m (MD+waterdepth) in well Pak-G2-1 (Fig. 4.4a). Exploratory wells (see Fig. 4.1b; Shahzad et al., 2018), including Patiani Creek-1, Daboo Creek-1, Shaikh Nadin-1, and Indus Marine-C1 were used to constrain the seismic interpretation of the Eocene stratigraphy (Fig. 4.5).

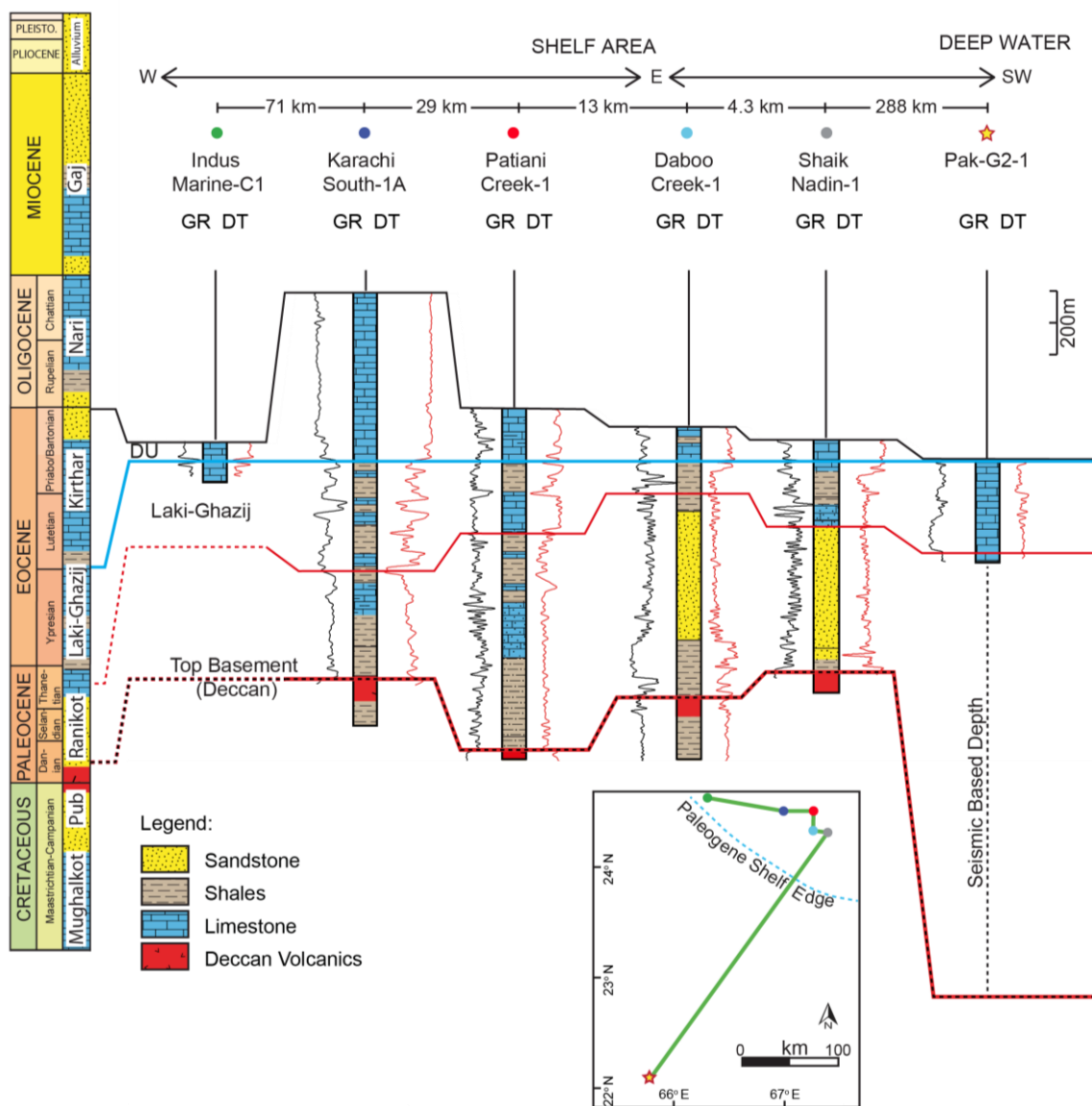


Figure 4.5: Well correlation of the Paleogene carbonate shelf with the isolated carbonate platforms in the Offshore Indus Basin. Well Pak-G2-1 is the only well which partially penetrated one of these isolated carbonate platforms.

On seismic sections, a persistent and high-amplitude seismic horizon is mapped as the Top Carbonates (Fig. 4.4c) which is a sharp transition between limestone and overlying siliciclastic and coincides with the drowning unconformity (DU) recovered in well Pak-G2-1 (Fig. 4.4b; Shahzad et al., 2018). The lower boundary of the carbonate succession was established as the Top Basement by identification of a high-amplitude seismic reflection and with well correlation (Figs. 4.3-4.5). This surface extends basin-wide and separates the Cenozoic succession from the Mesozoic (Carmichael et al., 2009). The scarcity of wells in the Offshore Indus Basin hinders an exact age assignment of this surface, and therefore the age model is based on magnetic lineations (Fig. 4.2) and a regional well correlation (Fig. 4.5). In this study, the designation isolated carbonate platform refers to a thick and mappable succession of carbonates detached from the main landmass. Isolated carbonate platforms are differentiated from carbonate buildups that here are features with significant topographic relief located in the platforms (Schlager, 2005; Saqab and Bourget, 2016). The isolated carbonate platforms were defined based on the diagnostic criteria defined by Burgess et al. (2013) such as a positive antecedent topography, marked stratal thickening, high angle flanks, stacking patterns, distinct reflection amplitude and geometry, and onlaps of surrounding sediments.

4.4 Results

4.4.1 Seismic facies analysis

The seismic facies analysis of the platform-to-basin transects has identified six seismic facies by applying the principles delineated by Ramsayer (1979). Interpretation of the depositional environment of each facies is based on the study performed by Bachtel et al. (2004) in a similar carbonate setting. A summary of each facies is provided in Tab. 4.1, the respective seismic expression is displayed in figure. 4.6.

4.4.2 Seismic morphology and distribution of isolated carbonate platforms

Nine isolated carbonate platforms are located in the study area, referred to as CP-1 to CP-9 (Figs. 4.4c, and 4.7a-d; Tab 4.2). These platforms are circular, sub-circular and elongated in shape, range in length between 4 and 80 km, and arranged into two NE-SW trending chains (Fig. 4.4c), covering the volcanic seamounts and ridges (Figs. 4.4 and 4.7). Slopes have an angle of up to $>12-15^{\circ}$ and are surrounded by younger (Oligocene to Miocene) onlapping basal sediments (e.g. SF5) (Figs. 4.3, 4.7 and 4.8). The western chain of carbonate platforms is named Somnath Ridge Carbonate Platforms and the eastern chain Saurashtra High Carbonate Platforms (Figs. 4.3, 4.4 and 4.7). The correlation between the two chains of platforms is purely based on seismic facies analysis, external form, and bounding surfaces. Therefore, the stratigraphic relationship has a certain degree of uncertainty due to insufficient drilling data in the study area.

The Somnath Ridge has four isolated carbonate platforms, labeled as CP-1 to CP-4 (Figs. 4.4c, 4.7 and 4.8). The CP-3 and CP-4 carbonate platforms are elongated in shape, over 85 km long, and extend in a northeast to the southwest direction (Figs. 4.7 and 4.8).

Table 4.1: Descriptions of seismic facies characteristics and their interpretation. The possible interpretation of the seismic is adopted from Misra et al. (2017) and Bachtel et al. (2004) in the similar kind of platform settings.

Seismic Facies	Internal reflection Configuration	Reflection Continuity	Amplitude	Bonding Relationship	Depositional Environment Interpretation
SF1: Mounded Seismic Facies (Fig. 6a)	Mounded with sub-parallel, upward convex to wavy internal reflections	Semi-continuous to discontinuous	Moderate to low	Strong, contorted to mound shaped upper reflection with moderate lower boundaries	Small isolated carbonate buildups, late stage buildups, pinnacles and patch reefs
SF2: Mounded Seismic Facies (Fig. 6b)	Chaotic reflections	Discontinuous	Low	Contorted to mound shaped reflection upper boundary, lower boundary is not traceable	Volcanic buildups and volcanic vents tops
SF3: Inner platform Facies (Fig. 6c)	Parallel	Continuous to semi-continuous	High to low alternate reflections	Strong amplitude reflective boundary with rugged top and slope onlaps surfaces	Platform interior facies. Alternates between low energy, shallow lagoonal to up-building shallow marine carbonate sediments with patch reefs on top
SF4: Chaotic (Platform) Facies (Fig. 6d)	Chaotic	Discontinuous	Moderate to low	Surrounded by SF1, SF3, SF5 seismic facies.	Confined slump and debris flow of carbonate sediments, carbonate growth associated with volcanic activity or fractured carbonate beds
SF5: Basinal Facies (Fig. 6e)	Parallel	Strongly continuous	Moderate to low	Conformable, continuous and draping underlying topography	Pelagic to hemipelagic and early fan deposits of low energy.
SF6: Volcanic Facies (Fig. 6f)	Chaotic	Discontinuous	Medium to low	Uneven and strong amplitude top non-conformable to disconformable surface	Volcanic basement with subaerial to submarine volcanic features, SDRs and hyaloclastite volcanic mounds.

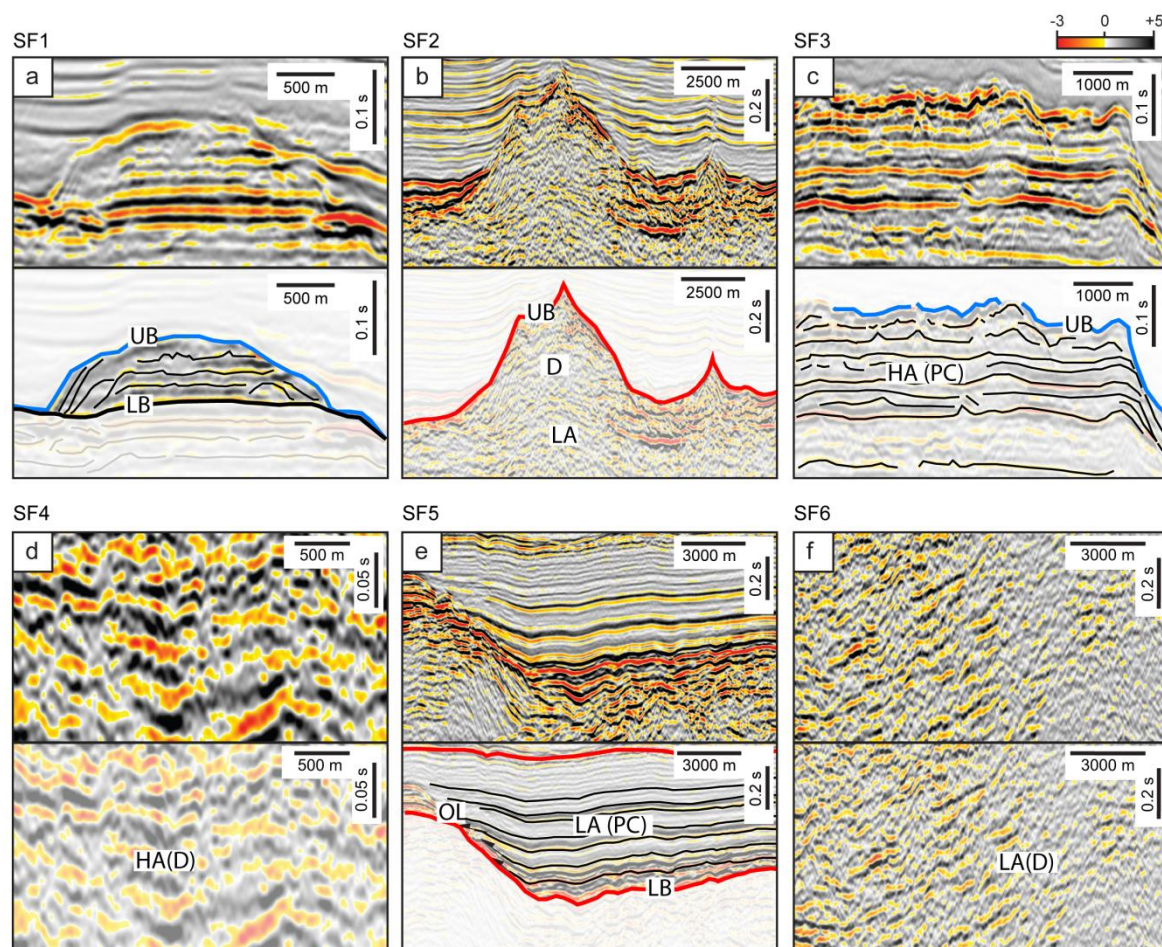
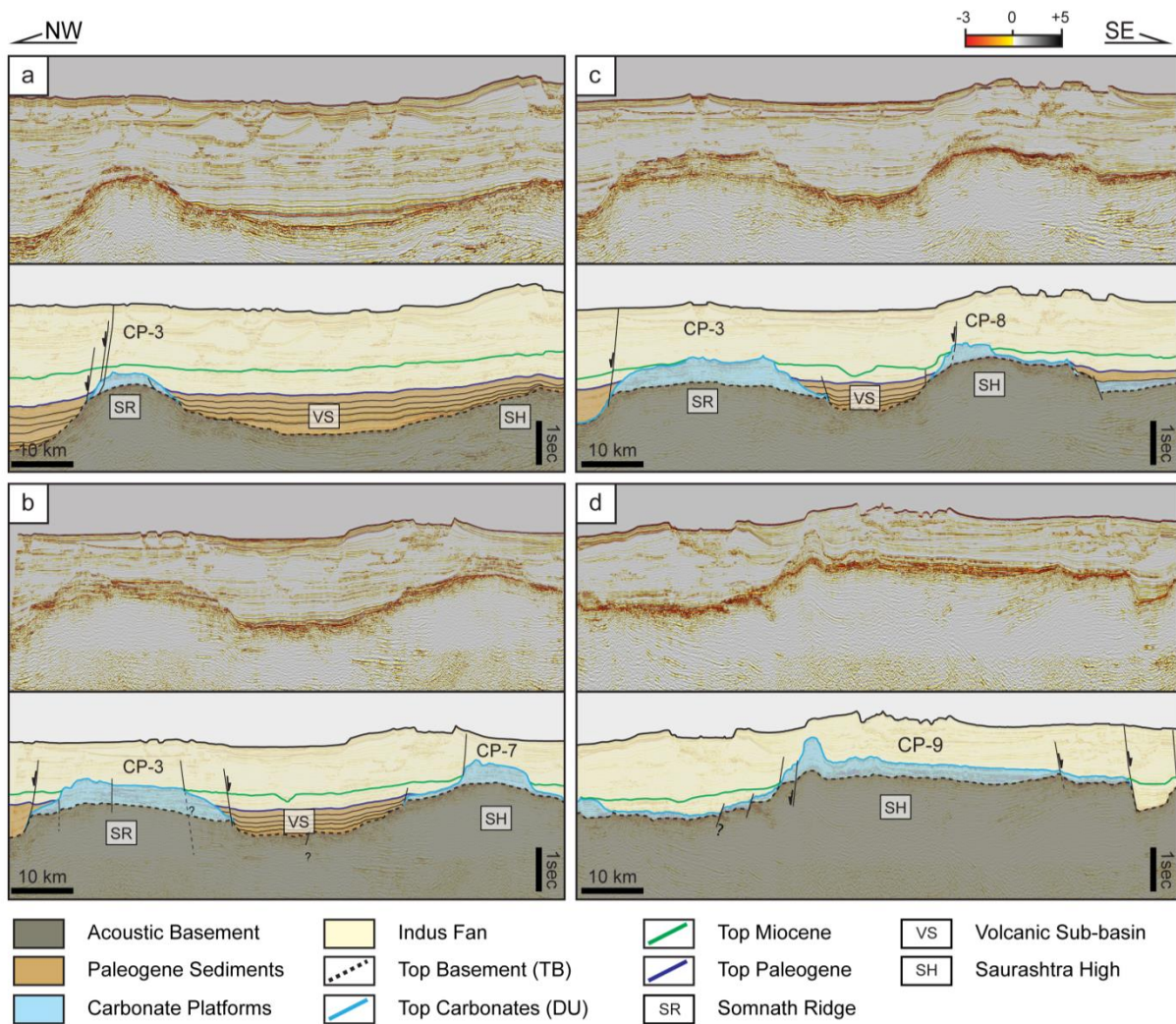


Figure 4.6: Seismic facies and expressions of depositional geometries defined in the high-resolution seismic data set (a-f); Seismic facies description is provided in table 4.1. UB: Upper Boundary, LB: Lower Boundary, HA: High Amplitude, LA: Low Amplitude, PC: Parallel Continuous, D: Discontinuous.

The data coverage of the Saurashtra High is limited to the EEZ of Pakistan, where platforms CP-5 to CP-9 are located (Fig. 4.4c), although the ridge extends into the EEZ of India (e.g. Fig. 4.2) where Misra et al. (2016) reports age-equivalent carbonate platforms. In general, these platforms are circular to sub-circular in shape and smaller in areal extent than the Somnath Ridge carbonate platforms (Figs. 4.4c and 4.7). The diameter of the individual carbonate platform ranges from 8 to 14 km where the areal extent of each carbonate platform varies from 200 to 1000 km² (Tab. 4.2). On average the carbonate platforms are more than 1000 m thick (500 to 800 ms; Tab. 4.2). Internally, the carbonate platforms display parallel and continuous reflectors (SF3), indicating a dominantly aggradational system, margins of the platforms step back. The seismic reflections of the sub-basin between both ridges appear as low amplitude, parallel and continuous succession attributed to the basinal seismic facies (SF5) (Fig. 4.7) onlapping against the basement highs and carbonate platforms. Deposits are interpreted as pelagic to hemipelagic and/or volcanoclastic in origin with a probable input of shallow marine mass wasting (Calvès et al., 2011). The regional correlations infer an Eocene to the Oligocene age of these sediments (Fig. 4.3; Carmichael et al., 2009).

Table 4.2: Location of carbonate platforms with their aerial extent and thickness. Coordinates represent the highest topographic point of each platform.

Name	Latitude	Longitude	Area (Sq. km)	Length in NW-SE (km)	Maximum Thickness (ms)
CP-1	22°31'02.6723"N	66°08'19.1462"E	1079.88	25	400
CP-2	22°06'24.4200"N	65°47'34.0300"E	818.10	28	700
CP-3	21°51'09.6559"N	65°25'44.6782"E	2318.75	68	730
CP-4	21°20'32.9380"N	64°58'31.7603"E	1366.61	35	780
CP-5	21°58'17.1064"N	66°18'05.3079"E	369.22	4	65
CP-6a	21°32'02.1115"N	66°06'48.6567"E	1016.11	21	784
CP-6b	21°31'50.0842"N	65°53'20.7305"E	212.74	10	500
CP-7	21°22'39.1449"N	64°58'13.5870"E	280.73	14	555
CP-8	21°21'31.1304"N	65°20'38.4606"E	277.96	10	600
CP-9a	20°51'16.2433"N	65°35'34.6884"E	771.34	50	800
CP-9b	20°55'28.1026"N	65°18'17.6269"E	390.00	40	784
CP-9c	20°46'09.0377"N	65°11'06.9387"E	634.36	45	770



4.4.3 Seismic stratigraphy of the isolated carbonate platforms

The carbonate succession is subdivided into seven seismic units delimited by high amplitude and laterally traceable bounding surfaces separating stratal packages with distinct facies associations, following the approach by Zampetti et al. (2004) and Kusumastuti et al. (2002). Among these seismic surfaces, two subaerial unconformities and one drowning unconformity were identified based on the associated stratal terminations and changes in the depositional environment in conjunction with the well data. The seismic stratigraphic units most commonly include parallel and aggradational geometries that can be interpreted as thin transgressive-regressive sequences (Figs. 4.8-4.13).

4.4.3.1 Top Basement (Cretaceous-Paleogene)

The Top Basement (Deccan Volcanics) horizon is a regional stratigraphic unconformity (Fig. 4.7 and 4.8). In the study area, Top Basement corresponds to the top of SVP (Fig. 4.2) and is mapped as a rough surface with strong basement reflections and associated diffractions. The depth of the Top Basement reflection ranges between 5 to 7s in two travel time map (Fig. 4.4d). The unit below the surface is typified by seismic facies SF6 and SF2 (Figs. 4.8-4.10) and encompasses many features (Planke et al., 2000; Calvès et al., 2011) indicative of an extrusive volcanic activity, such as seaward dipping reflectors (SDR), and local packages of clinofolds of lava flows and volcanic mounds, indicating subaerial to subaqueous volcanism (Corfield et al., 2010).

4.4.3.2 Seismic unit S1 (Middle to Late Paleocene)

Above the Deccan Volcanics, seismic unit S1 is the oldest unit of the carbonate platform succession (Figs. 4.8-4.10). S1 unit is typified by the mounded seismic facies (SF1 and SF2) in the basal part; the remaining part mostly contain discontinuous reflections with a high-amplitude seismic facies such as SF4 (Fig. 4.8). At places, the identification of the Top Basement becomes difficult because of the decreasing amplitude contrast between carbonates and underlying volcanics or volcanoclastic (Figs. 4.8 and 4.9). Locally, oblique downlapping reflections occur along the peripheries of the mounded facies (Fig. 4.8). The top of the unit is defined by the SH1 discontinuity surface characterized by high amplitude reflector associated with the toplaps and onlaps from the unit below and above respectively, depicting a change in seismic facies from discontinuous seismic reflection below to fairly continuous reflection of seismic unit S2 (Figs. 4.8 and 4.9). The thickness of unit S1 is variable and increases towards the southwest where it onlaps against the uplifted basement high of CP-4 (Fig. 4.8). In the absence of drilling data, a Middle to Late Paleocene age is tentatively assigned to this unit.

Figure 4.7 (previous page): Seismic transects across the carbonate platforms in northwest-southeast direction. Carbonate platforms are separated by a shallow basin (VS) filled with the mass-wasting deposits from the volcanic ridges and sediments of the early Indus Fan. The positions of the seismic lines are shown in the index map with mapped surface of Top Carbonate as drowning unconformity and their correlative conformity in the rest of the basin in the figure 4.4b. (Vertical Exaggeration=6)

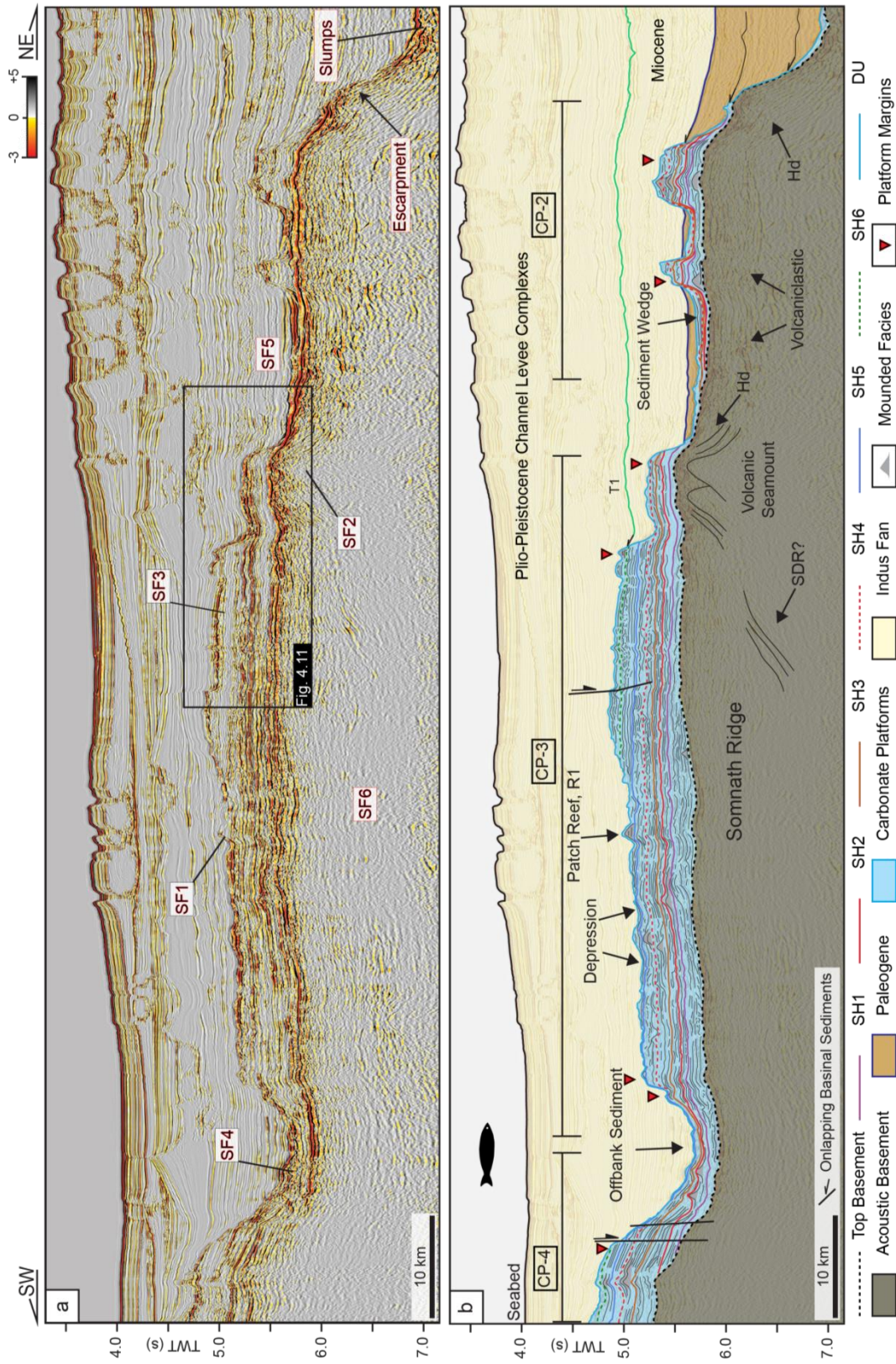


Figure 4.8: (a) Regional northeast-southwest oriented seismic profile (for location refers to figure 4.1b). (b) Interpretation showing the main identified seismic units and their bounding surfaces. SDR: Seismic Dipping Reflections, Hd: hyaloclastite (Vertical Exaggeration=10)

4.4.3.3 Seismic unit S2 and S3 (Late Paleocene)

Seismic unit S2 is a relatively thin unit (100 ms TWT). The seismic facies of this unit are low to medium amplitude and semi-continuous reflections in the platform area (SF 3; Figs. 4.8, 4.9 and 4.10) with few local SF1 facies patches (Fig. 4.9). Reflection continuity is low near sub-vertical packages of discontinuous seismic facies SF4 (e.g. fluid escape pipe; Fig. 4.10). Further to the south, unit S2 onlaps against the CP-4 structure (Fig. 4.8). S2 is bounded by the SH2 horizon at the top with several onlaps from the overlying seismic unit S3 in the southern part of the CP3.

Compared to seismic unit S2, Seismic unit S3 exhibits more continuous, parallel to sub-parallel seismic reflections with strong amplitudes (Figs. 4.8-4.11). The thickness of the unit decreases towards the southwest where it forms an onlapping set of reflections that climb up the basement high and forms the basal unit of CP-4 (Fig. 4.8). Between CP4 and CP3, S3 forms a thin section, comprising discontinuous to chaotic seismic facies (SF4). At the top, this unit is bounded by an irregular consistently traceable surface with strong amplitude defined as SH3.

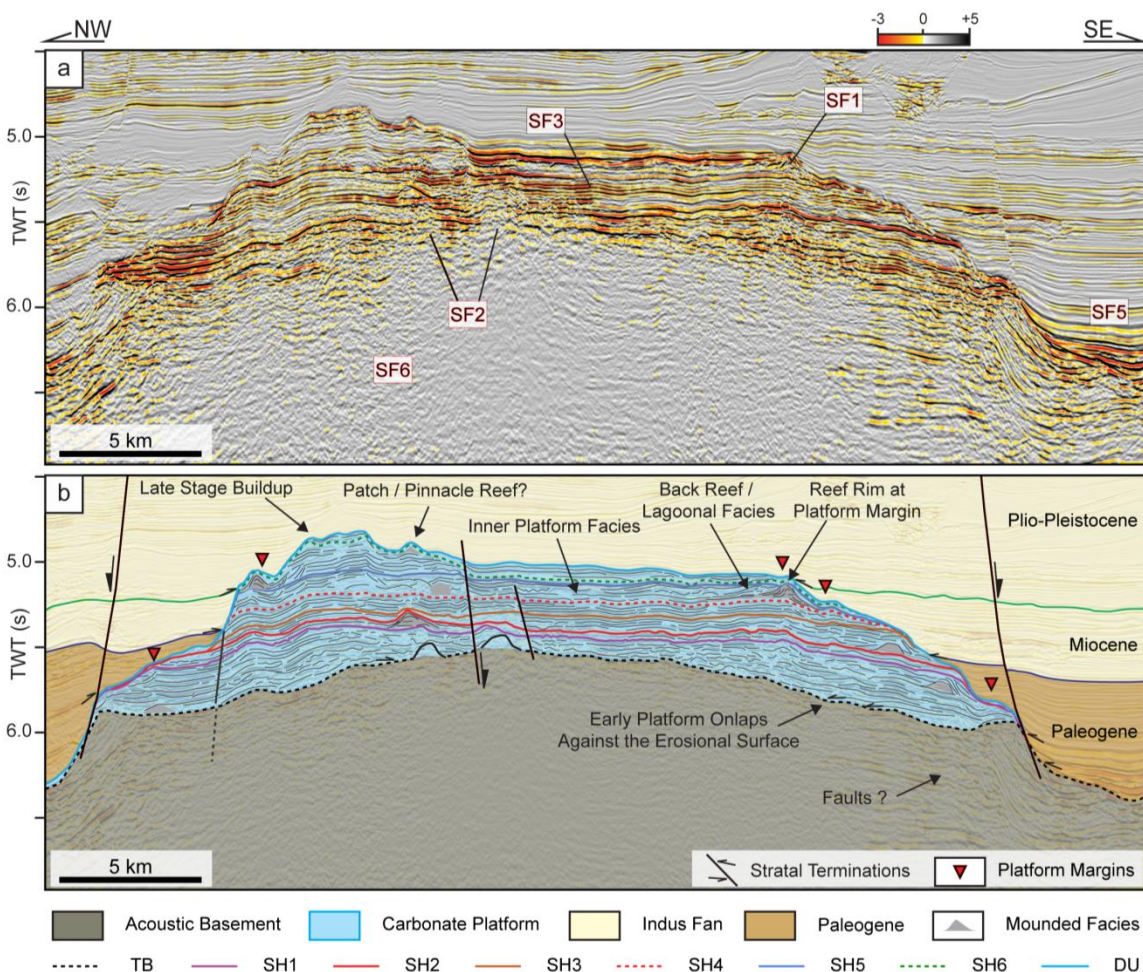


Figure 4.9: (a) Zoomed section of a northwest-southeast oriented regional seismic profile with interpretation in (b) showing the main seismic units and their respective bounding surfaces and facies changes (for location refers to figure 4.1b). (Vertical Exaggeration =6)

4.4.3.4 Seismic unit S4 (Late Paleocene to Early Eocene)

Seismic unit S4 is characterized by medium amplitude, parallel and continuous to sub-continuous reflections (SF3). The continuity of the seismic reflections are often interrupted by the mounded seismic facies (SF1) and subvertical zones of discontinuous seismic facies (SF4) associated with the high amplitudes anomalies (Figs. 4.8 and 4.10). Locally, the unit displays channel-like incisions (<500m wide and 50 ms in height) in CP-3 at the upper bounding surface SH4 (Figs. 4.10 and 4.11). SH4 further appears as an irregular surface with a strong amplitude (Figs. 4.9-4.11). Based on these characteristics, the surface is interpreted to have been subaerially exposed during formation of SH4. Based on the biostratigraphic information available from well Pak-G2-1 (Shahzad et al., 2018), a Late Paleocene to Early Eocene (Thanetian-Ypresian) age is assigned to unit S4.

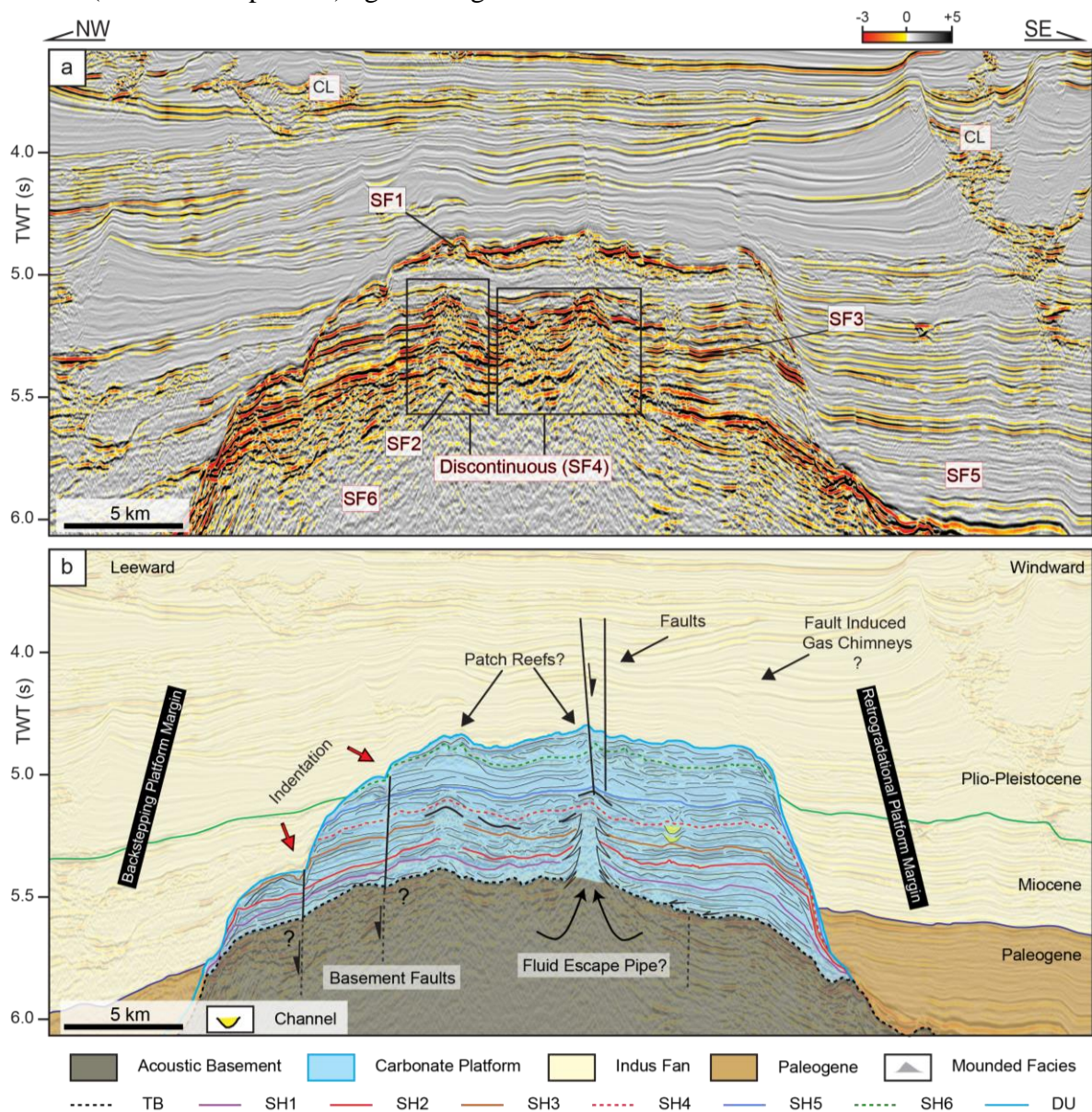


Figure 4.10: A closer view of the northwest-southeast oriented profile illustrated in figures 4.3. Uninterpreted (a) and interpreted section (b) the seismic units and their correlative boundaries are discussed in the text in details. The windward slope angle is steeper than the leeward angle. The northwestern margin shows large-scale backstepping. (Vertical Exaggeration =10)

4.4.3.5 Seismic unit S5 (Early Eocene)

The areal extent of the carbonate platform was reduced markedly after unit S4 deposition (Figs. 4.8-4.12). Seismic unit S5 has spatially variable stratal geometries, which clearly distinguishes this from the underlying unit S4 (Figs. 4.9-4.11). The unit mostly contains low to medium amplitude sub-continuous and sub-parallel seismic reflections (SF3) (Figs. 4.8-4.11). Mounded facies (SF 1) associated with a 1000 m wide channel-like incision also occurs in this unit (Fig. 4.11). Here mounded facies are associated with the set of prograding reflections towards the inner platform (Fig. 4.9), forming a localized regressive unit. Further, seismic reflections from the basal part of the unit onlap onto horizon SH4 (Fig. 4.8). To the northeast margin of CP3, unit S5 shows a stair-like backstepping of the platform flank which results in the formation of an 8 km wide terrace (T1; Fig. 4.11). The upper surface SH5 of unit S5 is a high amplitude concordant reflection (Figs. 4.8 and 4.11). Based on samples from well Pak-G2-1, Shahzad et al. (2018) assigned an Early Eocene age to this unit.

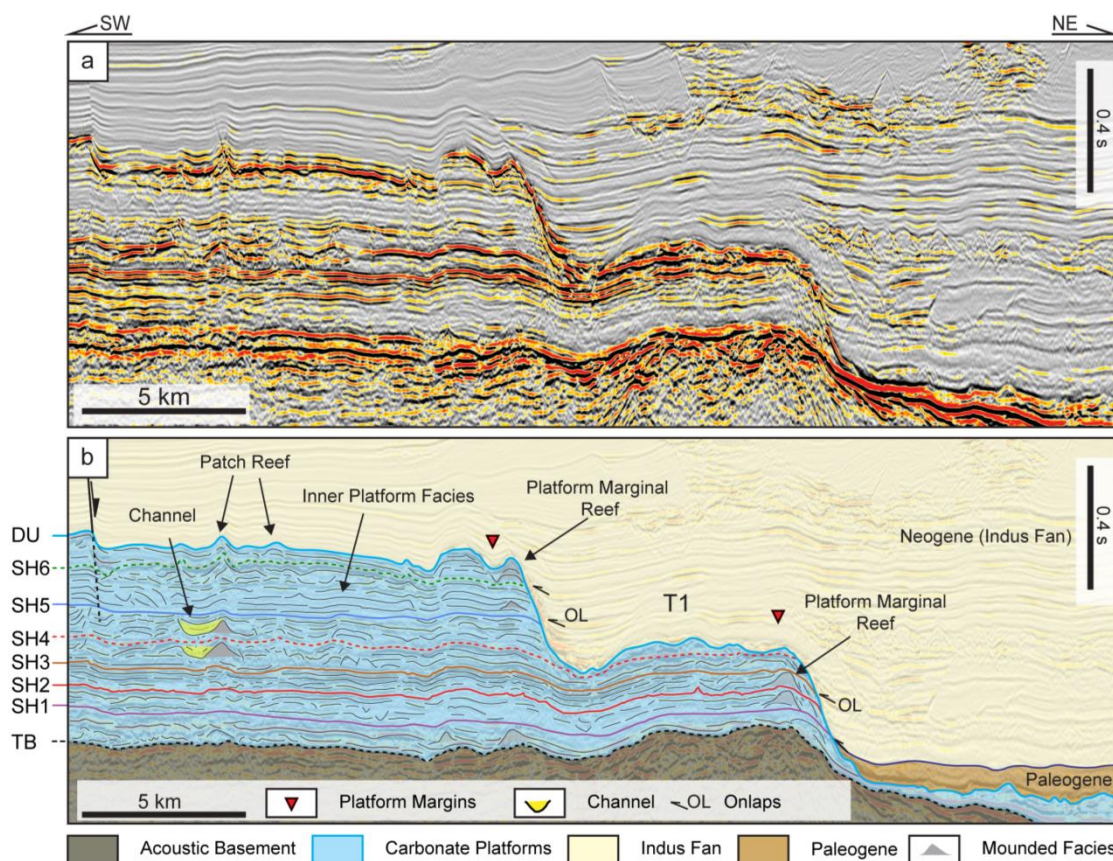


Figure 4.11: A closer view of the northeast-southwest oriented profile showed in figures 4.8. (a) Uninterpreted section and (b) interpreted section. T1 is the large-scale terrace along the northeastern edge of the carbonate platform CP-3 and interpreted to reflect backstepping of the platform margin. The reflections change above and below of the drowning surface are highlighted. (Vertical Exaggeration =10)

4.4.3.6 Seismic units S6 and S7 (Early to Middle Eocene)

Seismic unit S6 is characterized by a further shrinking of the platform extension along the northern margin of CP3, and CP4 (Figs. 4.8-4.13). Internally, this unit is dominated by SF3 with reflections of low amplitude (Figs. 4.8, 4.10 and 4.11). The continuity in the seismic

reflections locally decreases towards the top surface (Fig. 4.11). A small mound features (SF1) with ~100 ms height and ~1000 m width is observed in the platform CP3 and is interpreted to be a patch reef or late-stage buildups formed during the early drowning of the platform (R1: Fig. 4.8). From the top, this unit is bounded by the seismic surface SH6 that is interpreted as a seismic unconformity, retreating towards the top of the platform. Overall, unit S6 largely shows aggradational to backstepping stratal geometries at the margins. This unit inferred an Early Eocene to Earliest-Middle Eocene age. The age control is primarily derived from the well Pak-G2-1 (Shahzad et al., 2018).

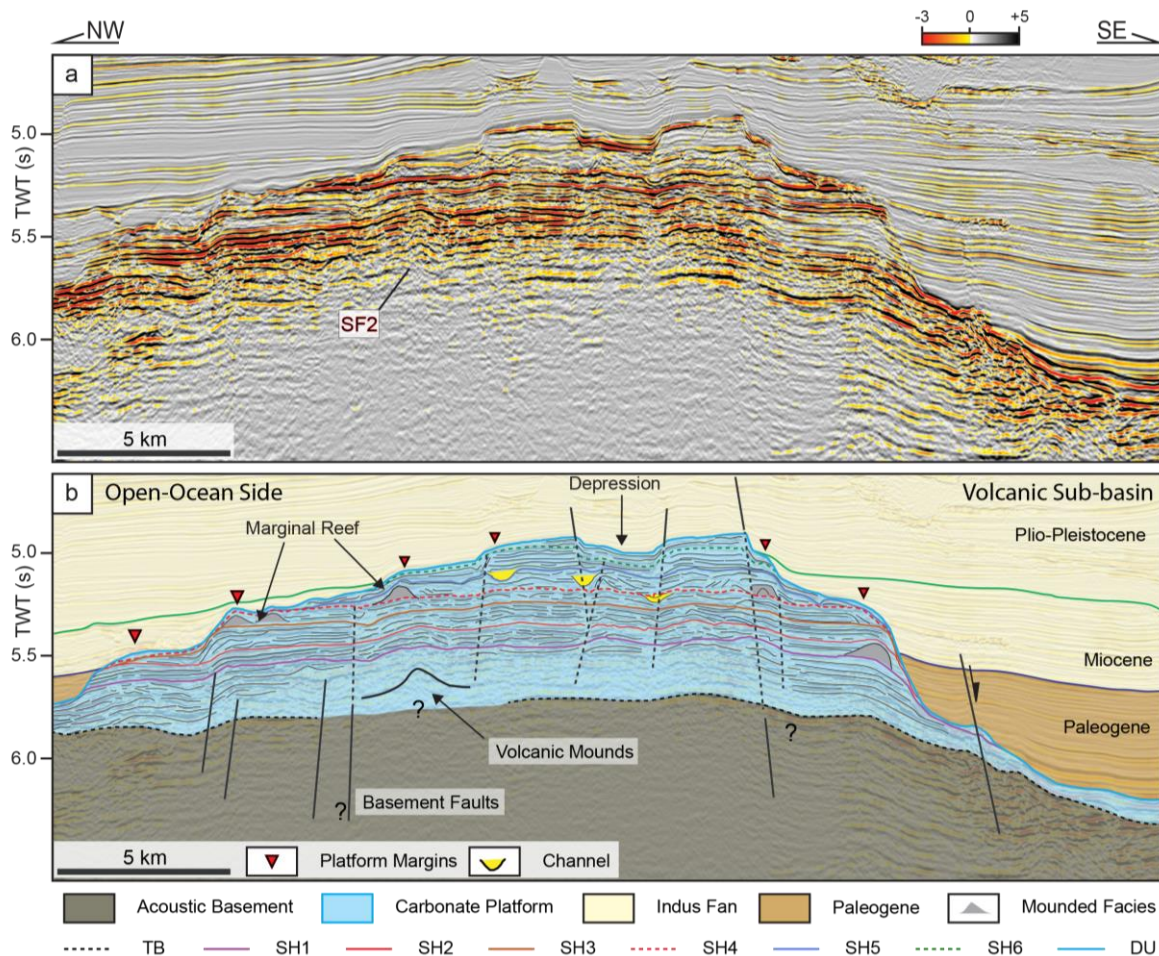


Figure 4.12: (a) A zoomed section of the northwest-southeast oriented regional seismic profile. (b) Interpreted section of a carbonate platform CP-3 showing the main seismic units and their respective bounding surfaces and characterization of the internal depositional geometries and structural deformation (for location refer to figure 4.1b). (Vertical Exaggeration =6)

Seismic unit S7 forms the youngest carbonate unit (Fig. 4.8). On average, this unit shows SF1 facies that are interpreted to represent late stage buildups (sensu Erlich, 1990) and patch reefs (Belopolsky and Droxler, 2003) with a significant relief. The thin unit between the mounds is seismically similar to the facies of unit S6. The unit is bounded at the top by a high amplitude DU surface. This surface has an irregular topographic relief with depressions up to 100 ms deep and 1 km wide (Figs. 4.8 and 4.12), which are draped by low amplitude reflections (Figs. 4.10 and 4.13). The DU surface is interpreted as the drowning unconformity, based on the localized growth of late-stage buildups, and reported deep water

facies lying above the shallow water carbonates in the well Pak-G2-1 (Shahzad et al., 2018). It can be traced regionally as the Top Carbonate surface.

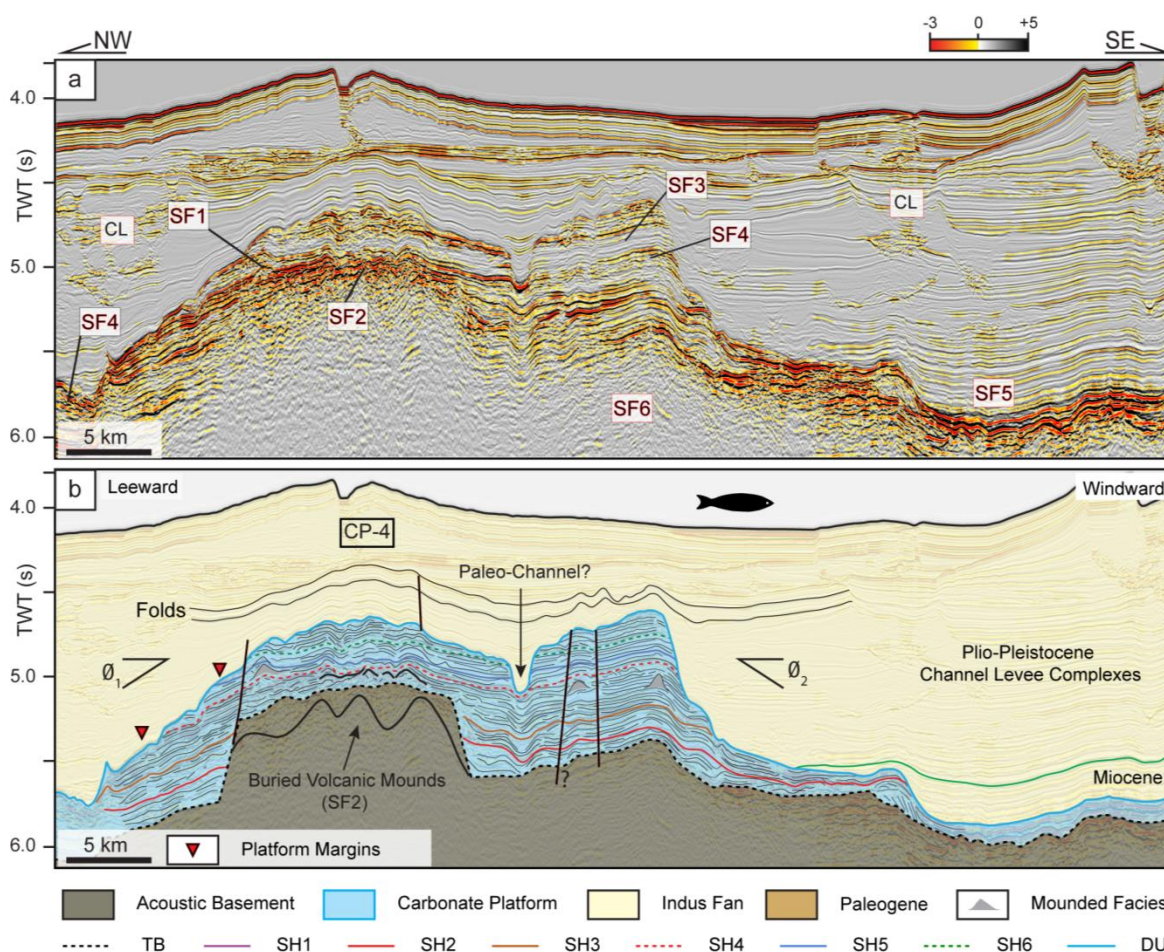


Figure 4.13: (a) Zoomed section of a northwest-southeast oriented regional seismic profile. (b) Interpreted section of carbonate platform CP-4 showing the main seismic units and their respective bounding surfaces and characterization of the internal depositional geometries. The identified windward margin is steeper (θ_2) than the leeward margin (θ_1) (for location refers to figure 4.1b). (Vertical Exaggeration =10)

4.4.4 Seismic interpretation and paleogeography

4.4.4.1 Carbonate platform evolution

The mapping of the seismic reflection data identify the structures CP-1 and CP-2 as the oldest carbonate platform growing in the study area (Fig. 4.14). A series of stacked reflectors, onlapping the Top Basement which forms the foundation of the carbonate banks (Fig. 4.9), indicates initiation of carbonate growth in the form of small patches around the subsiding volcanic substrate (Figs. 4.9 and 4.10). This is interpreted as a transgressive episode, which appears to be synchronous with deposition of marine shales on the shelf, overlying the shallow marine Paleocene sands encountered in the well Karachi-South-1A (e.g. Fig. 4.5). By keeping pace with the relative sea-level, the shallow water carbonate production spread over the basement highs. The discontinuous seismic reflections in unit S1 can be explained by the existence of small patches of shallow water carbonate bodies, which are below the seismic resolution and appear as discontinuous seismic reflections.

Following unit S1, the carbonate platform margins developed aggrading and backstepping geometries (Figs. 4.8 and 4.10). In response, the platforms contracted in size, forming high reliefs during formation of seismic unit S2, S3, and S4 (Figs. 4.9 – 4.12 and 4.14). Parallel to subparallel seismic reflections in the interior (Fig. 4.9) of the platforms are interpreted as lagoonal sediments (SF3), possibly alternating between mudstone to wackestones. The aggradational phase prevails up to horizon SH4. Small scale incisions are observed in the upper part of seismic unit S4 (e.g. Figs. 4.10 and 4.11) which are attributed to a relative sea-level fall that exposed the carbonate platform. The carbonate factory reinitiated with the next sea level rise along on the topographic highs (Fig. 4.14). This episode of rising sea level triggered the development of the large-scale terrace T1 (Fig. 4.11), and the areal extent of carbonate platform further contracted. This shrinking of the platform top through backstepping is associated with a significant increase in relief (Figs. 4.8-4.12). Several small scale patch and platform marginal reefs were also developed during the formation of this unit (Fig. 4.9).

During the deposition of seismic units S6 and S7, shallow-water platform areas shrank until they gave up and were drowned. With the drowning phase of the isolated carbonate platforms, the growth geometry of the flat-topped platforms turned into mound-shaped late stage buildups. This is interpreted to reflect submergence below wave base and a final episode of sub-photic mound growths, similar to examples described elsewhere (Erlich et al., 1990). Seismically, a high-amplitude condensed sequence covers the carbonate platforms after the final drowning. This sequence is interpreted to be composed of pelagic to hemipelagic sediments, based on the reported abundance of planktonic foraminifera in the well Pak-G2-1 (Fig. 4.4b; Shahzad et al., 2018). However, this condensed sequence can be diachronous as a function of the possible variations of the growth potential of each platform, because post-drowning onlapping strata are of different age (Fig. 4.7).

The drowning of carbonate platforms in the Offshore Indus Basin occurred in the Early to Middle Eocene (Figs. 4.3 and 4.14). However, the onlapping geometries of basinal sediments and lack of any terrigenous sediment in the well data suggest that the drowning event took place prior to the arrival of terrigenous sediments of the Indus Fan. Shallow-water carbonates continued accumulating on the shelf until the Oligocene (Figs. 4.5 and 4.14).

4.4.4.2 Carbonate platform margin development

Platform margins show different growth patterns leading to asymmetrical growth architecture (Figs. 4.10, 4.12 and 4.13). At the backstepping northwestern margins, the average width of the terraces is between 500 and 3000 m, (Figs. 4.9-4.10, 4.12 and 4.13). These terraces are draped by the seismically semi-transparent reflections of low to medium amplitude (Fig. 4.11). In contrast, platform margins facing southeast show aggradation and slight retrogradation, thus forming an escarpment slope towards the enclosed volcanic sub-basin (Fig. 4.7). This key observation is taken as the indication that the southeastern margins of the carbonate platform correspond to the windward margin, while the northwestern margins would be the leeward margin, taking the Great Bahama Bank margins as an analog where the aggrading margins are windward (Eberli and Ginsburg, 1989). Further, in contrast to the

windward margin, the slopes of the leeward margins show concave-upward features covering the terraces (Figs. 4.10, 4.12 and 4.13). These indentations are interpreted to reflect the post-depositional reworking of the slopes by ocean currents.

4.4.5 Structural trends

The study area comprises a series of horst and graben structures along the Somnath ridge aligned parallel to the Owen Fracture Zone (Fig. 4.2; Malod et al., 1997). However, the seismic data indicates that the Somnath Ridge Carbonate Platforms are structurally more deformed as compare to Saurashtra High carbonate platform, suggesting the structural deformation is not uniform in the carbonate platforms. On the seismic profiles, two different types of structural styles are recognized. A set of westward dipping faults are evident along the northwestern margin of platforms CP-3 and CP-4 that extends to the volcanic basement (Figs. 4.10, 4.12 and 4.13). These faults exhibit a net normal displacement with a relatively small throw of 20-30 ms and contributed to the development of the fault-bounded terraces along the northwestern margin during the development of unit S4 and S5 (Fig. 4.12). The fault-bounded terraces (e.g. in Fig. 4.12), are topped by the mounded facies as marginal reefs. These marginal reefs are seismically chaotic and reflection free- similarly to SF1 and are separated by intervals of more continuous, parallel and high amplitude reflectors representing the SF3 seismic facies. The backstepping pattern of marginal reefs associated with the large scale terraces indicates a synsedimentary movement along the actively subsiding blocks where the downward moving block turns carbonate growth into catch-up before leading to the partial drowning of carbonate margin. However, the homogenous nature of the volcanic basement constrains the recognition of fault displacement in the basement due to sub-basalt seismic imaging and the low impedance contrast between the displaced rocks. In contrast to the western margin, the eastern margin of the CP-4 platform is rarely typified by faulting.

Furthermore, the seismic profiles show that the carbonate platforms are blanketed by the draping of low amplitude reflections (Figs. 4.8, 4.10, 4.11 and 4.13). These reflections appear slightly folded above the carbonate platform with varying thickness between the carbonate platform and the rest of the basin. The folding of the draping reflections is interpreted as the result of varying subsidence rate over the rigid carbonate platform topographies. This interpretation is supported by the observation that the set of faults originate along the margins of the buildups and pierce upwards into overlying drape-over sequences (Figs. 4.7, 4.10 and 4.12). However, particularly in CP-4, the deformation of the overlying strata becomes more intense and strata are folded together with the younger units of carbonate platforms (Fig. 4.13). This deformation is interpreted as a post-depositional effect in response to the passive folding due to reactivation of the basement faults along the margin of the carbonate platform.

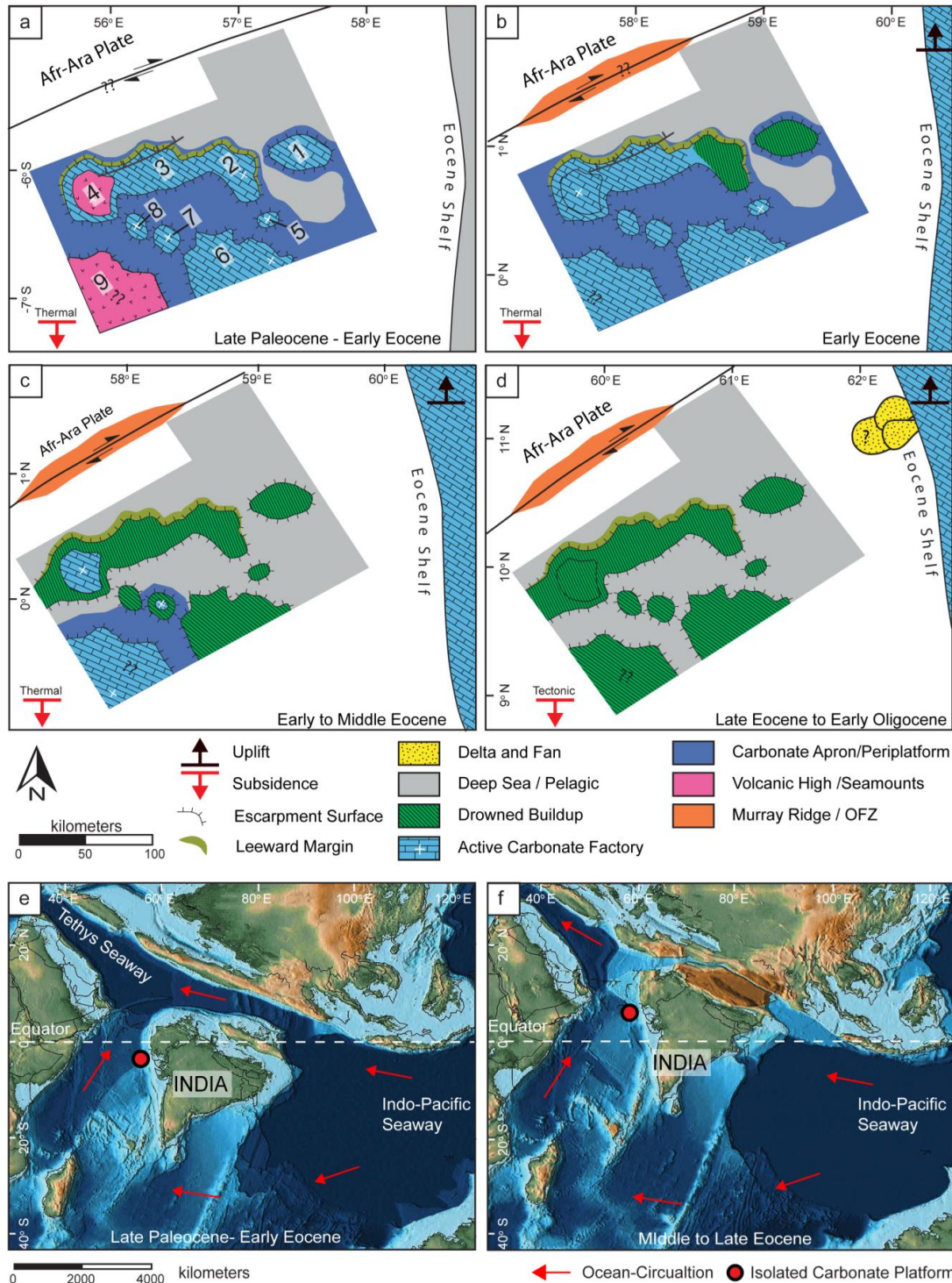


Figure 4.14: Seismic and well data based paleogeographic illustration of the Paleocene-Eocene carbonate platforms and buildups, with reference to their contemporaneous shelf margin. The maps represent the Late Paleocene to Early Oligocene development and reflect the interplay between carbonate platform growth and tectonic evolution. The Paleo-latitudes and rotation of the Indian Plate are calculated by Van Hinsbergen et al. (2015) and Copley et al. (2010). (a) Late Paleocene to Early Eocene: the carbonate growth was initiated during the Middle to Late Paleocene when most of the volcanic highs were inundated. The contemporaneous shelf region was dominated by the deep to shallow marine environment. During this time, leeward platform flanks developed staircase-shaped backstepping. (b) Early Eocene: during this time, the platforms located on the most proximal part of the basin drowned. Carbonate platform growth focused on elevated volcanic and structural highs. (Continued to the next page)

4.4.6 Subsidence and accommodation

The impact of the basement subsidence on accommodation during the deposition of the carbonate platforms is illustrated in a plot of the sedimentary thickness as a function of their ages (Fig. 4.15). The stratigraphic information such as thickness and ages of the stratigraphic units were obtained from well Pak-G2-1 (Calvès et al., 2008; Shahzad et al., 2018). The stratigraphic input data were de-compacted with the assumption that there was no significant erosion of platform strata occurred during the platform growth (Allen and Allen, 2013; Sclater and Christie, 1980). The paleobathymetric estimates of the pre- and post-drowning stratigraphic successions were derived from the micropaleontological data of well Pak-G2-1 (Shahzad et al., 2018), and based on the assumption that the volcanics erupted at or near sea level. The approximate age of this surface was estimated to 65 Ma (Calvès et al., 2008; Corfield et al., 2010). It is further assumed that the flat platform tops during growth essentially sea level, i.e. were lying in less than 30 m of water depth which is in the zone of the maximum growth potential of tropical carbonate factories (Calvès et al., 2008; Shahzad et al., 2018).

The graph represents the estimated burial rates as the subsidence of Top Basement which may have a corresponding error related to biostratigraphic age control, the de-compaction model and the sea level data in estimating paleobathymetry whereas the additional uncertainty relates to the depth conversion below the carbonates to the basement and a gap between the final cessation of volcanism and earliest carbonate deposition.

The plot shows three different phases with distinct subsidence patterns (Fig. 4.15). The oldest phase, i.e. the phase of basin subsidence following the breakup event of the West Indian Continental Margin. This time represents an accumulation rate of the carbonate platforms > 80 m/Ma. The second phase covered the pelagic deposition from Early Eocene to Middle Miocene, which reflects the lowest sedimentation rate (3–4 m/Ma) with increased water depths corresponding the post-drowning sediment starvation of the basin. This phase was followed by the higher sedimentation rate (> 130 m/Ma) due to the excessive sediments loading of the Indus Fan and the Neogene flexural modification in response to the Indian Plate interaction with the Arabian Plate.

The resultant burial curve as the basement subsidence follows the generalized trend of passive margins (Xie and Heller, 2009). Two different scenarios can be driven from this analysis: shallow-water carbonate sedimentation took place during an initial quick phase of subsidence that was followed by a slow subsidence phase.

(continued from Fig.4.14) (c) Early to Middle Eocene: a subsequent sea level rise caused the drowning of most of the carbonate buildups and carbonate growth was restricted to the tectonic highs along the most distal part of the basin. During this time, the shelf margin is characterized by an extensive shallow marine carbonate platform. (d) Late Eocene to Early Oligocene: Tectonic engagement between Indian and Arabian Plate increased significantly during this time, and the Murray Ridge was an initial topographic high. The detached carbonate platforms were completely submerged. However, the carbonate growth continued on the continental shelf that was tectonically uplifted. Probably, the proto-Indus delta began to develop during this time. (e) and (f) illustration of the Indian Plate with respect to the equatorial belt and paleo-seaways (Haq, 1981; Scotese, 2001).

In this scenario, the drowning of the isolated carbonate platforms can be attributed due to a relative sea level rise controlled by eustasy (Miller et al., 2011). In the second case, the slow cooling of the lithosphere following the rapid movement of the Indian Plate away from the Réunion Hotspot (Fig. 4.15) coincides with carbonate deposition and after that, the platforms drowned during the rapid subsidence phase of the volcanic margin as suggested by Calves et al. (2008).

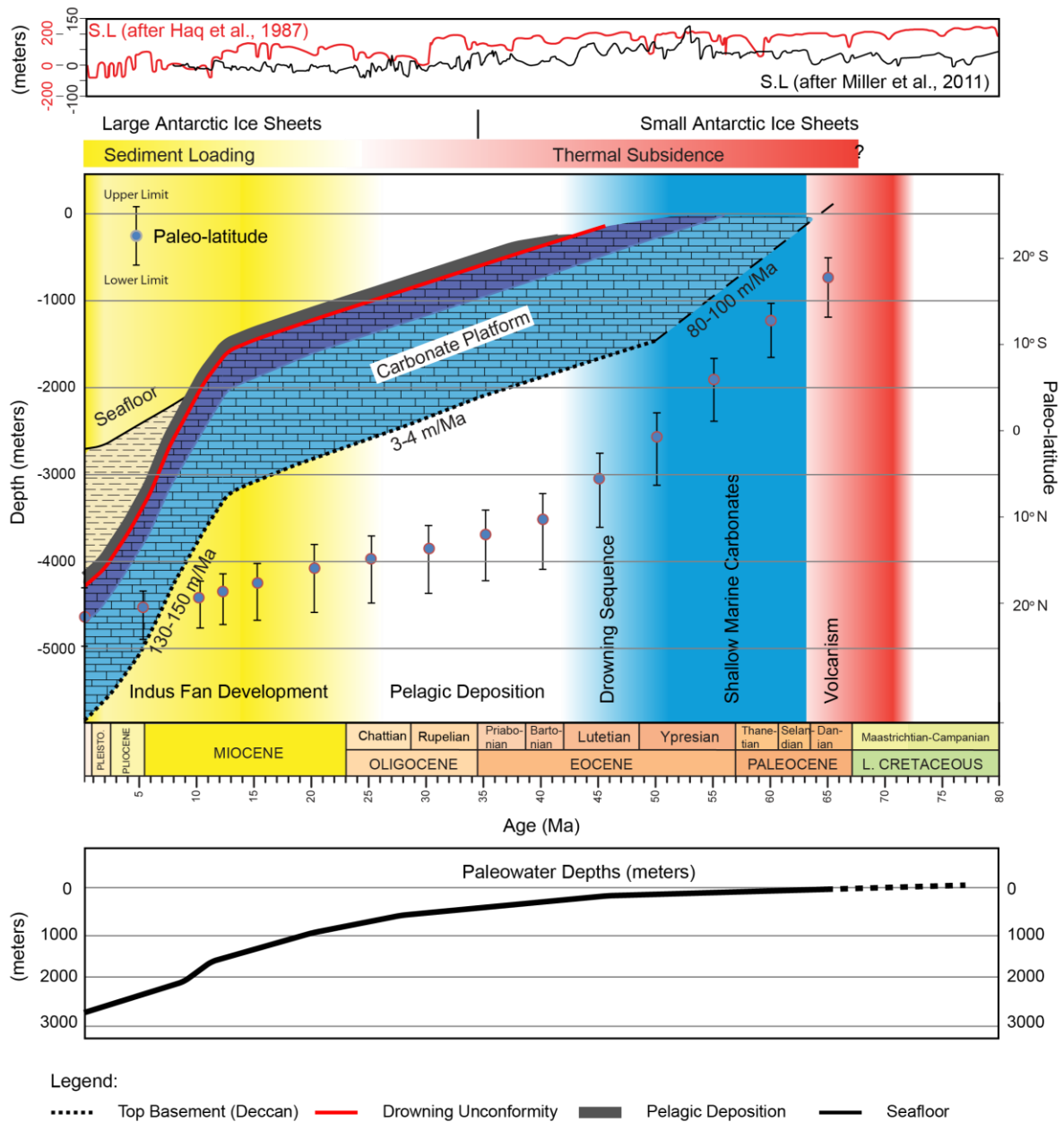


Figure 4.15: The burial history reconstruction of the well Pak-G2-1 and basement subsidence together with changing latitude (van Hinsbergen et al., 2015) and eustasy (Haq et al., 1987; Miller et al., 2011). SL: Sea level

4.5 Discussion

4.5.1 Controls on carbonate platform evolution

4.5.1.1 Volcanic ridges as antecedent topography

Isolated carbonate platforms of the Offshore Indus Basin are classified as of the volcanic pedestal platform type (*sensu* Bosence, 2005) which developed on the top of pre-existing volcanic seamounts and ridges, surrounded by deep water settings, and therefore isolated from any terrigenous sediment supply. In essence, the spatial distribution and morphologies of the isolated carbonate platforms, their steep slopes, their shapes and platform sizes seem strictly dictated by the volcanic basement. The contact between the Top Basement and the overlying carbonate succession has never been drilled in deeper part of the basin, however, a Late Cretaceous to Early Paleocene age has been suggested for the development of volcanic seamounts with respect to the volcanic eruption of the Réunion Hotspot and emplacement of the Deccan Traps during the northward movement of Indian Plate (Carmichael et al., 2009; Corfield et al., 2010; Calvès et al., 2011). This time period is associated with the recovery of the photic reef system of the Tethyan Realm, following the worldwide Cretaceous-Tertiary demise of reef builders (Baceta et al., 2005). The linear trends of the NE-SW oriented volcanic seamounts and ridges can be the result of the northward drift of the Indian Plate over the Réunion Hotspot mantle Plume (Duncan, 1990; Copley et al., 2010). Different cooling ages of the lithosphere can also explain the diachronous nature of the drowning surface as the seamount located in the north part of the basin subside comparatively earlier than the southern part basin with respect to the relative distance from the Réunion Plume.

Further, the volcanic ridges are nearly flattened in shape (e.g., Figs. 4.7 and 4.8). Since the final phase of volcanism occurred subaerially, the action of the surface waves resulted in the formation of guyots with subsequent onset of carbonate platforms. As analogous to volcanic ridge models (e.g. Hawaii or Réunion Hotspot volcanic islands and seamounts; Moore and Fornari, 1984; Moore and Clague, 1992; Duncan, 1990), this is comparable to the formation of guyots from relict volcanic seamounts, and the upward growth of shallow water carbonates into well-developed carbonate platforms (Courgeon et al., 2017; Paumard et al., 2017). These observations further elucidate that the nucleation of the carbonate platforms is controlled by the surface area of each volcanic edifice, (e.g. Figs. 4.3, 4.4c-d, 4.7 and 4.8) which was limited by the antecedent topography, and thus ultimately prevented the lateral expansion of shallow-water carbonate sedimentation to form coalesced platforms.

4.5.1.2 Platform geometries: sea level vs climate

The history of the major relative sea level fluctuations during the development of the isolated carbonate platforms is tentatively reconstructed from well facies, seismic facies and geometry such as platform aggradation, progradation, and erosion, interpreted to indicate phases of relative sea-level highstands and lowstands (Kendall and Schlager, 1981). However, the precise correlation of the seismic unit boundaries with an established eustatic curve is a rather difficult task because: 1) the age control of the deposits is not well constrained, 2) the long-

term thermal subsidence and the local tectonic control obscure the true eustatic impact, and/or 3) not all the mapped seismic surfaces are subaerial unconformities.

Following the initiation of the carbonate platform, the thick aggrading and backstepping geometries of the carbonate platforms are interpreted as the phase of long-term relative sea level rise that is interrupted by short-term sea level falls. The first sea level fall is recognized following the seismic unit S4 that generated unconformity SH5 with possible subaerial exposure. This time could be roughly comparable to the sea level fall around the Late Paleocene (Haq et al., 1987; Miller et al., 2011; Sluijs et al., 2008). A second sea level fall is proposed as having formed seismic surface SH6, in the Early Eocene, preceding the final drowning of the carbonate platform.

Relative sea level changes are the product of tectonically-induced vertical movements and eustasy (Posamentier et al., 1988). In the study area, the long-term increase in accommodation was driven by the thermal subsidence of the western continental margin of India during the Paleogene (Calvès et al., 2008; Misra et al., 2017). According to Zachos et al. (2001), this period of time is characterized by greenhouse climate conditions with small or no continental ice sheets. Sluijs et al. (2008) suggested the existence of small ice sheets on the elevated regions of Antarctica, which could be responsible for the low amplitude and high-frequency sea level fluctuations. Since the eustatic changes during the greenhouse interval are thought to be comparatively shorter than during ice-house climatic periods (Speijer et al., 1996; Abreu and Anderson, 1998), sea level falls would sub-aerially expose reefs and platforms for short time intervals.

Moreover, the climatic perturbations of this period also affected the Tethyan-wide coral communities. Reef-building coral species were replaced by extensive accumulations of larger benthic foraminifera at the Paleocene Eocene transition (Scheibner et al., 2005; Scheibner and Speijer, 2008b; Speijer et al., 2012). The larger benthic foraminifera assemblages reported for the well Pak-G2-1 (Shahzad et al., 2018) are similar to other assemblages described for the Paleocene-Eocene shallow water carbonate factories from the Tethyan realm. Therefore, it is suggested that the low amplitude eustatic changes and the lack of framework builders strongly affected the vertical growth of carbonate accumulation. Phases with small sea level rise created shallow lagoons with easily filled accommodation. This resulted in carbonate platforms to be composed of a markedly layer-cake stratigraphy, and prominent aggrading stratigraphic stacking cycles with only minor seismic reefs. Based on the anticipated age of the carbonate platforms, the bioconstruction of these seismic reefs can be compared with *Nummulites* or *Alveolina* banks (Arni, 1967; Eichenseer and Luterbacher, 1992; Racey, 2001; Jorjy et al., 2006) or marginal shoals (Markello et al., 2008) rather than coral reefs with frameworks that characterize modern atolls. As a result, the balance between subsidence and the low-amplitude eustatic fluctuations kept the carbonate platform uniformly aggrading and resulted in relatively thin packages of keep-up facies, rather than constructing a wave resistant-ring reef enclosing lagoons such as empty bucket platforms (Purdy and Gischler, 2005; Schlager and Purkis, 2013). Thus, facies are laterally well connected, and bank tops are laterally continuous and flat. The relative sea level falls and rises probably produced short-term exposure and drowning surfaces respectively and their signs might be

below seismic resolution. According to Kiessling et al. (2002), the basinward shedding of such type of carbonate factory is extremely rare during this time interval.

4.5.1.3 Tectonic influence and platform backstepping

The collision of the Indian and the Eurasian Plates with the related closure of the Tethys Seaway was one of the most important tectonic events in the Cenozoic geological history. It did not only impact onto the global paleoclimate and paleoceanography but also played a role in the local tectonics that in turn strongly influenced the deposition of carbonate platforms in the Indian-Ocean (Aubert and Droxler, 1996; Saqab and Bourget, 2015; Wilson, 2011).

Backstepping of carbonate platform margins is commonly attributed to phases of relative sea level rise that slightly outpace the platform growth potential and therefore platform margins retreat stepwise towards the interior lagoon (Menier et al., 2014). The particular event that has led to the drowning of the Paleogene carbonate platform is unclear, but it seems that the regional and local tectonic were primary drivers.

The differential subsidence due to the reactivation of basement faults is interpreted to be responsible for the formation of the stair-step like backstepping along the western margin. The syndepositional fault movements forced platform margins to repeatedly retreat which well-developed small reef rims along the edges of the footwall blocks (Fig. 4.16). We favor this interpretation because the carbonate platform margins did not backstep synchronously from all direction (Figs. 4.10 and 4.12). Alternatively, the terrace T1 could also bear controlled to a certain degree by a sea level rise following a phase of subaerial exposure. Sluijjs et al. (2008) reported episodes of quick eustatic rises during the Paleocene-Eocene Thermal Maximum following a short-term eustatic fall reported in the Late Paleocene succession.

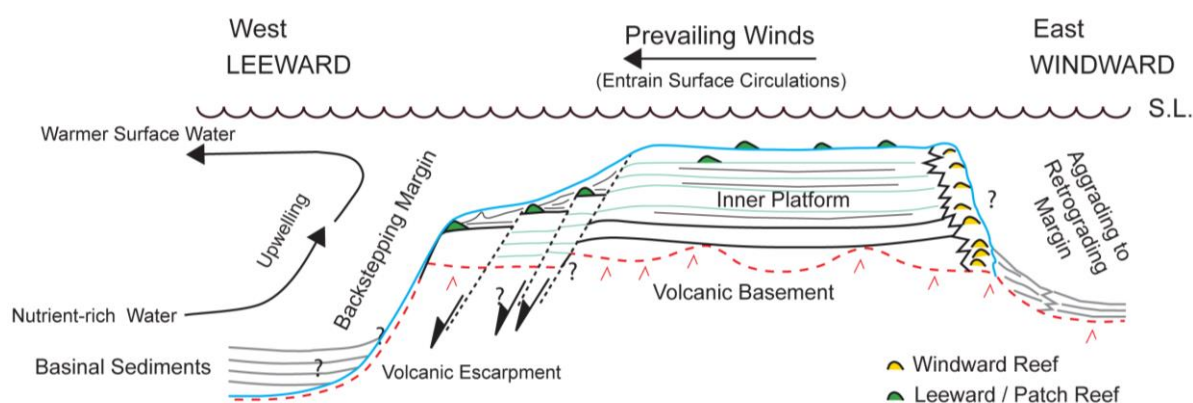


Figure 4.16: Line drawing of the NW-SE seismic transects which illustrates the features of the CP-3 carbonate platform. The windward side is characterized as an aggrading margin while the leeward margin is structurally modified. The high angle escarpment surfaces and faults modified the lateral facies distribution within the platform. S.L: Sea Level

The mechanism of backstepping margins could also be explained by the oceanic upwelling introducing eutrophic conditions. Assuming that atmospheric circulations similar to the

present day acted at the time of platform growth, the paleogeographical reconstruction of the Indian Plate suggests that the study area was located in the equatorial and tropical settings (10° Latitudes) within the Intertropical Convergence Zone (ITCZ) (Figs. 4.14e-f). Moreover, the currents in the Indo-pacific seaways were actively flowing westward connecting with the Tethys seaways and perhaps developed a local geostrophic flow along the western margin of the Indian continent. This circulation pattern could result in oceanic/coastal upwelling in the area of the isolated carbonate platforms. These conditions may have developed localized or regional eutrophic conditions that threatened the shallow water carbonate factories and forced the carbonate platform margins to retreat and backstep. However, in this scenario, the backstepping should be gradual rather than episodic.

4.5.2 Comparison with the Indian Ocean carbonate platform

Subsurface examples of Paleocene and Eocene carbonate platforms were rarely documented in the past. In comparison with the Maldives carbonate platforms, the observations concur with the Eocene platform succession as described by Aubert and Droxler (1996). In both examples, the accommodation space for carbonate sedimentation is provided by the thermal subsidence of the volcanic pedestal.

The Eocene succession of the Maldives carbonate platforms developed during a greenhouse time and internally contain an apparent layer cake stratigraphy with meter-scale stratigraphic cycles. The stratigraphic geometries are largely aggradational in this platform, escorted by the steep slopes descending to oceanic depths and apparently lacks wave resistant reefs structures. Because the sea level during greenhouse times does not change so drastically as during icehouse times, this resulted in a uniform deposition across the platform, and the marginal facies do not dramatically shift. Moreover, wave-resistant reef structures were absent or not very extensive during the Eocene and the carbonate factory could therefore not develop a high topographic relief, as it is the case in Neogene times. Consequently, the development of fringing or barrier reefs and therefore bucket geometries are less reported in greenhouse carbonate platforms (Purdy and Gischler, 2005). In term of biota, the quoted examples also share similarities with an abundance of benthic foraminifera such as nummulites. However, the Paleogene succession in the Maldives persisted until the Late Oligocene time (Aubert and Droxler, 1996). The Indus offshore example, on the contrary, drowned at the end of Early Eocene. These results confirm that, albeit the platforms are comparable in stratigraphy and morphology, the regional climatic and tectonic settings had a strong imprint on Indus Offshore carbonate platforms.

Chapter V

Seismic architecture and stratigraphy of the Indus Fan

5.1 Outline of the chapter

In contrast to chapters III and IV, which describe the evolution and stratigraphic architecture of the Paleocene-Eocene carbonate succession of the Offshore Indus Basin, Chapter V examines the shelf to basin stratigraphy and sedimentary dynamics of the Indus Fan that is deposited since the Paleogene. Previously published work (McHargue and Webb, 1986; Kolla and Coumes, 1987; Clift et al., 2001) discussed the evolution, internal structure, and sedimentation of the entire fan on very low-resolution seismic data. By using the high resolution seismic and well data, this chapter examines not only the architecture and stratigraphy of the Indus Fan but also of the coeval shelf deposits thus providing the understanding of the variability of the different depositional processes which acted along with the canyon-channel systems. Further, the chapter describes the evolution of one of the youngest channel-levee system based on seismic facies and interpreted depositional and erosional features.

5.2 Regional settings

5.2.1 Geological settings

The Indus Fan is the most pronounced sedimentary feature of the Arabian Sea as well as the second largest submarine fan in the world, after the Bengal Fan (Fig. 5.1; Kolla and Coumes, 1987). It developed in the northern Arabian Sea since the beginning of the Himalayan Orogeny during the Eocene. It is a mud-dominated fine-grained turbidite and submarine fan system, fed by the important northern rivers of the Indus drainage basin and contains much of the material eroded from the Himalaya, Karakoram and Hindukush mountain ranges (Clift et al., 2001).

Tectonically, the Indus Fan is located at the triple junction of the Indian, Arabian and Eurasian Plates. The fan is bounded to the north by the continental slope of Pakistan and India, to the east by the Chagos-Laccadive Ridge, and to the southwest by the Carlsberg Ridge (Fig. 5.1). To the northwest, it is boarded by the Murray Ridge and Owen Fracture Zone which is an important topographic feature that developed as a result of stresses induced by plate organization events (Rodriguez et al., 2014). The uplift of the Murray Ridge and Owen Fracture Zone has restricted the eastern sedimentary depocenters of the Offshore Indus Basin from the western depocenters of the Makran sedimentary province at least since the Late Miocene (Fig. 5.1 ; Clift et al., 2001; Gaedicke et al., 2002b; Bourget et al., 2013).

The structural evolution of the sedimentary province resulted from three main tectonic events including: i) the Late Cretaceous rifting and seafloor spreading at the Carlsberg Ridge that caused the separation of the Indian Plate from Seychelles during the Early Paleocene, ii) the northward drift of the Indian Plate along the Owen Fracture Zone and Murray Ridge, and iii)

the commencement of the Indian-Eurasian Plate collision during the Eocene with the formation of the Himalayan mountain belts (Edwards et al., 2000; Carmichael et al., 2009; Chatterjee et al., 2013). The collision event uplifted the northern and western mountains along plate boundaries episodically, first during the Miocene and then during the Late Pliocene to Middle Pleistocene (Gaedicke et al., 2002b). These tectonic events are evidenced by onshore and nearshore erosion which resulted in the significant deposition of detritus in the Greater Indus Basin (Clift et al., 2001).

The onset of the Indus Fan formation has been discussed for the last four decades (Clift et al., 2001; Droz and Bellaiche, 1991; Gaedicke et al., 2002b; Kolla and Coumes, 1987; McHargue and Webb, 1986). According to Clift et al. (2001), the sedimentation of the Indus Fan started at least during the Middle Eocene. Further Clift et al. (2008) postulated varying sedimentation phases of the Indus Fan during the Neogene Himalayan exhumation, coupled to the monsoon intensity and with the Miocene and Plio-Pleistocene sea level lowering (Kolla and Coumes, 1987; Prins et al., 2000).

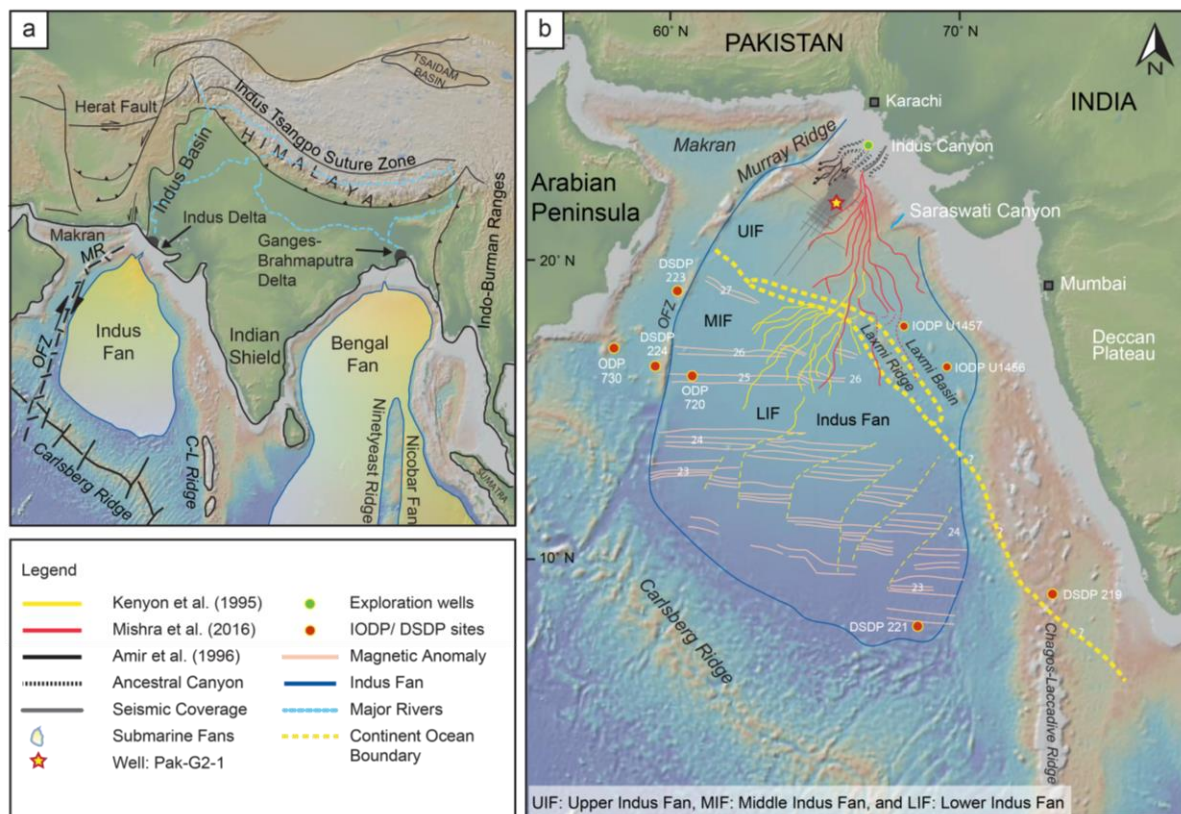


Figure 5.1: (a) Regional tectonic structure and bathymetry of the Arabian Sea and the Bay of Bengal (reproduced from Qayyum et al., 2001). The erosion products from the Himalayan ranges are transported by the Indus and Ganges-Brahmaputra River systems to the Indus and the Bengal Fan depocenters respectively. (b) Bathymetry of the Indus Fan and surroundings with the reconstruction of the Indus channel system (Kenyon et al., 1995; Deptuck et al., 2003; Mishra et al., 2016).

5.2.2 Fan morphology

The Indus Fan, covering an area of $1.1 \times 10^6 \text{ km}^2$, extends to the south over a length of 1500 km into the Indian Ocean from the present delta front with relative low gradients of c. 1 in

400 (Clift et al., 2001; Kenyon et al., 1995). The Indus Fan is approximately 9 km thick in its proximal setting, near the present-day shelf edge and thickness decreases towards the Carlsberg Ridge in the south where the water depth reaches 4500 m (Kolla and Coumes, 1987; Kenyon et al., 1995). Based on the fan morphology, Kolla and Coumes (1987) subdivided the Indus Fan into three fan territories, i.e., the Upper Indus Fan, the Lower Indus Fan and the Middle Indus Fan (Fig. 5.1). The study area considered here covers the present-day continental shelf to the upper and lower slope of the Upper Indus Fan.

The Upper Indus Fan is separated from the coastline by the 100 km wide continental shelf that is gently inclined basin-ward in the vicinity of the Indus Delta (von Rad and Tahir, 1997). The shelf break occurs at an average depth of ~125 m and is deeply incised by the Indus Canyon along the Pakistan-India margin (von Rad and Tahir, 1997). Today, the Indus canyon is the primary conduit for the source to sink sedimentary pathway of the Indus Basin which over a distance of 3000 km connects the Indus River to the ultra-deepwater settings of the Indus Fan (Inam et al., 2007; Clift et al., 2014).

The Indus Canyon is 185 km long with a starting water depth of less 20 m near the delta mouth and an average width of 8 km. It ends in a water depth of 1600 m where the canyon attains a width of about 20 km (von Rad and Tahir, 1997). The upper canyon floor (from 20 to 1350 m axial depth) is erosional (degradation) with steep walls, and the lower part (1350 m to 1500-1600 m axial depth) is the transition between the degradational canyon and the aggradational channel-levee systems of the Upper Indus Fan (von Rad and Tahir, 1997). At about 1000 m water depth, there is an eastward bend in the canyon which resembles turbiditic channel bends in the Northern Hemisphere attributed to the effects of the Coriolis force on the turbiditic flows (Kenyon et al., 1995). Further, several large channel-levee systems radiate from each canyon complex (McHargue and Webb, 1986; Kolla and Coumes, 1987).

5.3 Data and methods

5.3.1 Seismic and well data

A variety of data was used, including a dense grid of high-resolution 2D seismic surveys, lithological descriptions and log motifs of industrially wells (Fig. 5.2). The 2D time migrated seismic surveys consist of over 9000 km of high-resolution seismic data. The seismic surveys of the different vintages have been acquired for research and industrial (exploration) purposes during the 1990s and 2000s and serve as background for the herein presented interpretation. The seismic data cover the continental shelf to the ultra-deep-water settings of the basin (100 m to more than 3500 m; Fig. 5.2). This dataset covers an area further to the east to that studied by the McHargue and Webb (1986), and Deptuck et al. (2003).

5.3.2 Methodology

The post-stack time-migrated seismic sections and well data were introduced into the Petrel (Schlumberger) Software suite for stratigraphic and structural interpretation. Regional chronostratigraphic studies were incorporated to establish and map the regional stratigraphy. The stratigraphic model developed by Carmichael et al. (2009) was used for constraining our

interpretation of the deep-water settings. The seafloor surface was mapped on the seismic grid and was converted into bathymetry by using the standard water velocity of 1500 m/s (Fig. 5.2).

Much of our information about the sediments and age calibration of the Indus Fan comes from industrial and DSDP/IODP wells (Fig. 5.1). In this study, the Pak-G2-1 well is a primary source of lithological and stratigraphic information of the Neogene Fan deposits in the study area. However, no well reached to the base of the Indus Fan. The correlation of the Oligocene / Miocene horizons remains uncertain due to the distance of suitable well control, i.e. more than 1000 km to Karachi south-A1 well, whereas the Pak-G2-1 well recorded only sequences younger than the Middle Miocene (Fig. 5.3).

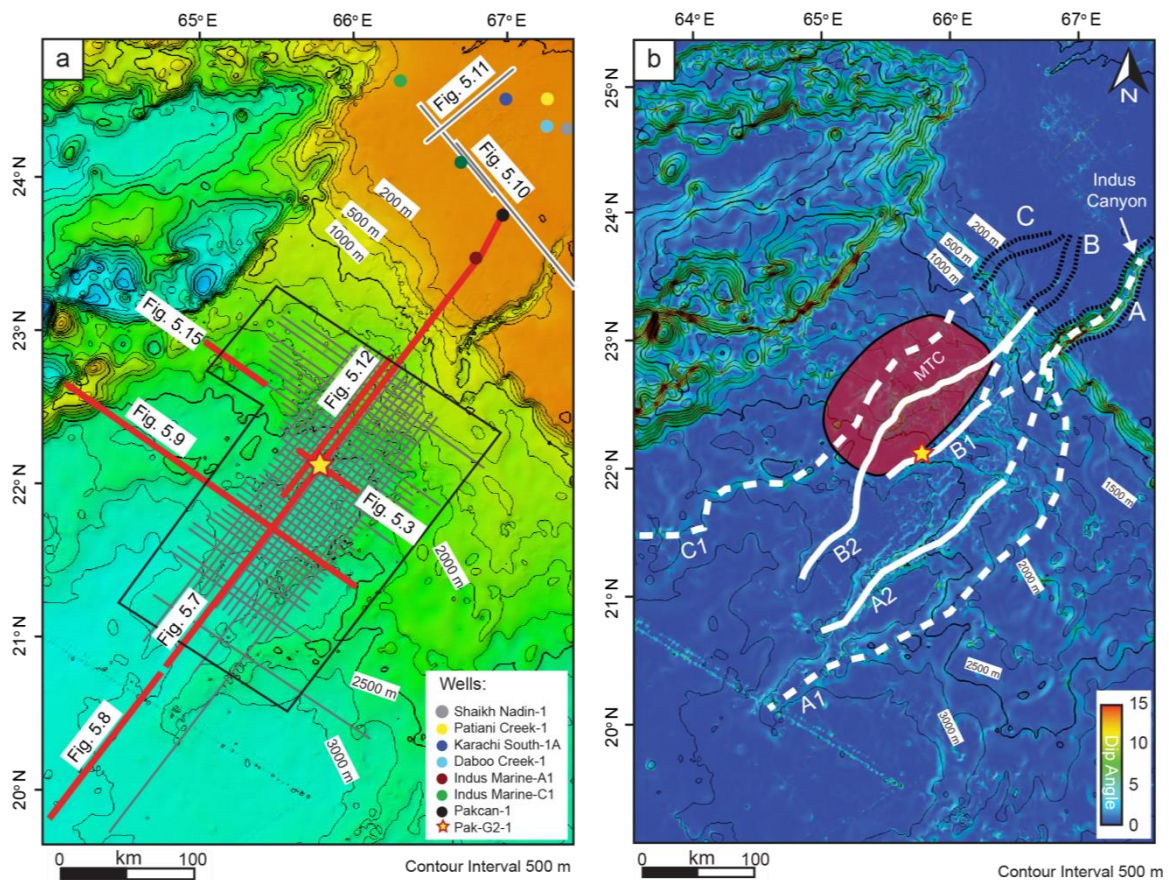


Figure 5.2: (a) Map of the Northern Arabian Sea with the position of the seismic profiles and industrial wells used within this study. (b) Calculated slope-angle map with the bathymetric contour lines. Continuous lines indicate the channel-levee complex with the better seismic coverage, and channel-levee complexes crossed by a limited number of the profiles are annotated with the dotted line. Red triangle indicates geographical position of mass transport complexes (MTCs).

In this study, the facies model of Posamentier and Kolla (2003) is adopted to characterize the individual sedimentary bodies of deep-water settings. This approach explains the organization of the depositional elements of the Indus Fan system into “architectural elements”. The subdivision of these architectural elements are based on key observations such as subtle seismic amplitude variations and reflection continuity (e.g. high versus low amplitude and continuous versus discontinuous), termination patterns against depositional and erosional bounding surfaces (e.g. erosive, gradual, planar and regular or irregular),

internal reflection configuration (e.g. longitudinal and lateral facies associations, sedimentary structures), and external forms (e.g. draping, wedge, channel filling, concave up, concave down and finger-like lenses, and sheets) (Prather et al., 2017). These seismic characteristics subdivide the primary facies into eight architectural elements (Tab. 5.1). With the integration of well data, the seismic data allow proposing an interpretation of the sediment type and the depositional environment. However, in the absence of lithological calibration from wells for certain elements, the interpretation of the facies composition and processes are inferred from drilling and seismic calibration of other geological studies previously published in the region or elsewhere (Fig. 5.3; McHargue and Webb, 1986; Kolla and Coumes, 1987; Flood et al., 1991; Hübscher et al., 1997; Posamentier and Kolla, 2003; Deptuck et al., 2003; Posamentier, 2003; Schwenk et al., 2005).

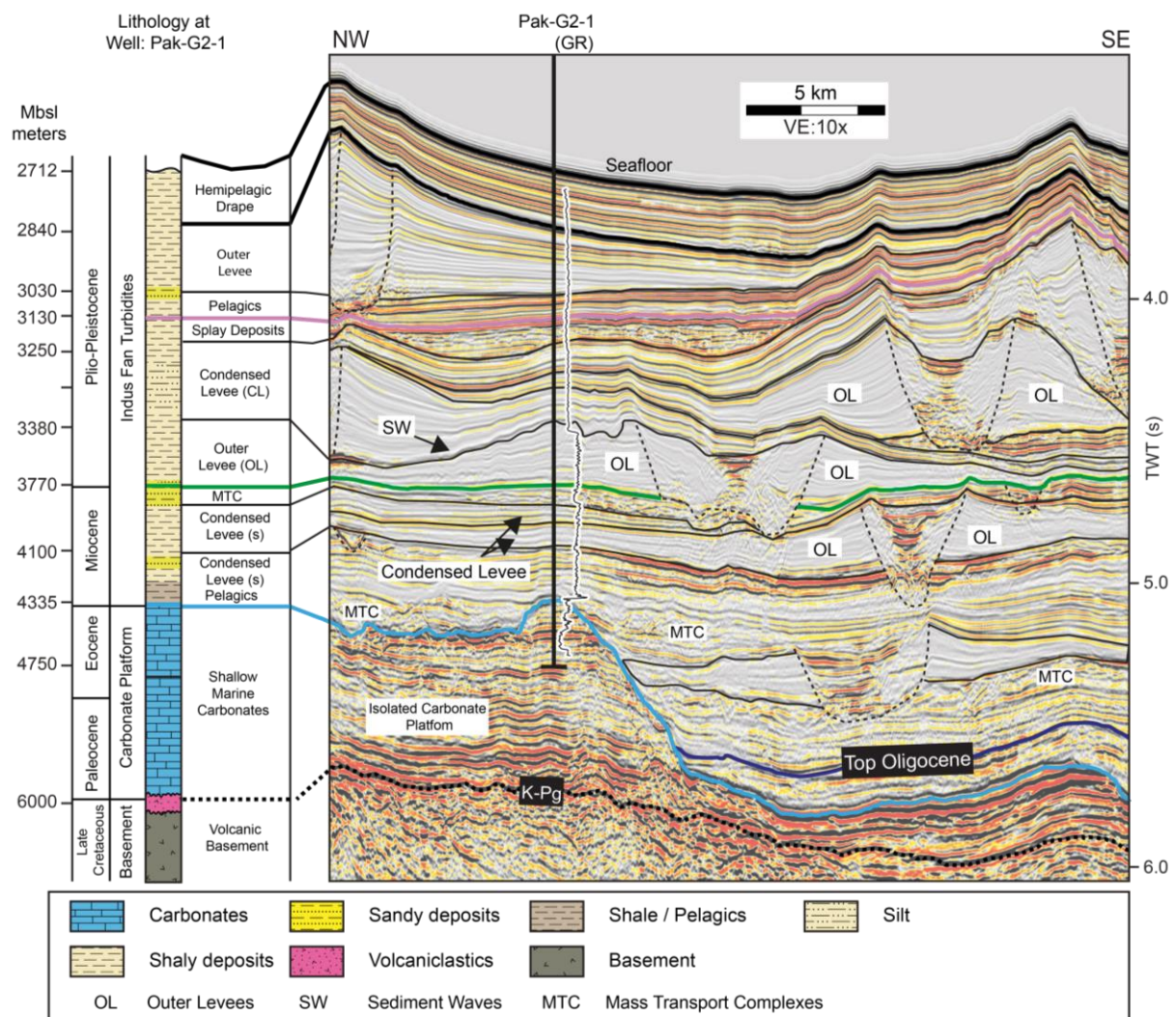


Figure 5.3: Well to seismic tie for the establishment of a chronostratigraphic framework of the Upper Indus Fan. Age, lithological information and Gamma-ray (GR) log are taken from the well Pak-G2-1. The interpretation of the depositional elements is based on the lithological information and seismic expressions observed in similar type of settings. Dotted lines mark the erosive surfaces of Channel-Levee Complexes.

5.3.3 Terminology

The term channel is used here to refer a conduit formed by conveying gravity flows. Submarine channels are V- or U-shaped negative relief features on at the seafloor that formed and maintained through the transportation and deposition of sediments by turbidity current flows over a relatively long period of time (Mutti and Normark, 1991). It may be either erosional or depositional (aggradational), or erosional/depositional mixed (McHargue and Webb, 1986).

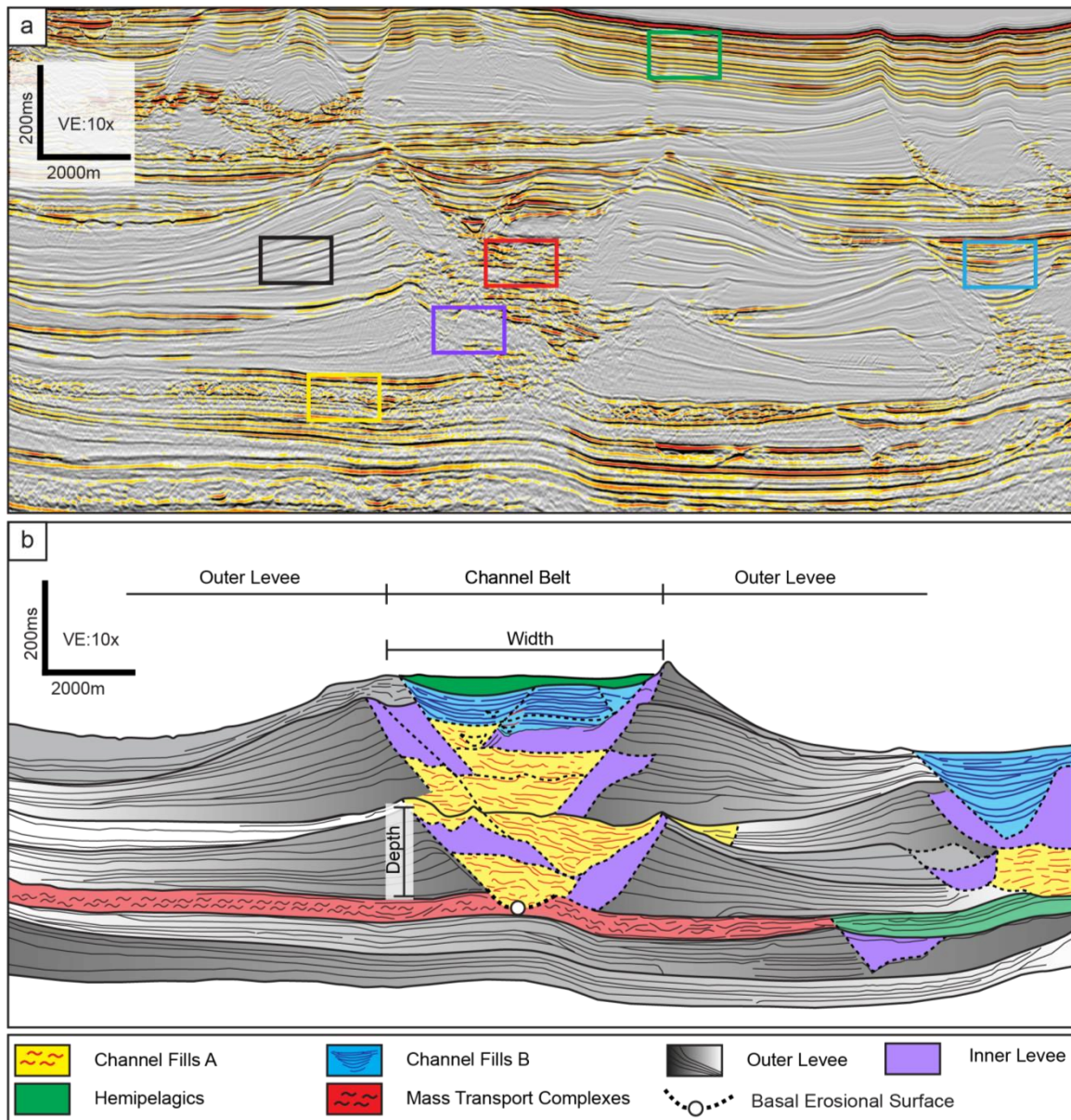


Figure 5.4: (a) Example of a channel-levee complex. Colored boxes show the spatial distributions of the facies examples in figure 5.5. (b) Figure highlighting the schematic distribution of the identified architectural elements of the channel-levee complexes of the Upper Indus Fan.

Channels with well-developed constructional wedges of sediments are known as channel-levee system or leveed channels. One or more leveed-channels overlap to form a channel-levee complex (CLC) (Wynn et al., 2007; Hansen et al., 2015). Channelized flow deposits

both inside and directly outside the conduit is referred as a channel belt. The deepest, hydraulic axial zone of the channel is termed as channel thalweg (Janocko et al., 2013; Hansen et al., 2015; Prather et al., 2017). Channel width is the maximum distance between the channel walls and the relief from the highest point of the outer levee to the channel base is referred as channel depth (Fig. 5.4). In order to avoid confusion amongst the terminology, submarine channels with well-developed margins (levees) are differentiated from erosional submarine valleys that markedly occur on the upper slope at the shelf edge, and without levees. The submarine leveed channels are a typical feature of the middle slope to basin floor that originates from shelf canyons, and radiate into the basin.

5.4 Results and discussion

5.4.1 Architectural elements of the Indus Delta and Fan system

Based on the seismic facies analysis in shelf to basin seismic transects, it is possible to identify several shelfal and deep-water depositional elements including shelf edge deltas, submarine erosional valleys as canyons, erosional surfaces, channel fills of deep-marine leveed channel complex and associated levees, frontal and crevasse splays, mass transport complexes, and hemipelagic deposits (Figs. 5.3, 5.4 and 5.6; Tab. 5.1). These deposits are presumed to be associated with turbidity flows and other mass transport processes, and their characteristics are discussed in detail in the following paragraphs.

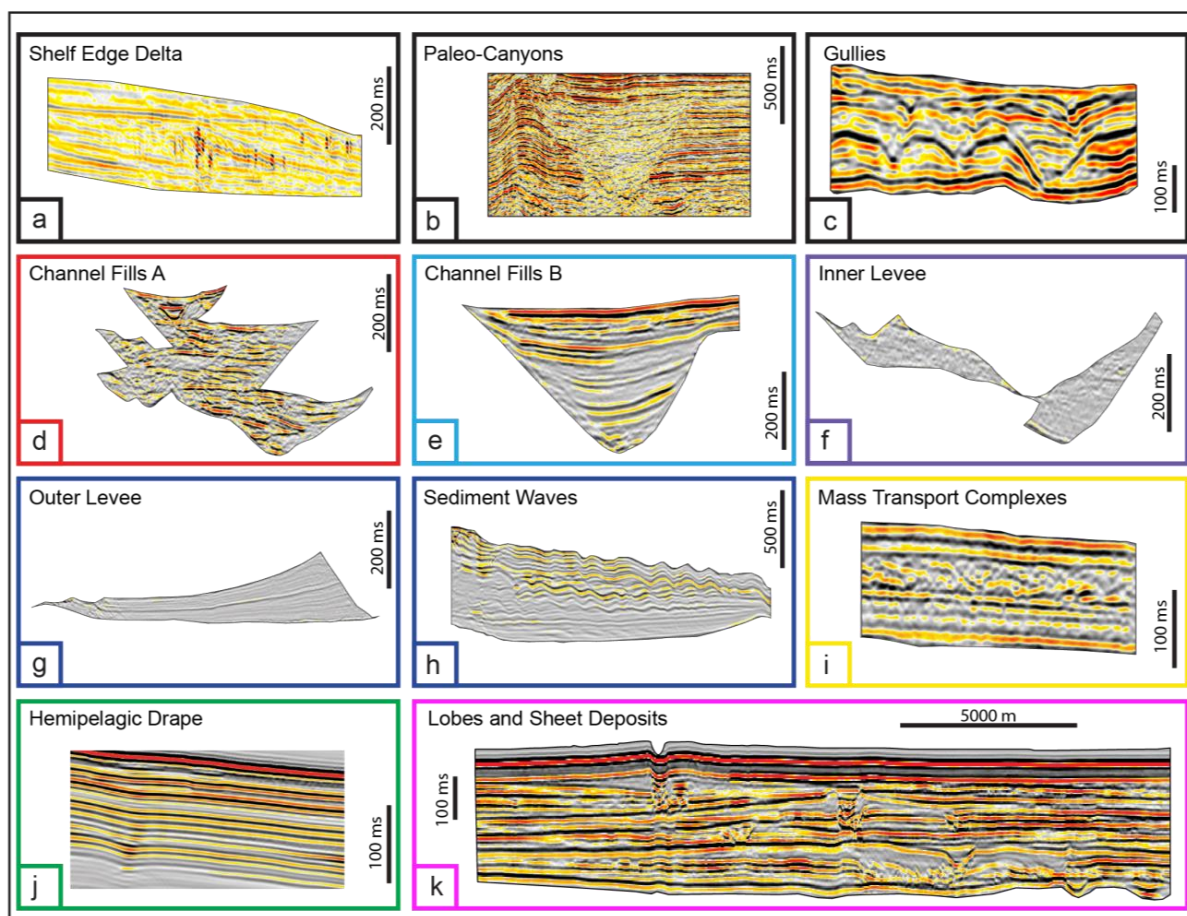


Figure 5.5: A catalogue of primary depositional elements identified on the seismic data.

Table 5.1: Summary of key seismic facies.

Seismic Facies	Amplitude	Continuity	Reflection Geometry	Environment/ sediment types	Bounding Surfaces
Shelf Edge Delta (fig. 5.5a)	Medium to low	Sigmoidal to oblique reflections	Progradational and wedge-shaped	Shelf edge	
Channel Fills A (fig. 5.5d)	High amplitude	Relatively discontinuous to chaotic	Package of organized to disorganized	Channel deposits of high energy turbidity currents	V- or U-shaped bounding surfaces / inner levees
Channel Fills B (fig. 5.5e)	Low to high alternating	Highly Continuous	Continuous and parallel	Channel deposit of decreasing to low energy turbidity currents	V- or U-shaped bounding surfaces with overlapping reflections
Inner Levees (fig. 5.5f)	Low	Discontinuous to chaotic	Wedge-shaped with/without terraces	Developed within the channel due to low intensity turbidity currents	Conformable with outer levees and erosional with channel fills.
Outer Levees (fig. 5.5g)	Dominantly low with high amplitude bed	Highly Continuous	Wedge-shaped and convergent		
Mass Transport Complexes (fig. 5.5i)	Medium to High	Discontinuous	Chaotic, and wavy with sheet like external form	Mass flow units of variable lithology	Erosional to grooved basal surface and continuous top bounding surface
Hemipelagic (fig. 5.5j)	Low to medium	Strongly continuous	Draping, and sheet like geometry	Muddy turbidite to condensed section and hemi (-pelagic) deposits	conformable continuous basal bounding surfaces
Frontal and crevasse splays (fig. 5.5k)	Medium to high	Moderate to high continuous	Concave-down external form and sheet like geometry	Channel mouths and breached channel, formed at slope to deep-marine	

5.4.1.1 Shelf Edge Delta

Shelf edge delta are recognized as oblique to sigmoidal reflections, gently dipping seawards and forms an external wedge-shaped pinch out towards the shelf (Fig. 5.5a). Shelf edge delta are characteristic features of relative sea level lowstands, when sand can be transported across the emerged shelf and exported towards deep water areas (Steel and Porębski, 2003).

5.4.1.2 Submarine canyons and gullies

Large scale negative relief features without any distinctly developed levees are classified as submarine erosional valleys, i.e. submarine canyons and gullies. Paleo-canyons are observed in Miocene and Pliocene that are stacked laterally. With a maximum incision of up to 500 ms, these canyons exhibit low amplitude chaotic reflections (Fig. 5.5b). In contrast, the gullies that are observed along the upper slope are straight, deeply incised and smaller in scale relative to that of submarine canyons i.e. with a maximum incision up to 100 ms (Fig. 5.5c).

5.4.1.3 Submarine channel fills

Two types of channel fills are observed, confined within V- or U- shaped erosional and/or bounding surfaces. The tightly grouped packages of discontinuous to chaotic and high amplitude seismic reflections are recognized as the Channel Fills A (Figs. 5.4 and 5.5). The reflection configuration of the Channel Fills A are interpreted to be coarse-grained sand prone or conglomerate sediments. In contrast, the second type of channel fill deposits, herein termed as Channel Fills B, are characterized by continuous, straight and parallel seismic reflections with varying amplitude (Figs. 5.4 and 5.5). These deposits show bidirectional, onlapping reflections with the bounding surfaces of the channel and interpreted as thin bedded turbidites to hemipelagic deposits.

5.4.1.4 Inner levee and intra-channel terraces

Inner levee deposits are recognized as incoherent to discontinuous and disorganized low amplitude reflections, confined within the channel belts (Figs. 5.4, 5.5 and 5.6). These deposits formed due to low intensity turbidite current flows (Posamentier, 2003). Inner levee deposits have been observed in many large fans such as the Bengal fan (Hübscher et al., 1997) as well as in other parts of the Indus Fan (Deptuck et al., 2003). The inner levee deposits vary in sizes and shapes, and occasionally are absent in small channels. On seismic data, inner levees are often observed as bench-like depositional stepped profiles in cross sections, and forms terraces. This type of feature is recognized as the intra-channel terraces that form through a variety of processes including remobilizing of sliding and slumping of the channel's levee (Fig. 5.6).

5.4.1.5 Outer levee/overbanking

Outer levees are seismically typified by the continuous and low to moderate amplitude reflections that downlap onto the underlying surface, forming wedge-shaped geometries thinning away from the channel belt (Figs. 5.4, 5.5 and 5.6). Outer levee flanks typically confine the channels belts as gull-winged shaped geometry (Fig. 5.4). Outer levees are the

product of over spilling and flow stripping of turbidity flows conveyed by the channel (Posamentier and Kolla, 2003; Janocko et al., 2013). According to Sylvester et al. (2011), the outer levee is composed of thin-bedded turbidites, becoming mud rich away from the channel.

5.4.1.6 Sediment waves

In some examples, the outer levees show sinuous structures as crests and troughs with parallel and well-bedded internal reflections of high to low amplitude (Figs. 5.5 and 5.6). These features are interpreted as sediment waves, and are formed by the spillover and flow stripping of the turbidity current that flows above the channel confinement. Sediments waves are best developed along the levees on the outer bends of the sinuous channels.

5.4.1.7 Mass transport complexes

On seismic profiles, mass transport complexes or MTCs are observed as structureless to complex reflective bodies which are characterized by discontinuous to chaotic reflections with varying amplitudes (Figs. 5.4 and 5.5). Spatially, MTCs are observed as sheet-like bodies in the different stratigraphic intervals (Figs. 5.4 and 5.6). Basal bounding surfaces of the sheet-like MTCs are erosional grooves whereas the top surfaces are smooth and regular. MTCs are also often developed above the basal erosive surfaces of the submarine channel. These deposits are formed of slumps and debris flows (Shanmugam, 2006). Only thin packages of MTCs are encountered in the well sections of Pak-G2-1 found to consist of coarse grain sediments of silt to sand lithology (Fig 5.3).

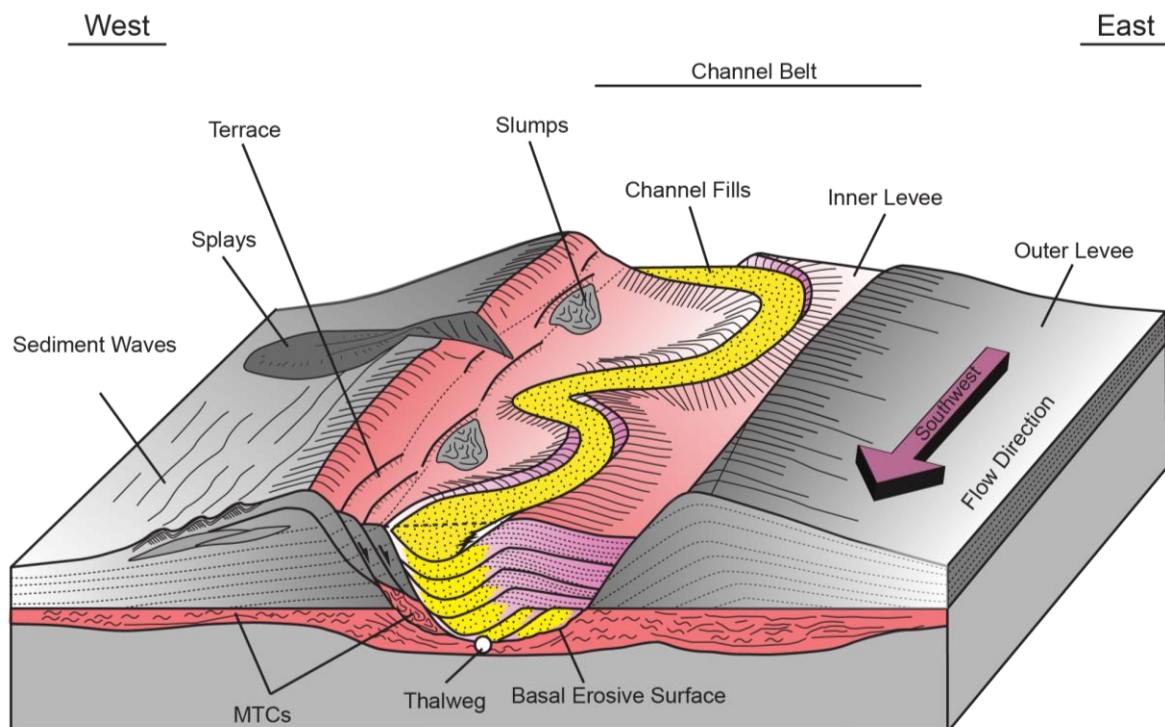


Figure 5.6: Block diagram of a channel-levee complex showing the distribution of the depositional elements.

5.4.1.8 Hemipelagic deposits

Hemipelagic deposits are characterized by parallel to sub-parallel and continuous seismic reflections with high to low amplitude, exhibiting sheet-like external form (Fig. 5.5). Lithologically, hemipelagic deposits composed of dark claystone and mudstone, deposited as background sediment (Prins et al., 2000).

5.4.1.9 Unconfined lobes and sheet deposits

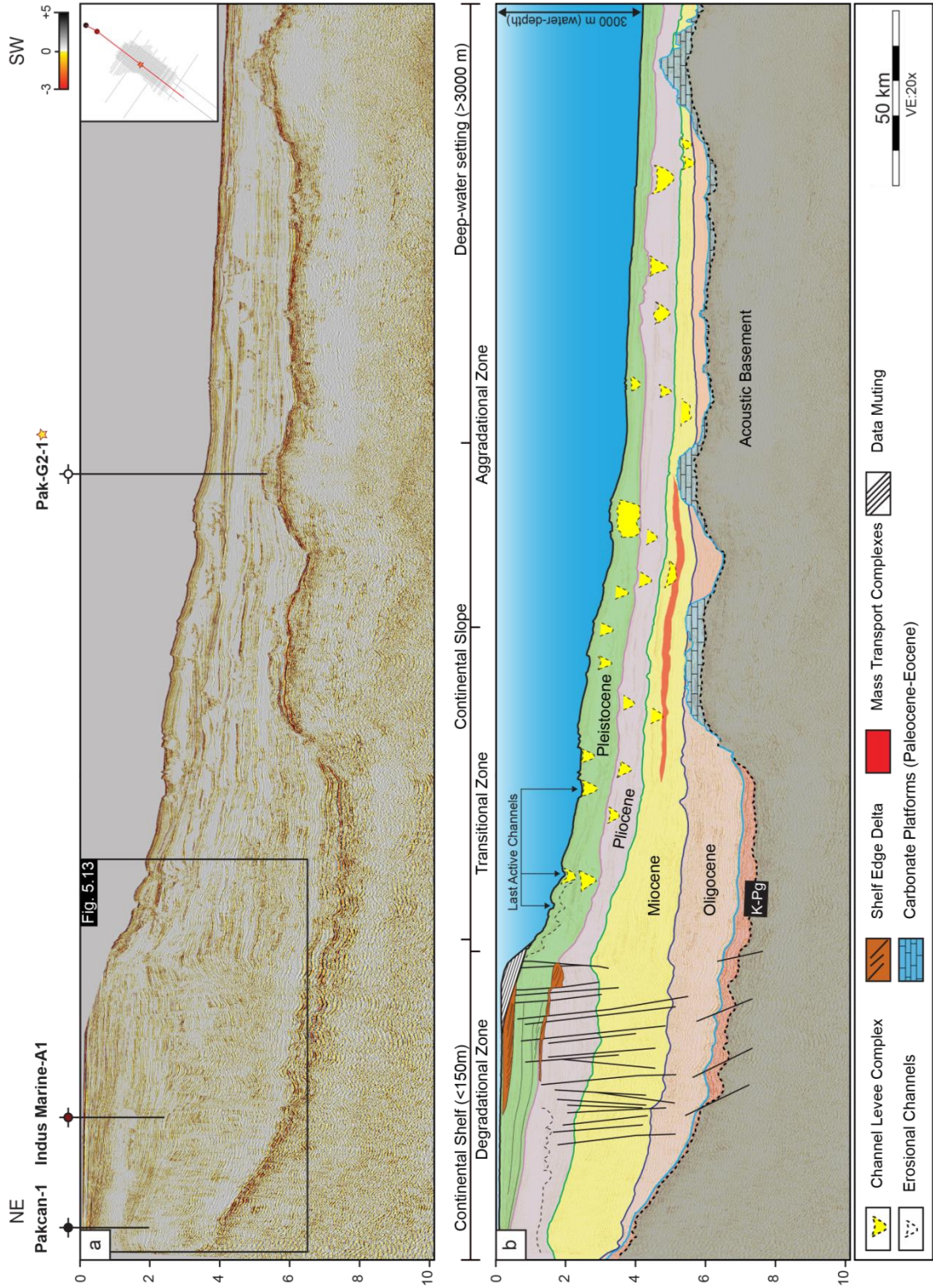
Unconfined lobes and sheet deposits are seismically characterized as thin packages of non-channelized deposits of high amplitude, parallel to subparallel and continuous seismic reflections (Fig. 5.5). According to Posamentier et al. (2003), these deposits develop at the mouth of the channels and form frontal lobe-shaped splays (Fig. 5.5.). The facies are interpreted as rich in coarse-grained sediments. At channel bends, the breaching of levees also commonly form unconfined lobes and sheet deposits (crevasse splay) (Fig. 5.6).

5.4.2 Seismic stratigraphy

5.4.2.1 Cretaceous-Paleogene boundary and prefan stratigraphy

The Cretaceous-Paleogene (K-Pg) boundary is recognized as the oldest strong seismic reflection that overlies the reflection-free acoustic basement of the Deccan Volcanics (Figs. 5.7 and 5.8; Shahzad et al., 2019). Along the continental shelf, this boundary is reported in wells Korangi Creek-1 and Karachi South-1A as the base of the Ranikot Fm. which contains basalt layers (Shuaib, 1982). The K-Pg boundary is characterized by a rough topography, associated with normal faults and horsts structures of the syn-rift phase of the Indian plate margin (Figs. 5.7 and 5.8; Malod et al., 1997; Gaedicke et al., 2002b; Carmichael et al., 2009). Below the K-Pg boundary, the crust type distally changes to a thin oceanic crust with the seismically delineated Mohorovicic discontinuity (Fig. 5.8). These results corroborate the interpretation of Corfield et al. (2010) and Carmichael et al. (2009) that determined a northward transition between the continental and oceanic crust.

Above K-Pg boundary, the Paleogene succession predominantly forms a carbonate shelf succession and contemporaneous detached carbonate platforms on the paleo-highs in the basin (e.g., Figs. 5.7 and 5.9; discussed in chapter III and IV; Shahzad et al., 2018, 2019). The intermittent topographic lows consist of Paleocene to Oligocene hemipelagic deposits, intercalated with the terrigenous clastic deposits. The Paleogene stratigraphic section has been drilled along the slope of the basin in the well Anne-ex-1 (Report: Anne ex 1 – unpublished), composed of deep-marine pelagic deposits with intercalation of the thin layers of coarse-grained sediments. The thickness of the Paleogene succession is up to 1950 ms in proximal settings of the Indus Fan (Fig. 5.7). Distally, the Paleogene succession is reduced to 400 ms and seismically appears as more continuous with closely spaced parallel to sub-parallel and low amplitude reflections (Fig. 5.8). The unit infills local depressions and shows onlaps against the preexisting volcanic paleo-highs, carbonate platforms and the Murray Ridge (Figs. 5.7 and 5.9).



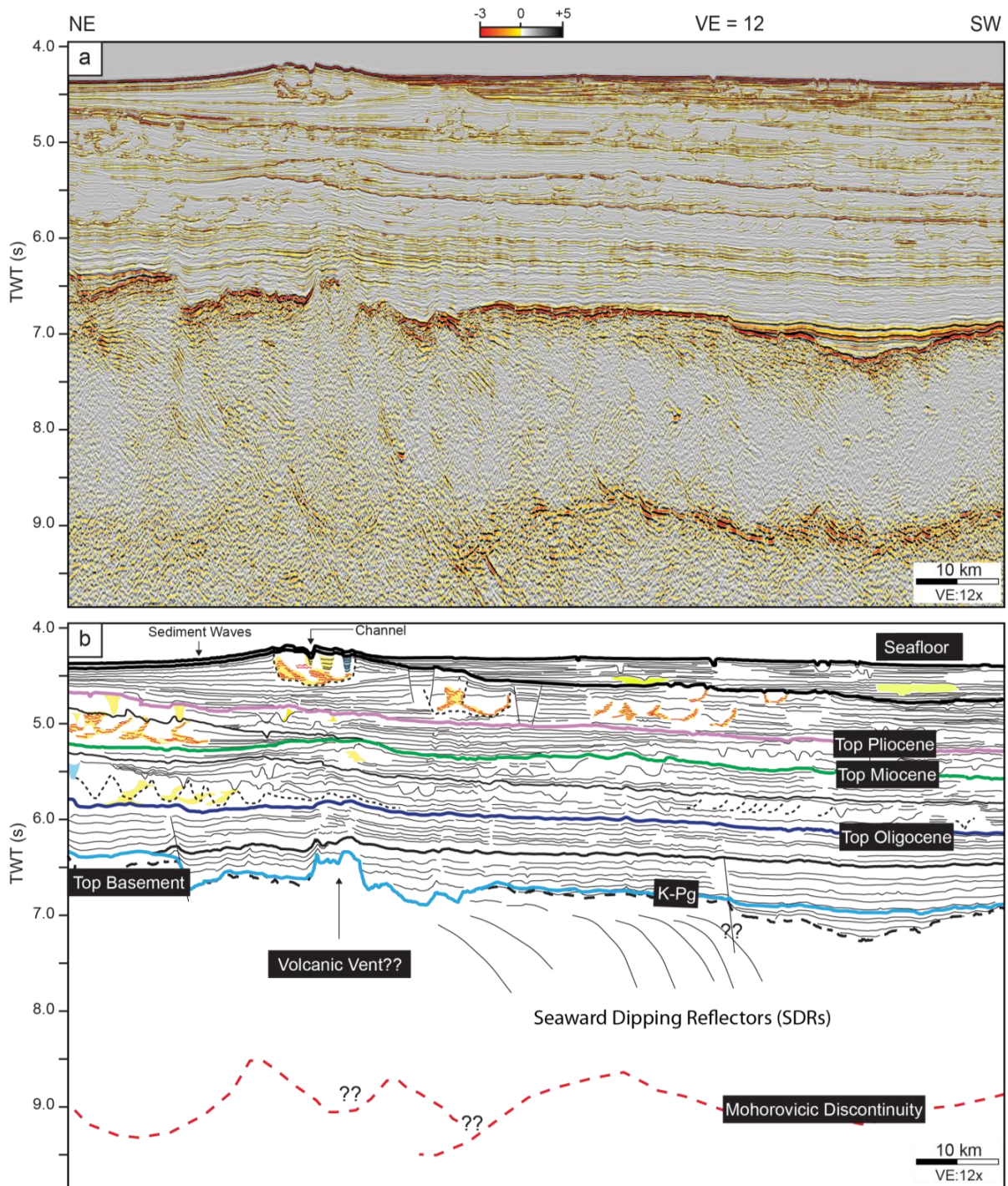
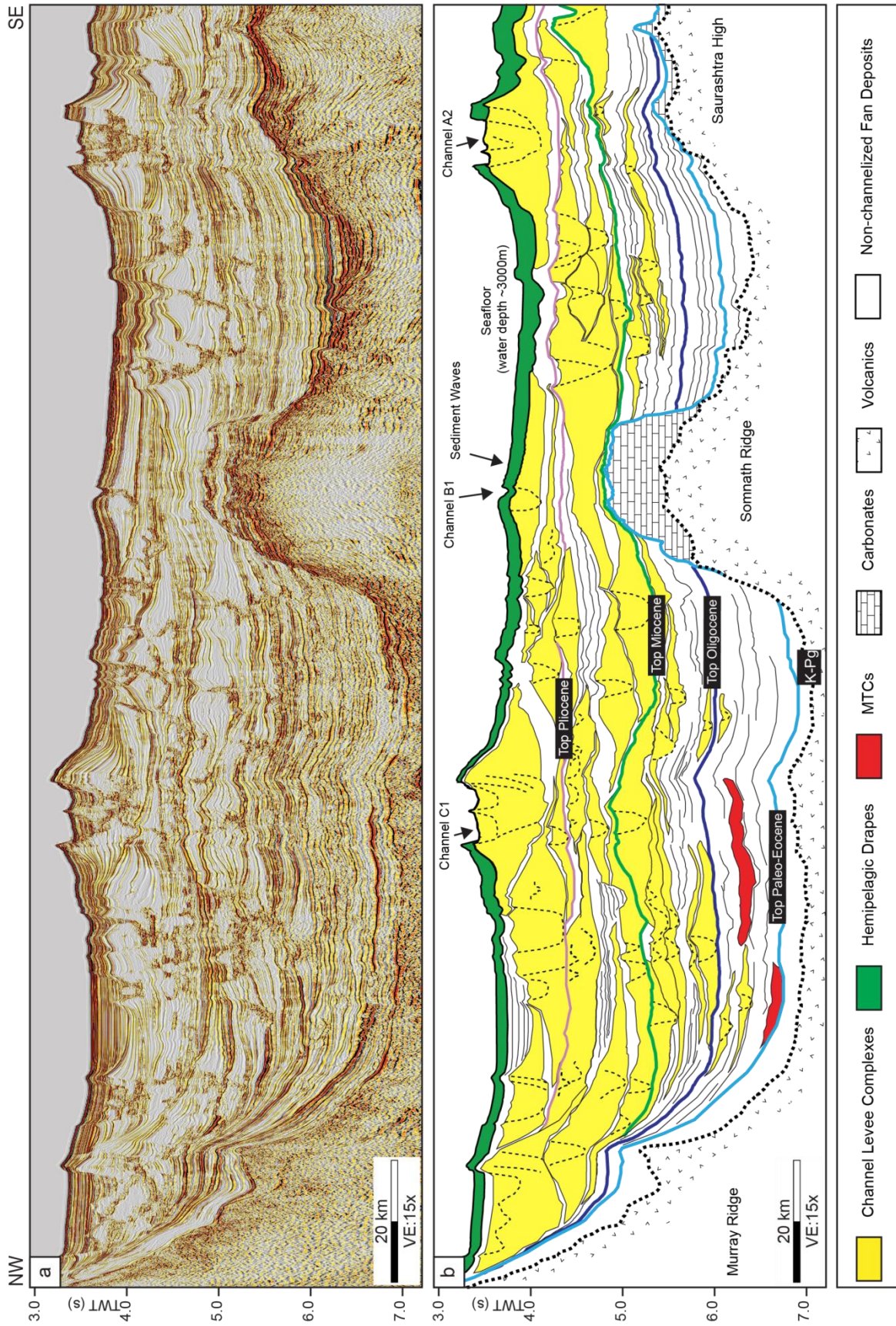


Figure 5.8: (a) Uninterpreted and (b) interpreted seismic profiles of the most distal setting of the Upper Indus Fan with lines drawing of the major stratigraphic boundaries and elements. A prominent deep seismic reflection (red line) is interpreted as Mohorovicic discontinuity (after Carmicheal et al., 2009 and Corfield et al., 2010). Fig. 5.2 shows the location of the seismic profile.

Figure 5.7 (previous page): Regional NE-SW seismic profile across the Offshore Indus Basin showing the important stratigraphic units and features discussed in the chapter. The black vertical lines represent the geological faults. Location of seismic profile is shown in Fig. 5.2.



5.4.2.2 Oligocene to Miocene

Outer Shelf

In industrial wells located on the continental shelf, the Oligocene is dominantly reported as shallow water carbonate with thin bands of shale (Nari Fm.), overlain by a thick interval of Early to Middle Miocene siliciclastic of the Gaj Fm. (Fig. 5.10; Shuaib, 1982). In seismic profiles, the carbonate succession is 200-400 ms thick, and exhibits parallel and continuous seismic reflections of low to medium amplitude, forming a distinct paleo-shelf with a slope dipping towards the southwest (Fig. 5.10). The overlying Middle Miocene Gaj Fm. shows aggradational to progradational reflections downlapping towards the basin (Fig. 5.10). This is interpreted as progradational deltaic deposits, filling the slope and basinal area developed during the Middle Miocene sea level lowering (Haq et al., 1987).

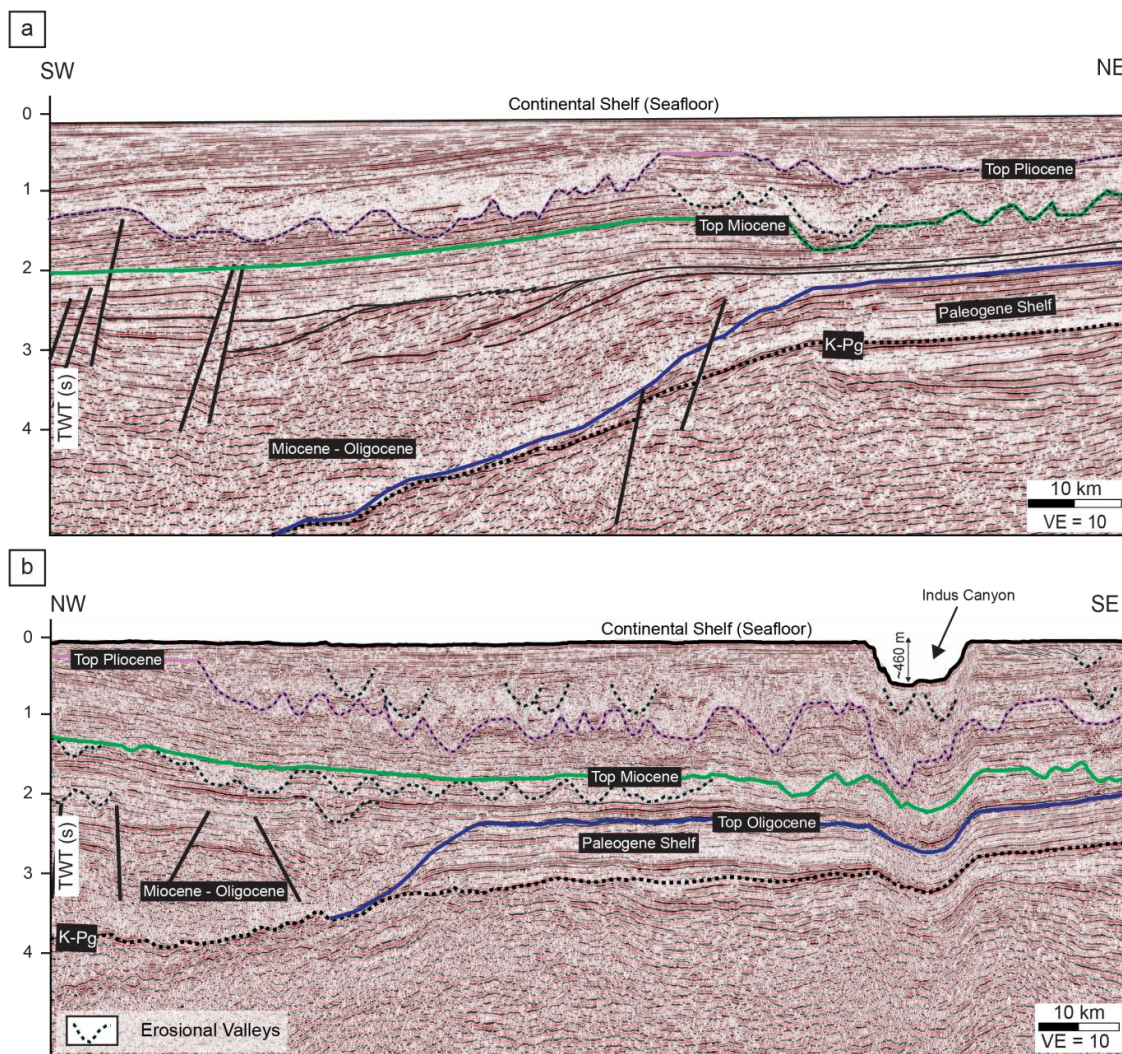


Figure 5.10: Two seismic sections showing the regional stratigraphic boundaries, and depositional features across the continental shelf. (a) Thin black lines indicate the clinoforms associated with Miocene progradation.

Figure 5.9 (previous page): (a) Regional NW-SE seismic profile through the Upper Indus Fan, and (b) interpretation of regional stratigraphic units and major depositional and tectonics subdivision of the basin. (Fig. 5.2 is referred for the location of seismic profile). The size of the channel levee complexes are increasing in stratigraphic order from Oligocene to Holocene.

Above the Gaj Fm. the Middle to Late Miocene succession is typified by medium amplitude and continues to incoherent seismic reflections with extensive erosional valleys along with the identified top Miocene reflector (Figs. 5.10 and 5.11). The valleys are infilled by sediments showing the low amplitude and discontinuous seismic reflections. These features are without levees and appear to be laterally stacked and coalesced on the seismic section, from west to east direction (Figs. 5.10 and 5.11).

The adjacent reflections terminate against the valleys walls (Figs. 5.10 and 5.11). It is proposed that the Miocene erosional valleys developed during a sea level fall in response to the incision of the paleo-shelf. In industrial wells, the Miocene is represented mainly by calcareous clastics. However, the seismic character of valley infills indicates the occurrence of shale to mud prone sediments of pro-delta deposits (Daley and Alam, 2002).

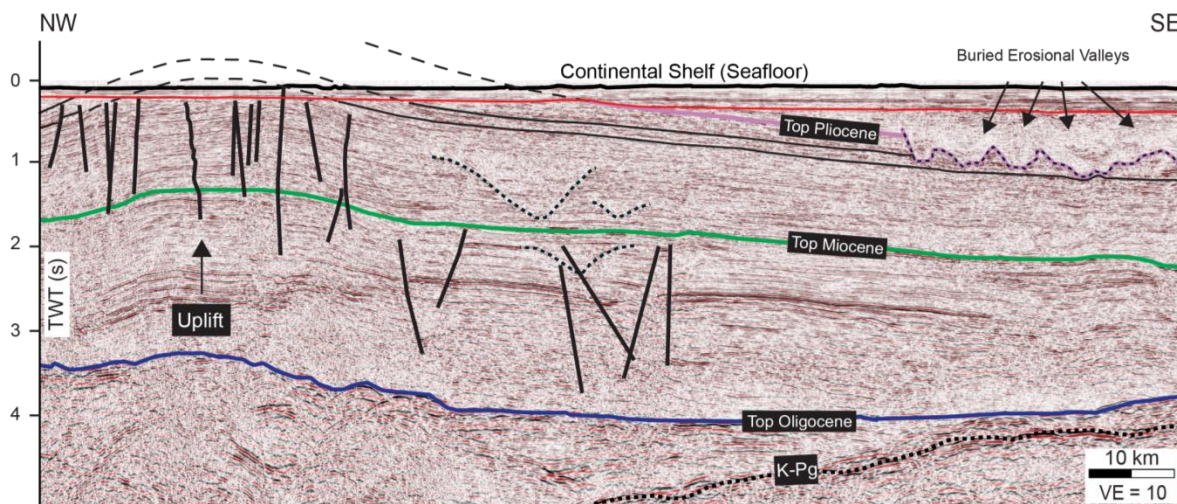


Figure 5.11: Regional seismic profile illustrating the stratigraphic boundaries and structural deformation across the continental shelf. (For location, Fig. 5.2 is referred).

Slope to deep-marine basin

From upper slope to the deep basin, the Middle Oligocene to Early Miocene stratigraphy shows discontinuous to chaotic seismic facies with occasional small-scale CLCs. Individual CLCs are up to 30 km wide with channel belts up to 5 km wide and levees up to 100 to 400 ms thick in the lower part of the Miocene succession. The size of the channel complexes gradually increases to the younger interval (Fig. 5.9) and decreases downdip along the slope (Fig. 5.7). The increasing width of the Miocene channel belts with multiple incisions infers an increase in the channel sinuosity and channel belt lateral migration. However, Miocene channel levees appear to be aggradational, and the cut-and-fill events of channel sinuosity are less evident.

The slope to basin seismic transect (Fig. 5.12) shows the presence of regional MTCs with a continuous to discontinuous and disorganized seismic character and varying reflection amplitudes. In two-way travel time, the thickness of these MTCs ranges from 150 to 300 ms. From regional seismic to well correlation, it is proposed that the mass transport events

occurred periodically, alternating between the CLCs, during the Late Oligocene to Late Miocene. These MTCs events were the main source of sediments influx in the basin from the shelf. The reasons behind the formation of regional MTCs are not well understood on the available seismic data, however, it is hypothesized that the rapid sedimentation accumulation rate from the Indus River and delta, the tectonically induced seismicity of the Owen Fracture Zone and Oligocene-Miocene sea level lowering could be the trigger of the shelf edge failure and subsequent deposition of the mass flows in the basin.

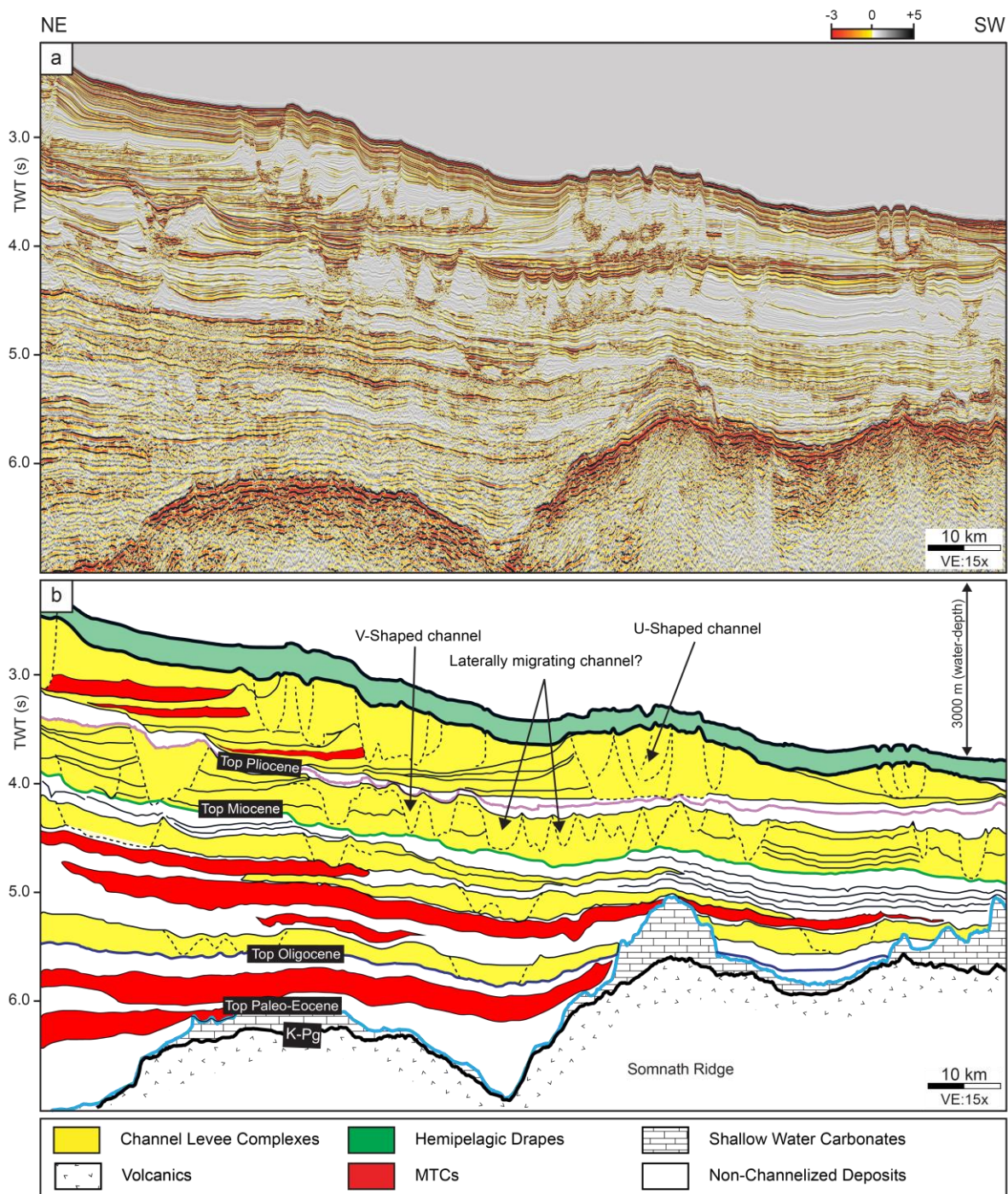


Figure 5.12: NE-SW oriented seismic profile along the slope, showing the depositional changes from the Cretaceous-Paleogene (K-Pg) to recent with the annotation of regional stratigraphic surfaces. (For location, see Fig. 5.2).

5.4.2.3 Pliocene – Pleistocene

Outer Shelf

Post-Miocene sediments are missing in many onshore wells. However, enormous thicknesses are encountered in the wells drilled on the continental shelf and deep Offshore Indus Basin (Shuaib, 1982; Shahzad et al., 2018). On the shelf, the lower part of the Plio-Pleistocene succession (?early Pliocene) shows high amplitude, parallel reflections dipping basinward, where the repeated phases of shelf edge delta growth episodes are observed (Figs. 5.7 and 5.13). On the shelf, the second phase of valleys incision is observed along with the poorly resolved Plio-Pleistocene transition. The erosional valleys are laterally continuous eastward in the dipping succession of Plio- Pleistocene (Fig 5.10). Seismically the channel fills are low amplitude to transparent, similar to the Miocene erosional valleys.

The Pliocene succession thins towards the west of the shelf. The top of the Pliocene forms an anticlinal structure associated with a set of normal faults with a nearly vertical throw (Fig. 5.11). Above the anticline, there are no post-Pliocene, which is interpreted to be a consequence of erosion. Seismically identified structural deformation is interpreted to develop as the products of contemporaneous transpressional tectonics caused by the Indian Plate reorganization and the uplift of the Murray Ridge. Erosional valleys were developed along the paleo-shelf, which acted as the conduit for the sediment supply to the basin during the sea level lows. The horizontal stacking of the erosional channels appears as the result of syndepositional transpressional tectonics; the tectonic uplift at the same time triggered an eastward migration of the valleys.

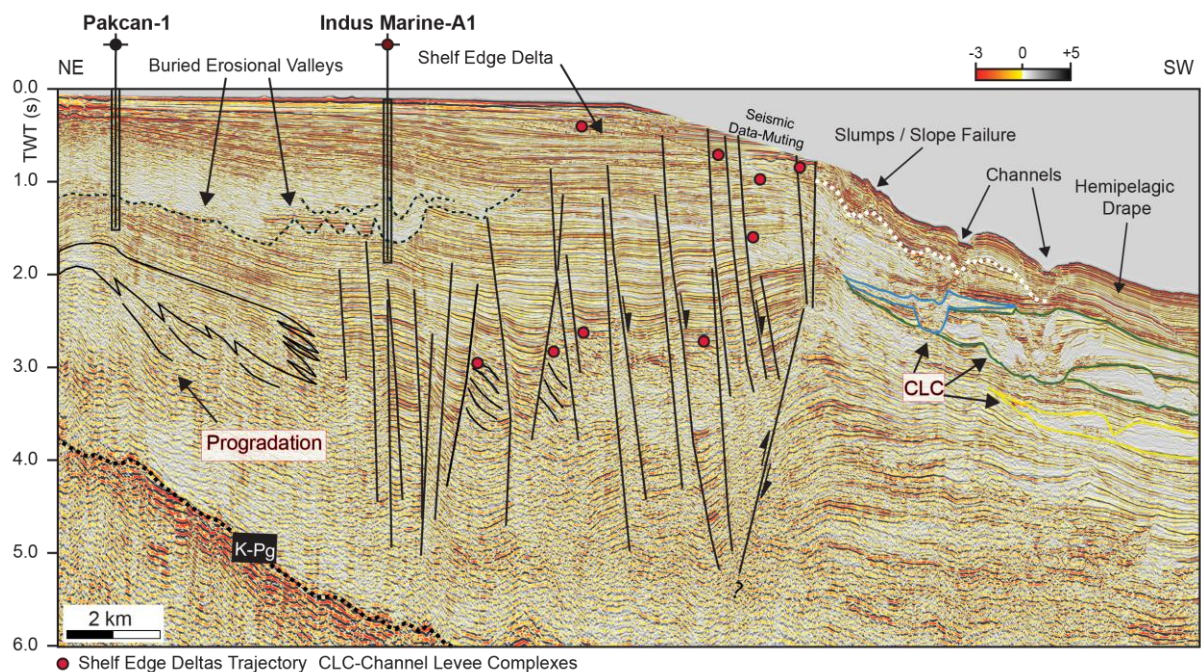


Figure 5.13: NE-SW oriented seismic profile along the outer shelf illustrating the changes in the depositional environment from the shelf to the upper slope.

The overall thickness of the Plio-Pleistocene succession varies along the shelf. In the Well Karachi South-1A, the Top Pliocene is missing, whereas it is encountered at a depth of 503 m in well Pakcan-1, located on the inner shelf. In the industrial wells, the Plio-Pleistocene succession is mainly calcareous, highly fossiliferous with intercalations of clay, siltstone, sandstone, and conglomerates (Shuaib, 1982).

Slope to deep-marine basin

According to Carmichael et al. (2009), the Plio-Pleistocene succession of the Indus Fan is characterized by the large scale CLCs. Mapping of the seismic images shows that these CLCs are up to 900 ms thick, 10-50 km wide and tens of kilometers long (Figs. 5.7, 5.9 and 5.12). CLCs are bounded by high amplitude seismic reflections, interpreted as a condensed section (Figs. 5.3 and 5.12). The Plio-Pleistocene succession is approximately 1000 ms to 1500 ms sec thick along the upper slope and is reduced to 400 ms on the middle to lower slope of the continental shelf (Figs. 5.7 and 5.9).

5.4.2.4 Holocene Hemipelagic drapes

Beneath the seafloor, the Plio-Pleistocene CLCs and fan deposits are overlain by a layered sequence of parallel and continuous seismic reflections of alternating, variable amplitude. With a sheet-like external form, these reflections drape the underlying succession with a continuous thickness of approximately ~100 ms tracing the paleo-seafloor undulations (Figs. 5.9 and 5.12). This draping unit is interpreted to represent hemipelagic drapes of the background sedimentation. According to Prins et al. (2000), the hemipelagic from the middle fan consists of a homogeneous mud unit with a few silty and sandy turbidites.

5.4.3 Sedimentary dynamics and growth of a Plio-Pleistocene channel-levee complex

The integration of seismic images, seismically mapped seafloor and satellite bathymetric data allows identifying five CLCs on seafloor (Fig. 5.2b). The CLC A2 has the best seismic coverage with excellent vertical and horizontal resolution and has been discussed in detail as representative of the Plio-Pleistocene CLCs. The CLC A2 is up to 30 km wide having a channel belt 8-10 km wide. This channel extends as an ancestral channel from the mouth of the present-day Indus Canyon to 210 km in the south (Fig. 5.14). The CLC A2 explored and described here is located to the east of the area studied by Deptuck et al. (2003). The seismic facies analysis suggests three growth stages of the CLCs.

5.4.3.1 Stage 1: Channel incision

The channel inception starts with the initial excavation of a buried CLC at the seafloor leading to the development of the erosional fairways by high-density turbidity currents (Fig. 5.14; Deptuck et al., 2003). The deepest incision of CLC A2 is nearest to the degradational canyon mouth at a water depth of ~2000 m, where the erosional fairway incised the seafloor multiple times due to channel migration and avulsion (Fig. 5.14). The channel incision into the seafloor is proposed to represent falling base level and net erosion of the pre-deposited strata on the upper slope.

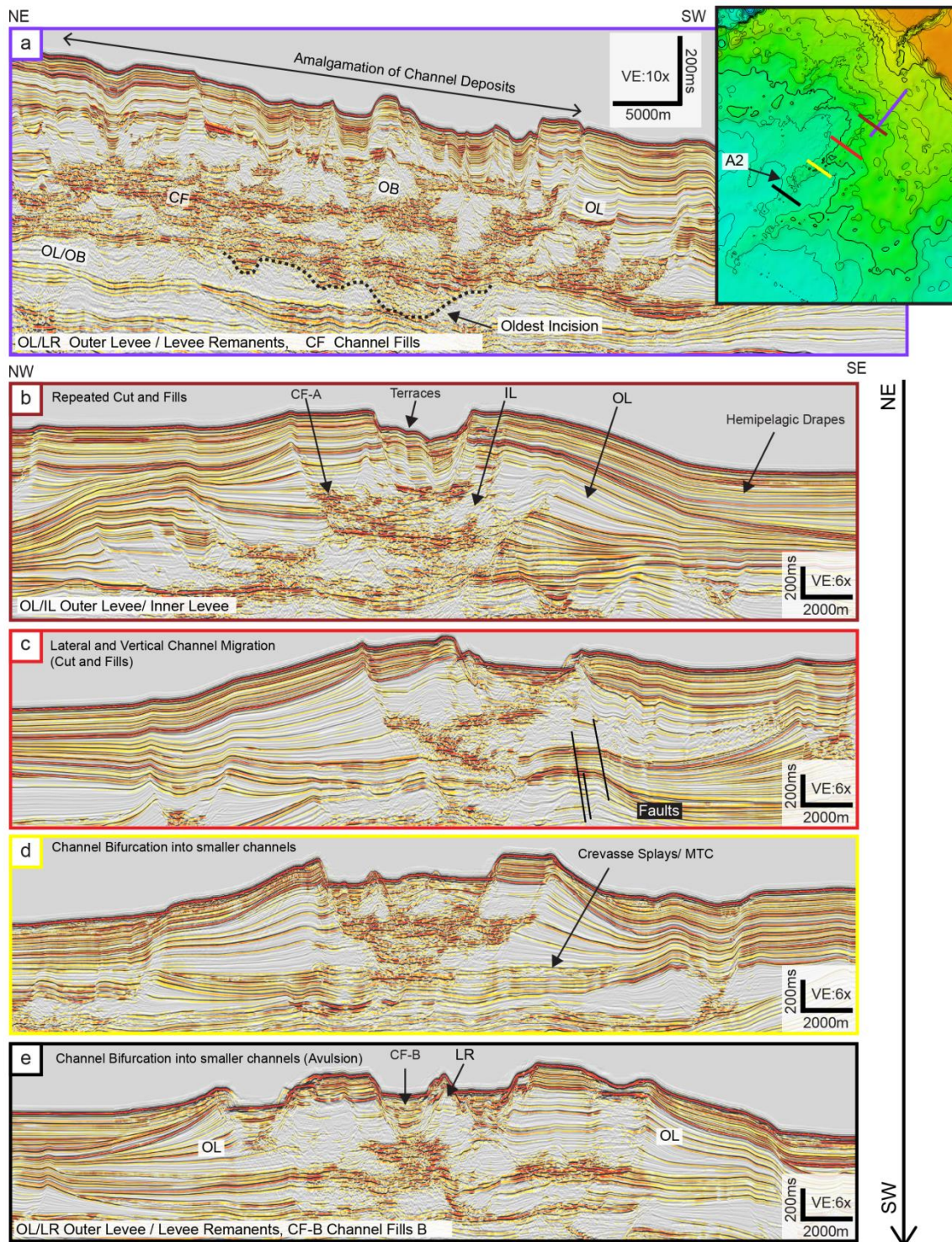


Figure 5.14: Seismic sections across the channel-levee complex A2 showing the variation in architectural elements.

Further, the basal erosional surfaces generally develop as V- or U- shaped incised valleys (Fig. 5.12). According to Peakall and Sumner (2015), the shape of V-shaped versus U-shaped incised valleys depends on the position of the channel along the slope gradient, the intensity of turbidity currents and the type of material being transported. This study finds that rapid and high-density turbidity currents develop V-shaped valleys and long-term erosion with repeated cut and fills produced U-shaped valleys in the Indus Fan. This finding are inline

with Janocko et al. (2013) who suggest that the V-shaped channels are typically characterized by upward fining deposits without any repeated cut and fill events. The degree of incisions along the channel belts are variable and depends on the channel position on the slope and the slope gradient, the intensity of turbidity currents and the type of sediments being transported (Janocko et al., 2013). This implies that the channel belts of CLC A2 were modified by multiple erosional and depositional events linked with the lateral channel migration after the initial excavation.

5.4.3.2 Stage 2: Channel fills and levee deposition

Stage 2 represents the phase of channel fill and levee deposition of CLC A2. Above the basal erosive surface, “channel fills A” are observed inside the channel belt as channel lag deposits of high-density turbidity flow, whereas overspill of turbidity currents developed fine-grained outer levees deposits and over banks on each side of the channel belt (Fig. 5.14). Based on the well to seismic correlation of a buried CLC example in figure 5.3, the outer levees of CLC A2 are interpreted to be composed of thin-bedded fine-grained turbidites, interbedded with sands and silts. As levee grew, the levee thickness increased and reached up to ~700 ms along the upper slope (Fig. 5.14).

The levees of the Plio-Pleistocene channels often contain large-scale sediment waves. For example, the seismic images of a buried channel show that these large-scale sediment waves developed along the western flanking levee (Fig. 5.15). The height of the sediment waves is up to 30-50 m. The sediment waves are moderately straight crested with an average spacing of 1000 m (crest to crest with increasing distance up-section). The wave crest trajectory is up-dip towards the crest of the levee, inferring upslope migration. These sediment waves are presumably developed at the channel bend of the sinuous channel.

5.4.3.3 Stage 2a: Channel migration and channel bifurcation

Figure 15.14 (a and b) shows that the channel fills A stacked vertically but also migrated laterally. These vertical and lateral stacking of the channel fills A are recognized as Lateral Accretionary Package or LAPs in term of Abreu et al. (2003). These vertical and lateral stacking of the channel fills A represent the lateral and vertical growth of the channel. LAPs exhibit the direction of migration of the channel. These packages either dip towards the axis of the channel or are parallel to the direction of migration of the channel (Abreu et al., 2003). LAPs that develop in the direction of lateral offset of the channel axis are the epitome of lateral channel migration. There are two sets of LAPs seen in the axis of the CLC A2. From the point of the first incision, the channel fills while aggrading vertically first migrated westward laterally up to 4500 m. In the second step, the channel fills show an eastward offset. These reflection stacking patterns are interpreted to represent the frequent lateral channel migration of a sinuous channel through time. Small scars in the basal erosive surface at multiple places are also observed that resulted from the erosion by the turbidite currents that widened the initial incisions and developed a U-shaped channel.

In figure 5.14 (a and b), it is observed that the inner levee deposits are significantly thinner in the direction of lateral offset of the channel axis in comparison to inner bank levee that

progrades in the direction of migration. This is because the thalweg migrates laterally towards the outerbank and erodes the levee. Further, it is observed that the channel fills A appears more aggradational with well-developed inner levees towards the distal side of the channel (Fig. 5.14c and 5.14d). This is interpreted as the southward decrease in channel sinuosity and lateral migration.

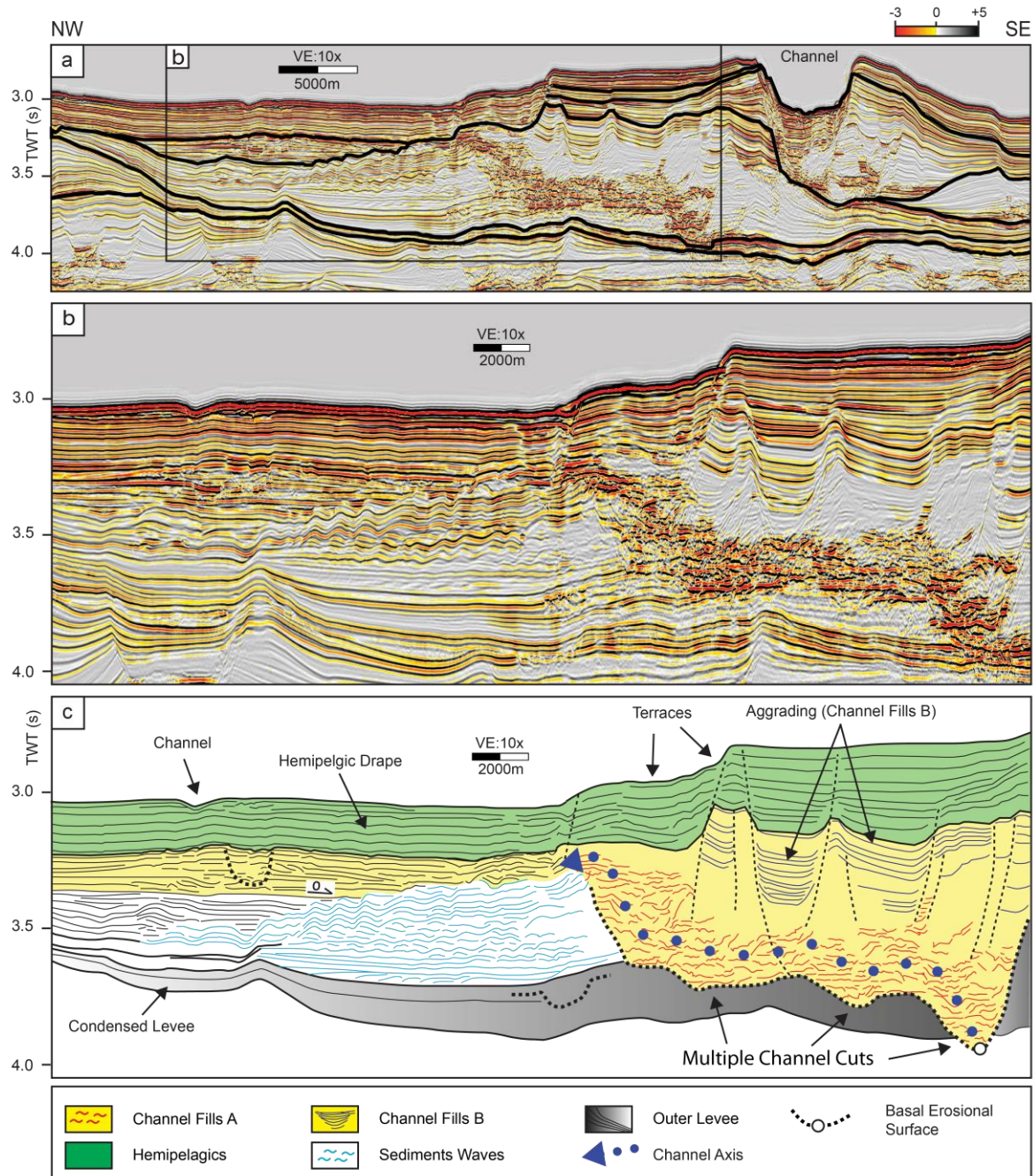


Figure 5.15: (a) Seismic profile across the channel-levee complex C1. (b) An Uninterpreted, and (c) interpreted section view across the sediment waves associated with the outer levee and changing trajectory of the channel axis.

The balance between lateral migration and upward filling of turbidite channels is primarily governed in response to changes in base level (Kolla et al., 2007). According to Deptuck et al. (2003), if the rate of sediment influx is higher than the rate of erosion, the channel thalweg

aggrades vertically and in case of inversed conditions, it offsets laterally. Further, the repeated cut and fill process resulted in the development of composite erosion surfaces within the channel which can be preserved after multiple cut-and-fill events. Furthermore, towards the distal part of the basin, the CLC A2 shows bifurcation into small channels as the vertical growth of the CLC diminishes. Development of small feeding channels may occur during the lateral migration caused by frequent avulsions that resulted in a deceleration of the turbidity currents. Reduction in flow parameters or avulsion also ceases the lateral migration, which is then followed by an abandonment phase (Fig. 5.14).

5.4.3.4 Stage 3: Passive channel filling and channel abandonment

Above the channel fills A, the parallel to subparallel seismic reflections of channel fills B marked the abandonment phase of the CLC A2 (Fig. 5.14). A similar change in the seismic facies is also evident in the CLC C1 (Fig 5.15). Turbidity currents with reducing flow velocity with impoverished columns of the sediments deposit their load that appears as parallel to subparallel seismic reflections. The abandonment of the CLC A2 may also be the consequence of channel avulsion as distally small feeding channels are evident on the seismic profiles. The hockey stick shape channel adjacent to CLC A2 (Fig. 5.14c) is suggestive of flow divergence and frequent avulsion events that significantly reduced the flow regime. Another factor for low sediment flow is the result of retaining of sediments along the shelf due to rising sea level and increasing accommodation at the shelf because of which sediment influxes to the basin decrease that increases the expanse of channel abandonment.

5.5 Controlling factors of the Indus Fan sedimentation

The stratigraphic evolution of the Indus Fan and associated CLCs is interpreted as the product of a variety of allogenic and autogenic mechanisms (Kenyon et al., 1995; von Rad and Tahir, 1997; Prins et al., 2000). Amongst these mechanisms, regional tectonics and changes in sea level have been widely regarded as the main factor for the growth and development of the Indus Fan in the current study.

The seismic stratigraphy discussed herein implies that the Paleo-Indus Fan existed since the Oligocene. Seismic data show the extensive development of MTCs during Oligocene to Early Miocene in the slope and upper fan with small channels incisions, whereas the CLCs of the Indus Fan preferentially start forming during Middle Miocene and Plio-Pleistocene sea level lowerings. The age of these MTCs roughly correlatable with the sea level falls occurred during the Middle Oligocene and Early Miocene (Haq et al., 1987), and therefore, these sea level falls can be attributed as main cause of triggering sediment failure as emplaced MTCs, along with the local tectonics impact. Further, the channel levee complexes development peaked during the sea level falls, and remained active until the next early rise. On contrary, the existence of thick hemipelagics infers that the current sediment supply became scarce in the basin due to sea level rise, and hemipelagic drapes developed (Fig. 5.16).

In addition, the local and regional tectonism also affected the stratigraphic architecture and evolution of the Indus submarine fan. According to Qayyum et al. (1997), the Paleogene fluvial and delta system existed to the north of the study area and formed after the uplift of

the northern Himalayan in the Eocene. During the Miocene, as a consequence of continued uplift of the northwestern mountain ranges and increased sediment supply, the delta developed, and the fluvial system diverted to the south. As per the seismic stratigraphy described herein, the first progradation of siliciclastics along the shelf, at least in the study area is recognized in the Middle to Late Miocene.

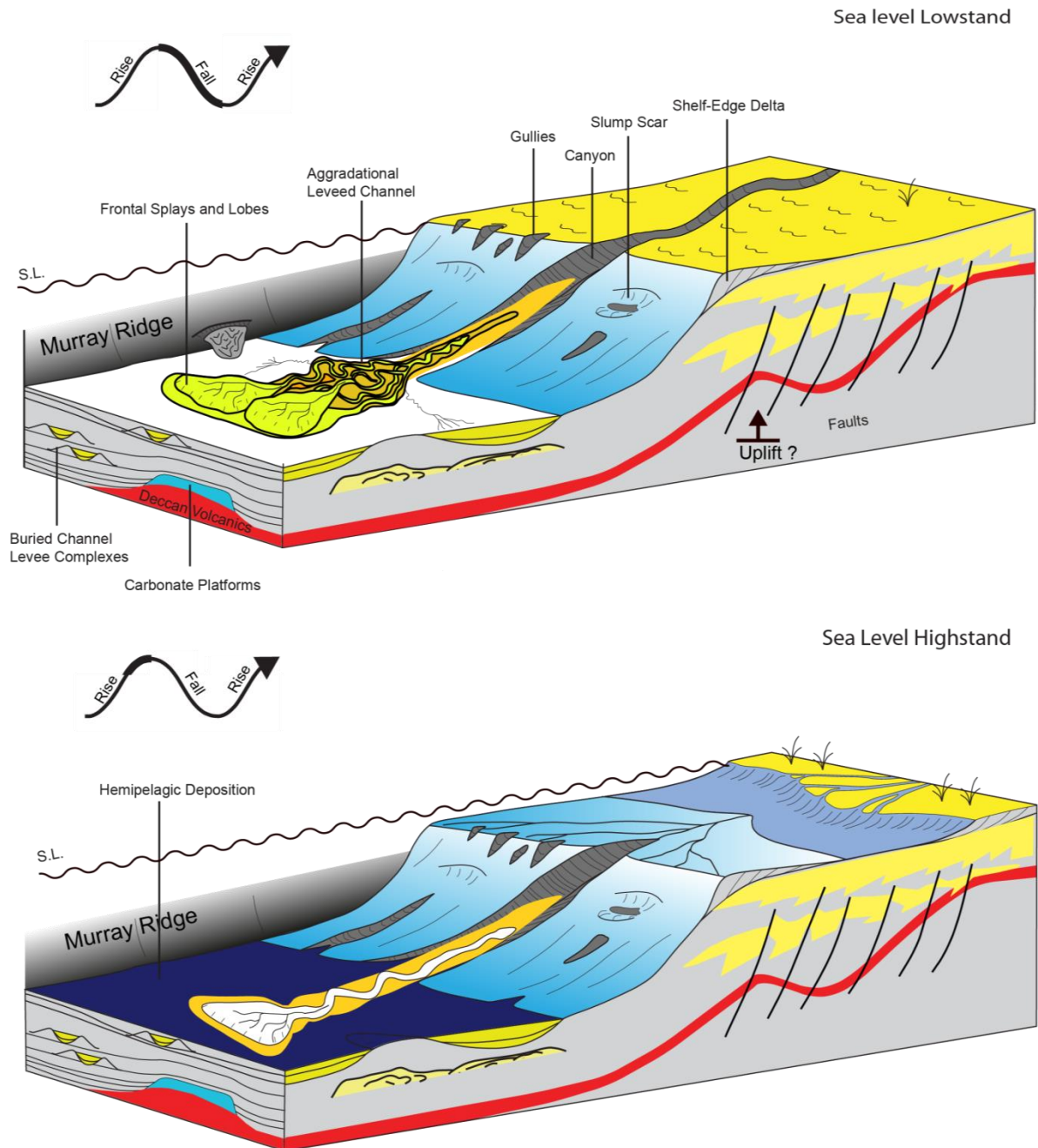


Figure 5.16: Schematic illustration of the Indus Fan sedimentation during sea level lowstand and early transgressive and highstand settings.

Furthermore, the Miocene and Pleistocene Plate re-organization of Indian Arabian Plate led to the uplift of the Murray Ridge and the surrounding area in the Early Miocene (Fournier et al., 2011). This event restricted the fan sedimentation to the eastern depocenter. Seismic

onlapping of the early Paleogene succession on the eastern Murray Ridge suggests that the ridge was a topographic high during the Paleocene-Eocene that further rejuvenated during the Miocene and then Plio-Pleistocene times. The Paleogene tectonic activity in the region also explains the thickness of the “prefan sediment succession” that is unrealistic solely for the pelagic to hemipelagic depositional regimes during the Indian Plate drift.

Qayyum et al. (1997) further suggested the deposition of a proto-Indus Fan in the Gulf of Oman, to the west of the Murray Ridge, prior to the shifting of depocenter. In the current study, the changing position of the erosional valleys along the shelf, from west to east, are also observed that corroborate the hypothesis of the occurrence of an older delta west of its present position. In response to the tectonic uplift caused by the Indian and Arabian plate transpression at the Murray Ridge, the delta migrated eastward where the uplift of the Pleistocene is evident on the presented seismic interpretation (Figs. 5.10b and 5.11).

The Indian-Eurasian collision is one of the most prominent Cenozoic tectonic events that not only caused mountains building, but also influenced the local and global climate. The Himalayan mountain building of high topography is seen as responsible for the intensification of South Asian Monsoon at least since the Late Oligocene (Clift et al., 2008). The high precipitation rate led to the unroofing of the mountains and provided the detrital sediments to the Arabian Sea (Ruddiman and Kutzbach, 1991). The wet climate of the monsoon has enhanced erosion and led to an increase in discharge and load of the Indus River (Clift et al., 2008). This increased run-off and thick flows of turbidity currents with dense volume of sediments have contributed to the establishment of new channels levee systems and the channel avulsion (McHargue, 1991; Prins et al., 2000). Contrary to the wet climate, the dry climate spells may be provide limited or decreased sediments to be carried by impoverished and depleted river flows. The combination of both the factors will impel the delta to recede and substantially decrease the sediment flow downslope.

Chapter VI

Conclusions and synthesis

This is the first comprehensive study, which uses seismic stratigraphy for a tectonostratigraphic synthesis of the depositional variations of the Pakistan passive margin. Detailed interpretation and facies analysis of high-resolution seismic data supported by log motifs and well cuttings allows an understanding of the Cenozoic stratigraphic evolution of the Offshore Indus Basin at a basinal scale. The post-rift succession of the Offshore Indus Basin is described, which encompasses the development of attached and detached carbonate platforms during the drift stage of the Indian Plate and the post-collision development of the Indus Fan. A summary of these findings is described in the following paragraphs.

In the first part, the age of the carbonates succession is evaluated on the basis of fossil record, and an investigation of the depositional architecture of nine mapped isolated carbonate platforms is presented, which developed above the Cretaceous-Paleogene boundary. Detached from the continental shelf, paleo-highs and ridges inherited from the multiphase rifting of the Indian Plate and associated volcanism of the Reunion hotspot provided the substratum for the development of these isolated carbonate platforms. Based on the micropaleontological analysis, a Late Paleocene-Early Eocene age of the isolated carbonate platforms is established. In the line of the results, the study proposes to subdivide the evolution of the carbonate platforms into five main stages:

1. *Carbonate initiation:* Shallow-water carbonate growth initiated following the submergence of the subaerially exposed volcanic basement during the Middle to Late Paleocene. Above the Cretaceous-Paleogene regional unconformity, the carbonates started to grow as small mounds and patches.
2. *Backstepping of carbonate margins:* During intervals of relative sea level rise, the carbonate platform aggraded with marked repeated backstepping phases.
3. *Platform emersion:* A drop in sea level led to the emersion of the carbonate platform tops during the Early Eocene, which resulted in extensive karstification.
4. *Late stage carbonate growth:* A subsequent fast sea level rise induced an overall shrinking of platform surface and led to the development of late-stage buildups. The sea level rise flooded the contemporaneous shelf, and coeval carbonate sedimentation started there.
5. *Drowning:* Drowning of the isolated carbonate platform took place in the Early to Middle Eocene. Following the drowning, a thin succession of planktonic rich pelagics covered the carbonate platform succession. Biostratigraphy indicates a depositional hiatus with a duration of more than ~30 Ma at the top of the carbonate, prior to the arrival of the Indus Fan sediments that wrapped the carbonate platform with turbiditic and channel-levee systems.

These results suggest that the architecture of the carbonate platforms is due to the combined effects of the local and regional topography, regional and local tectonics, eustasy as well as paleoclimate and paleoceanography. The size, shape, and locations for the carbonate platform growth are determined by the antecedent topography. Further, the long-term thermal subsidence was the main control on the creation of accommodation leading to the accumulation of a locally more than 1000 m thick carbonate succession. Eustatic fluctuations also acted as one dominant factor that influenced the internal heterogeneity and sequence formation.

The presence of a Late Paleocene to Early Eocene benthic assemblage with nummulitids and alveolinids permits assigning the platform to the Stage III of Scheibner's and Speijer (2005) subdivision of the circum-Tethyan platform stages. The growth of the studied carbonate platforms, therefore, coincided with the Paleocene-Eocene hyperthermal events and largely concurred with a phase of global warming corresponding to major biotic changes in coral-framework species during the Cenozoic Era. The low amplitude and high-frequency eustatic variations of the greenhouse world provided an ideal balance between the relative sea level fluctuations and rate of deposition. Short-term sea level rises or falls had the capacity to drown or expose the buildup for a short period, which is unresolvable through the conventional seismic interpretation of the available data. In the absence of framework species, the development of raised rims or bucket geometries during a sea level rise is uncommon in greenhouse carbonate platforms. This explains the depositional response of the platform-internal parallel and layer cake accumulations geometries with flat tops. A rapid relative rise in sea level, augmented by the subsidence of substratum drowned the carbonate platforms during the Eocene. The synsedimentary tectonic deformation largely controlled the internal architecture and the growth asymmetry of the carbonate platforms.

The post-collision uplift of the Himalayan and Hindukush established a fluvial system that transported the eroded sediment and started the fan sedimentation in the northern Indian Ocean. The second part of the dissertation work focuses on this topic and establishes a seismic stratigraphic framework of the Indus Fan sediments linking it with the shelf stratigraphy, thus documenting the shelf to basin changes in stratigraphy. The following conclusions are drawn:

1. Following the Indian-Seychelles volcanism associated to rifting, the sediment-starved basin was dominated by the sequence of pelagic and hemipelagic sediments and coeval shallow water carbonate platforms on the topographic highs, deposited during the drift phase of the Indian Plate. The unit is established as prefan succession and deposited from the Late Paleocene to the Oligocene. During this time, a carbonate shelf developed along the passive margin.
2. The Middle Oligocene to Early Miocene succession comprises the initial fan sediments. Levee dominated channel are small, alternating with massive mass transport complexes. Mass wasting processes predominant on the continental slope were controlled by higher sediment influx from the Himalayan region and by episodes of sea level lowering.

3. The Middle Miocene marks the time of shelf progradation with the development of prominent channel-levee complexes.
4. The channel size further increased during Plio-Pleistocene times.
5. The Recent hemipelagic highstand succession covers the Indus Fan and channel-levee deposits coincident with a retreating Indus Delta and recessive sediments influx.
6. The upper part of the Indus Fan, from the Middle Miocene to Recent, bears multiple cycles of incision to aggradation in comparison to the Oligocene to Early Miocene where multiple cycles of incision to aggradation are not frequent and excessive. Further, the lateral channel migration also increased from the Miocene to today, which is lacking or limited in the lower part of the Indus Fan.

References

- Abreu, J.B., Anderson, J.B.** (1998) Glacial eustasy during the Cenozoic: sequence stratigraphic implications. *AAPG Bulletin*, 82, 1385–1400.
- Afzal, J., Williams, M., Aldridge, R.J.** (2009) Revised stratigraphy of the lower Cenozoic succession of the Greater Indus Basin in Pakistan. *Journal of Micropalaeontology*, 28, 7–23.
- Afzal, J., Williams, M., Leng, M.J., Aldridge, R.J., Stephenson, M.H.** (2011) Evolution of Paleocene to Early Eocene larger benthic foraminifer assemblages of the Indus Basin, Pakistan. *Lethaia*, 44, 299–320.
- Agrawal, A., Rogers, J.J.W.** (1992) Structure and tectonic evolution of the western continental margin of India: Evidence from subsidence studies for a 25–20 Ma plate reorganization in the Indian Ocean. In: *Basement Tectonics 8: Characterization and Comparison of Ancient and Mesozoic Continental Margins* (Eds. Bartholomew, M.J., Hyndman, D.W., Mogk, D.W., Mason, R.). Springer Netherlands, Dordrecht, 583–590.
- Ahmad, A., Ahmad, N.** (2005) Paleocene petroleum system and its significance for exploration in the southwest lower Indus basin and nearby offshore of Pakistan. In: *Proceedings of Annual Technical Conference, 2005 Islamabad*, 1–22 pp.
- Akhter, M., Butt, A.A.** (1999) Lower Tertiary biostratigraphy of the Kala Chitta Range, northern Pakistan. *Revue de Paleobiologie*, 18, 123–146.
- Allen, P.A., Allen, J.R.** (2013) *Basin analysis: Principles and application to petroleum play assessment*. John Wiley & Sons, NJ, USA, 632 pp.
- Arni, P.** (1967) A comprehensive graph of the essential diagnostics of the nummulites. *Micropaleontology*, 13, 41–54.
- Aubert, O., Droxler, A.** (1996) Seismic stratigraphy and depositional signatures of the Maldivic carbonate system (Indian Ocean). *Marine and Petroleum Geology*, 13, 503–536.
- Baceta, J.I., Pujalte, V., Bernaola, G.** (2005) Paleocene corallgal reefs of the western Pyrenean basin, northern Spain: New evidence supporting an earliest Paleogene recovery of reefal ecosystems. *Palaeogeography, Palaeoclimatology, Palaeoecology*, 224, 117–143.
- Bachtel, B., Steven L., Kissling, R.D., Martono, D., Raharjanto, S.P., Dunn, P.A., Macdonald, B.A.** (2004) Seismic stratigraphic evolution of the Miocene-Pliocene Segitia Platform, East Nauna Sea, Indonesia: The origin, growth, and demise of an isolated carbonate platform. In: *Seismic Imaging of Carbonate Reservoirs and Systems* (Eds. By Eberli, G.P., Masferro, J.L., Sarg, J.F.). *AAPG Memoir*, 81, 309–328.

References

- Belopolsky, A., Droxler, A.** (2003) Imaging Tertiary carbonate system—the Maldives, Indian Ocean: Insights into carbonate sequence interpretation. *The Leading Edge*, 22, 646–652.
- Berggren, W.A.** (2005) A revised tropical to sub-tropical Paleogene planktonic foraminiferal zonation. *The Journal of Foraminiferal Research*, 35, 279–298.
- Betzler, C., Eberli, G.P., Kroon, D., Wright, J.D., Swart, P.K., Nath, B.N., Alvarez-Zarikian, C.A., Alonso-García, M., Bialik, O.M., Blättler, C.L.** (2016) The abrupt onset of the modern South Asian Monsoon winds. *Scientific Reports*, 6.
- Betzler, C., Fürstenau, J., Lüdmann, T., Hübscher, C., Lindhorst, S., Paul, A., Reijmer, J.J.G., Droxler, A.W.** (2013) Sea level and ocean-current control on carbonate-platform growth, Maldives, Indian Ocean. *Basin Research*, 25, 172–196.
- Betzler, C., Hübscher, C., Lindhorst, S., Reijmer, J.J., Römer, M., Droxler, A.W., Fürstenau, J., Lüdmann, T.** (2009) Monsoon-induced partial carbonate platform drowning (Maldives, Indian Ocean). *Geology*, 37, 867–870.
- Bhattacharya, G.C., Chaubey, A.K., Murty, G.P.S., Srinivas, K., Sarma, K.V.L.N.S., Subrahmanyam, V., Krishna, K.S.** (1994) Evidence for seafloor spreading in the Laxmi Basin, northeastern Arabian Sea. *Earth and Planetary Science Letters*, 125, 211–220.
- Bosence, D.** (2005) A genetic classification of carbonate platforms based on their basinal and tectonic settings in the Cenozoic. *Sedimentary Geology*, 175, 49–72.
- Bourget, J., Zaragosi, S., Rodriguez, M., Fournier, M., Garlan, T., Chamot-Rooke, N.** (2013) Late Quaternary megaturbidites of the Indus Fan: Origin and stratigraphic significance. *Marine Geology*, 336, 10–23.
- Burgess, P.M., Winefield, P., Minzoni, M., Elders, C.** (2013) Methods for identification of isolated carbonate buildups from seismic reflection data. *AAPG Bulletin*, 97, 1071–1098.
- Calvès, G., Clift, P.D., Inam, A.** (2008) Anomalous subsidence on the rifted volcanic margin of Pakistan: No influence from Deccan plume. *Earth and Planetary Science Letters*, 272, 231–239.
- Calvès, G., Schwab, A.M., Huuse, M., Clift, P.D., Gaina, C., Jolley, D., Tabrez, A.R., Inam, A.** (2011) Seismic volcanostratigraphy of the western Indian rifted margin: The pre-Deccan igneous province. *Journal of Geophysical Research : Solid Earth*, 116, 1–28.
- Carmichael, S.M., Akhter, S., Bennett, J.K., Fatimi, M.A., Hosein, K., Jones, R.W., Longacre, M.B., Osborne, M.J., Tozer, R.S.J.** (2009) Geology and hydrocarbon potential of the offshore Indus Basin, Pakistan. *Petroleum Geoscience*, 15, 107–116.
- Catuneanu, O.** (2006) Principles of Sequence Stratigraphy. Elsevier. 386 pp.

- Chatterjee, S., Goswami, A., Scotese, C.R.** (2013) The longest voyage: tectonic, magmatic, and paleoclimatic evolution of the Indian plate during its northward flight from Gondwana to Asia. *Gondwana Research*, 23, 238–267.
- Clift, P., Gaedicke, C.** (2002) Accelerated mass flux to the Arabian Sea during the middle to late Miocene. *Geology*, 30, 207–210.
- Clift, P.D., Giosan, L., Henstock, T.J., Tabrez, A.R.** (2014) Sediment storage and reworking on the shelf and in the Canyon of the Indus River-Fan System since the last glacial maximum. *Basin Research*, 26, 183–202.
- Clift, P.D., Hodges, K.V., Heslop, D., Hannigan, R., Van Long, H., Calves, G.** (2008) Correlation of Himalayan exhumation rates and Asian monsoon intensity. *Nature Geoscience*, 1, 875–880.
- Clift, P.D., Shimizu, N., Layne, G.D., Blusztajn, J.S., Gaedicke, C., Schlüter, H.-U., Clark, M.K., Amjad, S.** (2001) Development of the Indus Fan and its significance for the erosional history of the Western Himalaya and Karakoram. *Geological Society of America Bulletin*, 113, 1039–1051.
- Copley, A., Avouac, J.-P., Royer, J.-Y.** (2010) India-Asia collision and the Cenozoic slowdown of the Indian plate: Implications for the forces driving plate motions. *Journal of Geophysical Research : Solid Earth*, 115, B03410.
- Corfield, R.I., Carmichael, S., Bennett, J., Akhter, S., Fatimi, M., Craig, T.** (2010) Variability in the crustal structure of the West Indian Continental Margin in the Northern Arabian Sea. *Petroleum Geoscience*, 16, 257–265.
- Courgeon, S., Jorry, S.J., Camoin, G.F., BouDagher-Fadel, M.K., Jouet, G., Révillon, S., Bachèlery, P., Pelleter, E., Borgomano, J., Poli, E., Droxler, A.W.** (2016) Growth and demise of Cenozoic isolated carbonate platforms: New insights from the Mozambique Channel seamounts (SW Indian Ocean). *Marine Geology*, 380, 90–105.
- Courgeon, S., Jorry, S.J., Jouet, G., Camoin, G., BouDagher-Fadel, M.K., Bachèlery, P., Caline, B., Boichard, R., Révillon, S., Thomas, Y., Thereau, E., Guérin, C.** (2017) Impact of tectonic and volcanism on the Neogene evolution of isolated carbonate platforms (SW Indian Ocean). *Sedimentary Geology*, 355, 114–131.
- Daley, T., Alam, Z.** (2002) Seismic stratigraphy of the offshore Indus Basin. In: *The Tectonic and Climatic Evolution of the Arabian Sea Region* (Eds. Clift, P.D., Kroon, D., Gaedicke, C., Craig, J.). *The Geological Society of London, Special Publications*, 105, 259–271.
- de Groot, P., Huck, A., de Bruin, G., Hemstra, N., Bedford, J.** (2010) The horizon cube: A step change in seismic interpretation. *The Leading Edge*, 29, 1048–1055.
- Deptuck, M.E., Steffens, G.S., Barton, M., Pirmez, C.** (2003) Architecture and evolution of upper fan channel-belts on the Niger Delta slope and in the Arabian Sea. *Marine and Petroleum Geology*, 20, 649–676.

References

- Droz, L., Bellaiche, G.** (1991) Seismic facies and geologic evolution of the central portion of the Indus Fan. In: *Seismic Facies and Sedimentary Processes of Submarine Fans and Turbidite Systems* (Eds. Weimer, P., Link, M.H.). Springer, New York 383–402.
- Duncan, RA.,** (1990) The volcanic record of the Reunion hotspot. In: *Proceedings of the Ocean Drilling Program, Scientific Results* (Eds. Backman J, Peterson L, Duncan RA) 115, 3–10
- Eberli, G.P. Ginsburg, R.N.** (1989) Cenozoic progradation of northwestern Great Bahama Bank, a record in lateral platform growth and sea level fluctuations. In: *Controls on Carbonate Platform and Basin Development* (Eds. Crevello, P.D., Wilson J.L., Sarg J.F & Read J.F.), *SEPM Special Publication*, 44, 339–351.
- Edwards, R.A., Minshull, T.A., White, R.S.** (2000) Extension across the Indian–Arabian plate boundary: the Murray Ridge. *Geophysical Journal International*, 142, 461–477.
- Eichenseer, H., Luterbacher, H.** (1992) The marine Paleogene of the temp region (NE Spain)-depositional sequences, facies history, biostratigraphy and controlling factors. *Facies*, 27, 119–151.
- Embry, A.F.** (1993) Transgressive–regressive (T–R) sequence analysis of the Jurassic succession of the Sverdrup Basin, Canadian Arctic Archipelago. *Canadian Journal of Earth Sciences*, 30, 301–320.
- Erlich, R.N., Barrett, S.F., Ju, G.B.** (1990) Seismic and Geologic Characteristics of Drowning Events on Carbonate Platforms. *AAPG Bulletin*, 74, 1523–1537.
- Flood, R.D., Manley, P.L., Kowsmann, R.O., Appi, C.J., Pirmez, C.** (1991) Seismic Facies and Late Quaternary Growth of Amazon Submarine Fan. In: *Seismic Facies and Sedimentary Processes of Submarine Fans and Turbidite Systems* (Eds. Weimer, P., Link, M.H.). Springer, New York, 415–433.
- Fontaine, J.M., Cussey, R., Lacaze, J., Lanaud, R., (5), L.Y.** (1987) Seismic interpretation of carbonate depositional environments. *AAPG Bulletin*, 71, 281–297.
- Fournier, F., Borgomano, J., Montaggioni, L.F.** (2005) Development patterns and controlling factors of Tertiary carbonate buildups: Insights from high-resolution 3D seismic and well data in the Malampaya gas field (Offshore Palawan, Philippines). *Sedimentary Geology*, 175, 189–215.
- Fraser, S.I., Fraser, A.J., Lentini, M.R., Gawthorpe, R.L.** (2007) Return to rifts – the next wave: fresh insights into the petroleum geology of global rift basins. *Petroleum Geoscience*, 13, 99–104.
- Fürstenau, J., Lindhorst, S., Betzler, C., Hübscher, C.** (2010) Submerged reef terraces of the Maldives (Indian Ocean). *Geo-Marine Letters*, 30, 511–515.
- Gaedicke, C., Prexl, A., Schlüter, H.-U., Meyer, H., Roeser, H., Clift, P.D.** (2002a) Seismic stratigraphy and correlation of major regional unconformities in the northern Arabian Sea. In: *The Tectonic and Climatic Evolution of the Arabian Sea Region*

- (Eds. Clift, P.D., Kroon, D., Gaedicke, C., Craig, J.). *The Geological Society of London, Special Publications*, 105, 25–36.
- Gaedicke, C., Schlüter, H.-U., Roeser, H.A., Prexl, A., Schreckenberger, B., Meyer, H., Reichert, C., Clift, P., Amjad, S.** (2002b) Origin of the northern Indus Fan and Murray Ridge, Northern Arabian Sea: interpretation from seismic and magnetic imaging. *Tectonophysics*, 355, 127–143.
- Green, O.R., Searle, M.P., Corfield, R.I., Corfield, R.M.** (2008) Cretaceous-Tertiary Carbonate Platform Evolution and the Age of the India-Asia Collision along the Ladakh Himalaya (Northwest India). *The Journal of Geology*, 116, 331–353.
- Hallock, P.** (1987) Fluctuations in the trophic resource continuum: A factor in global diversity cycles? *Paleoceanography*, 2, 457–471.
- Hallock, P., Glenn, E.C.** (1986) Larger Foraminifera: A tool for paleoenvironmental analysis of Cenozoic carbonate depositional facies. *Palaios*, 1, 55–64.
- Hallock, P., Premoli Silva, I., Boersma, A.** (1991). Similarities between planktonic and larger foraminiferal evolutionary trends through Paleogene paleoceanographic changes. *Palaeogeography, Palaeoclimatology, Palaeoecology*, 83, 49–64.
- Hallock, P., Schlager, W.** (1986) Nutrient excess and the demise of coral reefs and carbonate platforms. *Palaios*, 1, 389–398.
- Hansen, L.A.S., Callow, R.H.T., Kane, I.A., Gamberi, F., Rovere, M., Cronin, B.T., Kneller, B.C.** (2015) Genesis and character of thin-bedded turbidites associated with submarine channels. *Marine and Petroleum Geology*, 67, 852–879.
- Haq, B.** (1981) Paleogene paleoceanography: Early Cenozoic oceans revisited. *Oceanologica Acta*, Special issue, 71–82.
- Haq, B.U., Hardenbol, J., Vail, P.R.** (1987) Chronology of Fluctuating Sea Levels Since the Triassic. *Science*, 235, 1156–1167.
- Höntzsch, S., Scheibner, C., Kuss, J., Marzouk, A.M., Rasser, M.W.,** (2011) Tectonically driven carbonate ramp evolution at the southern Tethyan shelf: the Lower Eocene succession of the Galala Mountains, Egypt. *Facies*, 57, 51–72.
- Höntzsch, S., Scheibner, C., Brock, J., Kuss, J.** (2013) Circum-Tethyan carbonate platform evolution during the Palaeogene: the Prebetic platform as a test for climatically controlled facies shifts. *Turkish Journal of Earth Sciences*, 22, 891–918.
- Hottinger, L.** (1971) Larger foraminifera common to Mediterranean and Indian Paleocene and Eocene formations. *Annals of the Hungarian Geological Institute*, 54, 143–150.
- Hübscher, C., Spieß, V., Breitzke, M., Weber, M.E.** (1997) The youngest channel-levee system of the Bengal Fan: results from digital sediment echosounder data. *Marine Geology*, 141, 125–145.

References

- Inam, A., Clift, P.D., Giosan, L., Tabrez, A.R., Tahir, M., Rabbani, M.M., Danish, M.** (2007) The geographic, geological and oceanographic setting of the Indus River. In: *Large Rivers* (Ed. Gupta, A.). John Wiley & Sons, Ltd, Chichester, UK, pp. 333–346.
- Janocko, M., Nemec, W., Henriksen, S., Warchol, M.** (2013) The diversity of deep-water sinuous channel belts and slope valley-fill complexes. *Marine and Petroleum Geology*, 41, 7–34.
- Jerram, D.A., Single, R.T., Hobbs, R.W., Nelson, C.E.** (2009) Understanding the offshore flood basalt sequence using onshore volcanic facies analogues: an example from the Faroe–Shetland basin. *Geological Magazine*, 146, 353–367 .
- Jones, B., Desrochers, A.** (1992) Shallow platform carbonates. In: *Facies Models - Response to Sea level Changes* (Eds. Walker, R., James, N.). *Geological Association of Canada*, 277–301.
- Jorry, S.J., Hasler, C.-A., Davaud, E.** (2006) Hydrodynamic behaviour of Nummulites: implications for depositional models. *Facies*, 52, 221–235.
- Kendall, C.G.S.C., Schlager, W.** (1981) Carbonates and relative changes in sea level. *Marine Geology*, 44, 181–212.
- Kent, D.V., Muttoni, G.** (2008) Equatorial convergence of India and Early Cenozoic climate trends. *Proceedings of the National Academy of Sciences of the United States of America*, 105, 16065–16070.
- Kenyon, N.H., Amir, A., Cramp, A.** (1995) Geometry of the younger sediment bodies of the Indus Fan. In: *Atlas of Deep Water Environments* (Eds. Pickering, K.T., Hiscott, R.N., Kenyon, N.H., Ricci Lucchi, F., Smith, R.A.). Springer Netherlands, Dordrecht, pp. 89–93.
- Khan, N., Rehman, K., Ahmad, S., Khokher, J., Hajana, M.I., Hanif, M.** (2016) Sequence stratigraphic analysis of Eocene Rock Strata, Offshore Indus, southwest Pakistan. *Marine Geophysical Research*, 37, 207–228.
- Kiessling, W., Flügel, E.** (2002) Paleoreefs—a database on Phanerozoic reefs. In: *Phanerozoic Reef Patterns* (Eds. Kiessling, W., Flügel, E., Golonka, J.). SEPM (Society for Sedimentary Geology), Tulsa, Okla., U.S.A.
- Kim, W., Fouke, B.W., Petter, A.L., Quinn, T.M., Kerans, C., Taylor, F.** (2012) Sea level rise, depth-dependent carbonate sedimentation and the paradox of drowned platforms: Slowly drowned platforms. *Sedimentology*, 59, 1677–1694.
- Kolla, V., Coumes, F.** (1987) Morphology, internal structure, seismic stratigraphy, and sedimentation of Indus Fan. *AAPG Bulletin*, 71, 650–677.
- Kolla, V., Posamentier, H.W., Wood, L.J.** (2007) Deep-water and fluvial sinuous channels—Characteristics, similarities and dissimilarities, and modes of formation. *Marine and Petroleum Geology*, 24, 388–405.

- Kusumastuti, A., Rensbergen, P.V., Warren, J.K.** (2002) Seismic sequence analysis and reservoir potential of drowned Miocene carbonate platforms in the Madura Strait, East Java, Indonesia. *AAPG Bulletin*, 86, 213–232.
- Lucia, F.J.** (2007) *Carbonate Reservoir Characterization*. Springer, Berlin, Germany, 332 pp.
- Malod, J.A., Droz, L., Kemal, B.M., Patriat, P.** (1997) Early spreading and continental to oceanic basement transition beneath the Indus deep-sea fan: northeastern Arabian Sea. *Marine Geology*, 141, 221–235.
- Mann, P., Gahagan, L., Gordon, M.B.** (2003) Tectonic setting of the world's Giant Oil and Gas Fields. In: *Giant Oil and Gas Fields of the Decade: 1990-1999* (Eds. Halbouty, M.T.). 15–105.
- Markello, J.R., Keopnick, R.B., Waite, L.E., Collins, J.F.** (2008) The Carbonate Analogs Through Time (Catt) Hypothesis and the Global Atlas of Carbonate Fields—A Systematic and Predictive Look at Phanerozoic Carbonate Systems. In: *Controls on Carbonate Platform and Reef Development* (Eds. Lukasik, J., Simo, J.A.). *SEPM (Society for Sedimentary Geology)*.
- McHargue, T.R.** (1991) Seismic facies, processes, and evolution of Miocene inner fan channels, Indus submarine fan. In: *Seismic Facies and Sedimentary Processes of Submarine Fans and Turbidite Systems* (Eds. Weimer, P., Link, M.H.). Springer, New York 403–413.
- McHargue, T.R., Webb, J.E.** (1986) Internal geometry, seismic facies, and petroleum potential of canyons and inner fan channels of the Indus submarine fan. *AAPG Bulletin*, 70, 161-180.
- Menier, D., Pierson, B., Chalabi, A., Ting, K.K., Pubellier, M.** (2014) Morphological indicators of structural control, relative sea level fluctuations and platform drowning on present-day and Miocene carbonate platforms. *Marine and Petroleum Geology*, 58, 776–788.
- Miller, K., Mountain, G., Wright, J., Browning, J.** (2011) A 180-Million-Year Record of Sea Level and Ice Volume Variations from Continental Margin and Deep-Sea Isotopic Records. *Oceanography*, 24, 40–53.
- Miller, K.G., Fairbanks, R.G., Mountain, G.S.** (1987) Tertiary oxygen isotope synthesis, sea level history, and continental margin erosion. *Paleoceanography*, 2, 1–19.
- Miller, K.G., Kominz, M.A., Browning, J.V., Wright, J.D., Mountain, G.S., Katz, M.E., Sugarman, P.J., Cramer, B.S., Christie-Blick, N., Pekar, S.F.** (2005) The Phanerozoic record of global sea level change. *Science*, 310, 1293–1298.
- Minshull, T.A., Edwards, R.A., Flueh, E.R.** (2015) Crustal structure of the Murray Ridge, northwest Indian Ocean, from wide-angle seismic data. *Geophysical Journal International*, 202, 454–463.

References

- Mishra, R., Pandey, D.K., Ramesh, P., Clift, P.D.** (2016) Identification of new deep sea sinuous channels in the eastern Arabian Sea. *SpringerPlus*, 5.
- Misra, A.A., Banerjee, S., Kundu, N., Mukherjee, B.** (2017) Subsidence around oceanic ridges along passive margins: NE Arabian Sea. In: *Tectonics of the Deccan Large Igneous Province: An Introduction* (Eds. Mukherjee, S., Misra, A.A., Calvès, G., Nemčok, M.). Geological Society of London, Special Publications, London, UK, 119–149.
- Mitchum, R.M., Vail, P.R., Sangree, J.B.** (1977) Seismic Stratigraphy and Global Changes of Sea Level: Part 6. Stratigraphic Interpretation of Seismic Reflection Patterns in Depositional Sequences: Section 2. Application of Seismic Reflection Configuration to Stratigraphic Interpretation. In: *Seismic Stratigraphy--Applications to Hydrocarbon Exploration* (Eds. Playton, C.E.). *AAPG Memoir*, 26, 83–97.
- Mohan, M.** (1985) Geohistory analysis of Bombay High region. *Marine and Petroleum Geology*, 2, 350–360.
- Moore, J.G., Clague, D.A.** (1992) Volcano growth and evolution of the island of Hawaii. *Geological Society of America Bulletin*, 104, 1471–1484.
- Moore, J.G., Fornari, D.J.** (1984) Drowned Reefs as Indicators of the Rate of Subsidence of the Island of Hawaii. *The Journal of Geology*, 92, 752–759.
- Mutti, E., Normark, W.R.** (1991) An Integrated Approach to the Study of Turbidite Systems. In: *Seismic Facies and Sedimentary Processes of Submarine Fans and Turbidite Systems* (Eds. Weimer, P., Link, M.H.). *Springer*, 75–106.
- Naini, B.R., Talwani, M.** (1982) Structural Framework and the Evolutionary History of the Continental Margin of Western India: Rifted Margins: Field Investigations of Margin Structure and Stratigraphy. In: *Studies in Continental Margin Geology* (Eds. Watkins, J.S., Drake, C.L.). *AAPG Memoir*, 34, 167–191.
- Parrish, J.T.** (1987) Palaeo-upwelling and the distribution of organic-rich rocks. *The Geological Society of London*, 26, 199–205.
- Paumard, V., Zuckmeyer, E., Boichard, R., Jorry, S.J., Bourget, J., Borgomano, J., Maurin, T., Ferry, J.-N.** (2017) Evolution of Late Oligocene - Early Miocene attached and isolated carbonate platforms in a volcanic ridge context (Maldives type), Yadana field, offshore Myanmar. *Marine and Petroleum Geology*, 81, 361–387.
- Peakall, J., Sumner, E.J.** (2015) Submarine channel flow processes and deposits: A process-product perspective. *Geomorphology*, 244, 95–120.
- Pearson, P.N., Palmer, M.R.** (2000) Atmospheric carbon dioxide concentrations over the past 60 million years. *Nature*, 406, 695–699.
- Perrin, C.** (2002) Tertiary: the emergence of modern reef ecosystems. In: *Phanerozoic Reef Patterns* (Eds. Kiessling, Flügel, E., Golonka, J.). *SEPM Special Publication*, 72, 587–618.

- Planke, S., Symonds, P.A., Alvestad, E., Skogseid, J.** (2000) Seismic volcanostratigraphy of large-volume basaltic extrusive complexes on rifted margins. *Journal of Geophysical Research: Solid Earth*, 105, 19335–19351.
- Posamentier, H.W.** (2003) Depositional elements associated with a basin floor channel-levee system: case study from the Gulf of Mexico. *Marine and Petroleum Geology*, 20, 677–690.
- Posamentier, H.W., Jervey, M.T., Vail, P.R.** (1988) Eustatic controls on clastic deposition I—conceptual framework. In: *Sea level Changes: An Integrated Approach* (Eds. Wilgus, C.K., Hastings, B.S., Posamentier, H., Wagoner, J.V., Ross, C.A., Kendall, C.C.G.). SEPM, Tulsa, Okla., U.S.A, 109–124.
- Posamentier, H.W., Kolla, V.** (2003) Seismic Geomorphology and Stratigraphy of Depositional Elements in Deep-Water Settings. *Journal of Sedimentary Research*, 73, 367–388.
- Prather, B.E., O’Byrne, C., Pirmez, C., Sylvester, Z.** (2017) Sediment partitioning, continental slopes and base-of-slope systems. *Basin Research*, 29, 394–416.
- Prins, M.A., Postma, G., Cleveringa, J., Cramp, A., Kenyon, N.H.** (2000) Controls on terrigenous sediment supply to the Arabian Sea during the late Quaternary: the Indus Fan. *Marine Geology*, 169, 327–349.
- Purdy, E.G., Betram, G.T.** (1993) Carbonate Concepts from the Maldives, Indian Ocean. *AAPG Studies in Geology*, 34, 56pp.
- Purdy, E.G., Gischler, E.** (2005) The transient nature of the empty bucket model of reef sedimentation. *Sedimentary Geology*, 175, 35–47.
- Qayyum, F., Paul, de G., Hemstra, N.** (2012) Using 3D Wheeler diagrams in seismic interpretation – the Horizon-Cube method. *First Break*, 30, 103–109.
- Qayyum, M., Lawrence, R.D., Niem, A.R.** (1997) Discovery of the palaeo-Indus delta-fan complex. *Journal of the Geological Society*, 154, 753–756.
- Qayyum, M., Niem, A.R., Lawrence, R.D.** (2001) Detrital modes and provenance of the Paleogene Khojak Formation in Pakistan: Implications for early Himalayan orogeny and unroofing. *Geological Society of America Bulletin*, 113, 320–332.
- Racey, A.** (2001) A review of Eocene Nummulite accumulations: Structure, formation and reservoir potential. *Journal of Petroleum Geology*, 24, 79–100.
- Ramsayer, G.R.** (1979) Seismic Stratigraphy, a Fundamental Exploration Tool, in: *Offshore Technology Conference Proceeding*. Presented at the Offshore Technology Conference, Houston, Texas.
- Raymo, M.E., Ruddiman, W.F.** (1992) Tectonic forcing of late Cenozoic climate. *Nature*, 359, 117–122.

References

- Rebesco, M., Hernández-Molina, F.J., Van Rooij, D., Wåhlin, A.** (2014) Contourites and associated sediments controlled by deep-water circulation processes: State-of-the-art and future considerations. *Marine Geology*, 352, 111–154.
- Rodriguez, M., Chamot-Rooke, N., Huchon, P., Fournier, M., Lallemand, S., Delescluse, M., Zaragosi, S., Mouchot, N.** (2014) Tectonics of the Dalrymple Trough and uplift of the Murray Ridge (NW Indian Ocean). *Tectonophysics*, 636, 1–17.
- Ruddiman, W.F., Kutzbach, J.E.** (1991) Plateau Uplift and Climatic Change. *Scientific American*, 264, 66–75.
- Ryan, W.B.F., Carbotte, S.M., Coplan, J.O., O’Hara, S., Melkonian, A., Arko, R., Weissel, R.A., Ferrini, V., Goodwillie, A., Nitsche, F., Bonczkowski, J., Zemsky, R.** (2009) Global Multi-Resolution Topography synthesis. *Geochemistry, Geophysics, Geosystems*, 10, 1–9.
- Sandwell, D.T., Muller, R.D., Smith, W.H.F., Garcia, E., Francis, R.** (2014) New global marine gravity model from CryoSat-2 and Jason-1 reveals buried tectonic structure. *Science*, 346, 65–67.
- Saqab, M.M., Bourget, J.** (2016) Seismic geomorphology and evolution of early–mid Miocene isolated carbonate build-ups in the Timor Sea, North West Shelf of Australia. *Marine Geology*, 379, 224–245.
- Saqab, M.M., Bourget, J.** (2015) Controls on the distribution and growth of isolated carbonate build-ups in the Timor Sea (NW Australia) during the Quaternary. *Marine and Petroleum Geology*, 62, 123–143.
- Scheibner, C., Speijer, R.P.** (2008a) Decline of coral reefs during Late Paleocene to Early Eocene global warming. *eEarth*, 3, 19–26.
- Scheibner, C., Speijer, R.P.** (2008b) Late Paleocene–Early Eocene Tethyan carbonate platform evolution — A response to long- and short-term paleoclimatic change. *Earth-Science Reviews*, 90, 71–102.
- Scheibner, C., Speijer, R.P., Marzouk, A.M.** (2005) Turnover of larger foraminifera during the Paleocene-Eocene Thermal Maximum and paleoclimatic control on the evolution of platform ecosystems. *Geology*, 33, 493–496.
- Schlager, W.** (2005) *Carbonate sedimentology and sequence stratigraphy*. SEPM Tulsa-Oklahoma, 193 pp.
- Schlager, W.** (1981) The paradox of drowned reefs and carbonate platforms. *Geological Society of America Bulletin*, 92, 197–211.
- Schlager, W., Purkis, S.J.** (2013) Bucket structure in carbonate accumulations of the Maldives, Chagos and Laccadive archipelagos. *International Journal of Earth Sciences*, 102, 2225–2238.
- Schwenk, T., Spieß, V., Breitzke, M., Hübscher, C.** (2005) The architecture and evolution of the Middle Bengal Fan in vicinity of the active channel–levee system imaged by high-resolution seismic data. *Marine and Petroleum Geology*, 22, 637–656.

- Sclater, J.G., Christie, P.A.F.** (1980) Continental stretching: An explanation of the Post-Mid-Cretaceous subsidence of the central North Sea Basin. *Journal of Geophysical Research: Solid Earth*, 85, 3711–3739.
- Scotese, C.R.** (2001) Atlas of Earth History, Volume 1, Paleogeography, PALEOMAP Project, Paleogeography, PALEOMAP Project, Arlington, Texas.
- Scotese, C.R., Summerhayes, C.P.** (1986) Computer model of palaeoclimate predicts coastal upwelling in the Mesozoic and Cenozoic. *Geobyte*, 1, 28–42.
- Serra-Kiel, J., Hottinger, L., Caus, E., Drobne, K., Ferrandez, C., Jauhri, A.K., Less, G., Pavlovec, R., Pignatti, J., Samso, J.M., Schaub, H., Sirel, E., Strougo, A., Tambareau, Y., Tosquella, J., Zakrevskaya, E.** (1998) Larger foraminiferal biostratigraphy of the Tethyan Paleocene and Eocene. *Bulletin de la Société Géologique de France*, 169, 281–299.
- Shahzad, K., Betzler, C., Ahmed, N., Qayyum, F., Spezzaferri, S., Qadir, A.** (2018) Growth and demise of a Paleogene isolated carbonate platform of the Offshore Indus Basin, Pakistan: effects of regional and local controlling factors. *International Journal of Earth Sciences*, 107, 481–504.
- Shahzad, K., Betzler, C., Qayyum, F.** (2019) Controls on the Paleogene carbonate platform growth under greenhouse climate conditions (Offshore Indus Basin). *Marine and Petroleum Geology*, 101, 519–539.
- Shanmugam, G.** (2006) *Deep-water processes and facies models: Implications for sandstone petroleum reservoirs*. Elsevier, 496 pp.
- Shuaib, S.M.** (1982) Geology and Hydrocarbon Potential of Offshore Indus Basin, Pakistan: Geologic Notes. *AAPG Bulletin*, 66, 940–946.
- Sluijs, A., Brinkhuis, H., Crouch, E.M., John, C.M., Handley, L., Munsterman, D., Bohaty, S.M., Zachos, J.C., Reichert, G.-J., Schouten, S., Pancost, R.D., Damsté, J.S.S., Welters, N.L.D., Lotter, A.F., Dickens, G.R.** (2008) Eustatic variations during the Paleocene-Eocene greenhouse world. *Paleoceanography*, 23, PA4216.
- Smith, W.H., Sandwell, D.T.**, (1997) Global Sea Floor Topography from Satellite Altimetry and Ship Depth Soundings. *Science*, 277, 1956–1962.
- Speijer, R., Scheibner, C., Stassen, P., Morsi, A.-M.M.** (2012) Response of marine ecosystems to deep-time global warming: A synthesis of biotic patterns across the Paleocene-Eocene thermal maximum (PETM). *Austrian Journal of Earth Sciences*, 105, 6–16.
- Speijer, R.P., Van Der Zwaan, G.J., Schmitz, B.** (1996) The impact of Paleocene/Eocene boundary events on middle neritic benthic foraminiferal assemblages from Egypt. *Marine Micropaleontology*, 28, 99–132.
- Speijer, R.P., Wagner, T.** (2002) Sea level changes and black shales associated with the late Paleocene thermal maximum: Organic-geochemical and micropaleontologic evidence from the southern Tethyan margin (Egypt-Israel). In: *Catastrophic Events and Mass*

References

- Extinctions: Impacts and Beyond*. (Eds. Koeberl, C., MacLeod, K.) *Geological Society of America Special Publication*, 356, 533–549.
- Steel, R.J., Porebski, S.J.** (2003) Shelf-edge delta types and their sequence-stratigraphic relationships. In: *Shelf Margin Deltas and Linked Down Slope Petroleum Systems: Global Significance and Future Exploration Potential* (Eds. Roberts, H.R., Rosen, N.C., Fillon, R.F., Anderson, J.B.). *SEPM*, 21, PP-PP.
- Sylvester, Z., Pirmez, C., Cantelli, A.** (2011). A model of submarine channel-levee evolution based on channel trajectories: Implications for stratigraphic architecture *Marine and Petroleum Geology*, 28, 716–727.
- Talwani, M., Reif, C.** (1998) Laxmi Ridge – A continental sliver in the Arabian Sea. *Marine Geophysical Researches*, 20, 259–271.
- Todal, A., Edholm, O.** (1998) Continental margin off Western India and Deccan Large Igneous Province. *Marine Geophysical Researches*, 20, 273–291.
- Torsvik, T.H., Amundsen, H., Hartz, E.H., Corfu, F., Kuszniir, N., Gaina, C., Doubrovine, P.V., Steinberger, B., Ashwal, L.D., Jamtveit, B.** (2013) A Precambrian microcontinent in the Indian Ocean. *Nature Geoscience*, 6, 223–227.
- van Hinsbergen, D.J.J., de Groot, L.V., van Schaik, S.J., Spakman, W., Bijl, P.K., Sluijs, A., Langereis, C.G., Brinkhuis, H.** (2015) A Paleolatitude Calculator for Paleoclimate Studies. *Plos One*, 10, e0126946.
- von Rad, U., Tahir, M.**, (1997) Late Quaternary sedimentation on the outer Indus shelf and slope (Pakistan): evidence from high-resolution seismic data and coring. *Marine Geology*, 138, 193–236.
- Wade, B.S., Pearson, P.N., Berggren, W.A., Pälike, H.** (2011) Review and revision of Cenozoic tropical planktonic foraminiferal biostratigraphy and calibration to the geomagnetic polarity and astronomical time scale. *Earth-Science Reviews*, 104, 111–142.
- Wandrey, C., Law, B., Shah, H.A.** (2004) Sembar-Goru/Ghazij Composite Total Petroleum System, Indus and Sulaiman-Kirthar Geologic Provinces, Pakistan and India, In: *Petroleum Systems and Related Geologic Studies in Region 8, South Asia* (Eds Wandrey, C.J.). *U.S. Geological Survey Bulletin*, 2208-A, 29 pp.
- Ward, W.B.** (1999) Tectonic control on backstepping sequences revealed by mapping of Frasnian Backstepped Platforms, Devonian Reef Complexes, Napier Range, Canning Basin, Western Australia. In: *Advances in Carbonate Sequence Stratigraphy* (Eds. Harris, P.M., Simo, J.A.). *SEPM Special Publications*, 63, 47–74.
- White, R., McKenzie, D.** (1989) Magmatism at rift zones: The generation of volcanic continental margins and flood basalts. *Journal of Geophysical Research: Solid Earth*, 94, 7685–7729.

- Whiting, B.M., Karner, G.D., Driscoll, N.W.** (1994) Flexural and stratigraphic development of the west Indian continental margin. *Journal of Geophysical Research: Solid Earth*, 99, 13791–13811.
- Wilson, M.E.J.** (2011) SE Asian carbonates: tools for evaluating environmental and climatic change in equatorial tropics over the last 50 million years. In: *The SE Asian Gateway: History and Tectonics of the Australia–Asia Collision* (Eds. Hall, R., Cottam, M.A., Wilson, M.E.). *The Geological Society of London Special Publications*, 355, 347–372.
- Wynn, R.B., Cronin, B.T., Peakall, J.** (2007). Sinuous deep-water channels: Genesis, geometry and architecture. *Marine and Petroleum Geology*, 24, 341–387.
- Xie, X., Heller, P.L.** (2009) Plate tectonics and basin subsidence history. *Geological Society of America Bulletin*, 121, 55–64.
- Zachos, J., Pagani, M., Sloan, L., Thomas, E., Billups, K.** (2001) Trends, Rhythms, and Aberrations in Global Climate 65 Ma to Present. *Science*, 292, 686–693.
- Zachos, J.C.** (2003) A Transient Rise in Tropical Sea Surface Temperature During the Paleocene-Eocene Thermal Maximum. *Science*, 302, 1551–1554.
- Zampetti, V., Schlager, W., van Konijnenburg, J.-H., Everts, A.-J.** (2004) Architecture and growth history of a Miocene carbonate platform from 3D seismic reflection data; Luconia province, offshore Sarawak, Malaysia. *Marine and Petroleum Geology*, 21, 517–534.